

AFFDL-TR-76-112

ADA 042369

## EFFECTS OF FIGHTER ATTACK SPECTRUM ON CRACK GROWTH

*MCDONNELL DOUGLAS CORPORATION  
MCDONNELL AIRCRAFT COMPANY  
P.O. BOX 516  
ST. LOUIS, MISSOURI 63166*

MARCH 1977

FINAL REPORT FOR PERIOD MAY 1975 - JULY 1976

Approved for public release; distribution unlimited

AIR FORCE FLIGHT DYNAMICS LABORATORY  
AIR FORCE WRIGHT AERONAUTICAL LABORATORIES  
AIR FORCE SYSTEMS COMMAND  
WRIGHT-PATTERSON AIR FORCE BASE, OHIO 45433

20060921182

## NOTICES

When Government drawings, specifications, or other data are used for any purpose other than in connection with a definitely related Government procurement operation, the United States Government thereby incurs no responsibility nor any obligation whatsoever; and the fact that the government may have formulated, furnished, or in any way supplied the said drawings, specifications, or other data, is not to be regarded by implication or otherwise as in any manner licensing the holder or any other person or corporation, or conveying any rights or permission to manufacture, use or sell any patented invention that may in any way be related thereto.

This technical report has been reviewed and is approved for publication.



JOHN M. POTTER  
Project Engineer



ROBERT M. BADER, Chf  
Structural Integrity Br

FOR THE COMMANDER



HOWARD L. FARMER, Colonel, USAF  
Chief, Structural Mechanics Division

Copies of this report should not be returned unless return is required by security considerations, contractual obligations, or notice on a specific document.

"This report has been reviewed and cleared for open publication and/or public release by the appropriate Office of Information (OI) in accordance with AFR 190-17 and DODD 5230.9. There is no objection to unlimited distribution of this report to the public at large or by DDC to the National Technical Information Service (NTIS)."

UNCLASSIFIED

SECURITY CLASSIFICATION OF THIS PAGE (When Data Entered)

REPORT DOCUMENTATION PAGE		READ INSTRUCTIONS BEFORE COMPLETING FORM
1. REPORT NUMBER AFFDL-TR-76-112	2. GOVT ACCESSION NO.	3. RECIPIENT'S CATALOG NUMBER
4. TITLE (and Subtitle) EFFECT OF FIGHTER ATTACK SPECTRUM ON CRACK GROWTH		5. TYPE OF REPORT & PERIOD COVERED Final Technical Report May 1975-July 1976
		6. PERFORMING ORG. REPORT NUMBER
7. AUTHOR(s) H. D. Dill C. R. Saff		8. CONTRACT OR GRANT NUMBER(s) F33615-75-C-3112
9. PERFORMING ORGANIZATION NAME AND ADDRESS McDonnell Aircraft Company P.O. Box 516 St. Louis, Mo. 63166		10. PROGRAM ELEMENT, PROJECT, TASK AREA & WORK UNIT NUMBERS 486U0213
11. CONTROLLING OFFICE NAME AND ADDRESS Air Force Flight Dynamics Laboratory (FBE) Wright-Patterson Air Force Base Ohio 45433		12. REPORT DATE March 1977
		13. NUMBER OF PAGES 159
14. MONITORING AGENCY NAME & ADDRESS (if different from Controlling Office) Same		15. SECURITY CLASS. (of this report) Unclassified
		15a. DECLASSIFICATION/DOWNGRADING SCHEDULE
16. DISTRIBUTION STATEMENT (of this Report) Approved for public release; distribution unlimited		
17. DISTRIBUTION STATEMENT (of the abstract entered in Block 20, if different from Report)		
18. SUPPLEMENTARY NOTES		
19. KEY WORDS (Continue on reverse side if necessary and identify by block number) Spectrum Generation 7075-T7351 Aluminum Spectrum Loads Overloads Crack Growth Interaction Mathematical Models		
20. ABSTRACT (Continue on reverse side if necessary and identify by block number) The purpose of this program was to systematically evaluate the effect of variations in flight stress spectra on crack propagation using current analysis techniques in conjunction with experimental correlations. Over 100 spectra variations were generated, derived from four baseline load factor spectra. The spectra variation types considered were (a) Reordering of loads within a mission, (b) Sequence of missions, (c) Mission mix, (d) Individual flight length, (e) High and low load truncation, (f) Compression loads, (g) Exceedance curve, (h) Coupling of peaks and valleys, (i) Test limit stress. Crack growth was predicted for each		

DD FORM 1473  
1 JAN 73

EDITION OF 1 NOV 65 IS OBSOLETE

UNCLASSIFIED

SECURITY CLASSIFICATION OF THIS PAGE (When Data Entered)

UNCLASSIFIED

SECURITY CLASSIFICATION OF THIS PAGE(When Data Entered)

baseline spectrum and spectra variation prior to test with the exception of tests for one baseline spectrum. The generalized Willenborg Model was the primary method of crack growth analysis. Additionally, predictions were made using a closure model based on analyses of crack surface contact, the Contact Stress Model. Three constant amplitude and thirty spectrum tests were performed to verify the predictions of the analysis methods, to evaluate the effects of spectra variations, and to provide data useful for defining guidelines for structural verification of future aircraft. Spectrum variations shown to have the greatest impact on crack growth life are those involving modifications of the maximum peak stresses. The experimental data was evaluated and summarized, and recommendations and guidelines were developed for deriving spectra for multi-mission tactical fighter aircraft.

UNCLASSIFIED

SECURITY CLASSIFICATION OF THIS PAGE(When Data Entered)

## FOREWORD

This report was prepared by McDonnell Aircraft Company (MCAIR), St. Louis, Missouri, for the Structural Integrity Branch, Structural Mechanics Division, Air Force Flight Dynamics Laboratory, Wright-Patterson Air Force Base, Ohio under Contract F33615-75-C-3112, Project 486U "Advanced Metallic Structures", Work Unit 486U0213, "Effect of Fighter Attack Spectrum on Crack Growth". The contract was administered by John M. Potter, Project Engineer, AFFDL/FBE.

The Strength Department of McDonnell Aircraft Company has the responsibility for the performance of this program. The program manager for MCAIR was J. F. Schier. Principal authors of this report are H. D. Dill and C. R. Saff. L. F. Impellizzeri and F. R. Foster contributed to spectra development, and H. T. Young assisted in computer program development. R. E. Whaley and M. E. Reindl, MCAIR Structural Laboratories, performed the test program.

This report covers work accomplished during the period May 1975 through July 1976.

This report was released by the authors in August 1976 for publication.

## TABLE OF CONTENTS

<u>Section</u>	<u>Page</u>
1. INTRODUCTION	1
2. BASELINE EXCEEDANCE DATA	3
2.1 Load Factor Exceedance Curves	3
2.2 Stress Exceedance Curves	7
3. SPECTRUM DEVELOPMENT USING RANDOM NOISE THEORY	13
3.1 Random Noise Theory	13
3.2 Gaussian Process Simulation	19
3.3 Mapping of Gaussian Process to Real History	22
3.4 Rise and Fall Counting	23
3.5 Search for Peaks and Valleys	25
4. CRACK PROPAGATION ANALYSIS METHODS	27
4.1 Selection of Analysis Method	27
4.2 Willenborg Model	28
4.3 Contact Stress Model	32
4.4 Contact Stress Model-II	33
4.5 Model Calibration	35
5. SPECIMEN DEFINITION AND TEST PROCEDURES	39
5.1 Test Program Summary	39
5.2 Specimens	40
5.3 Test Procedure, Crack Growth Monitoring, and Instrumentation	43
5.4 Constant Amplitude Crack Growth Results	45
6. SPECTRA, CRACK GROWTH ANALYSES, AND TEST RESULTS	48
6.1 Overview	48
6.2 Data Presentation	49
6.3 Baseline Spectra, Crack Growth Analyses, and Test Results	52
6.4 Spectra Variations, Crack Growth Analyses, and Test Results	55
6.4.1 Re-Ordering of Loads Within a Mission	57
6.4.2 Sequence of Missions	57
6.4.3 Mission Mix	58
6.4.4 Individual Flight Length	62
6.4.5 High and Low Load Truncation	62
6.4.6 Compression Loads	65
6.4.7 Exceedance Curve Variations	66
6.4.8 Coupling of Peaks and Valleys	69
6.4.9 Combined Variations	69
6.4.10 Test Limit Load Variations	72

7. SUMMARY AND RECOMMENDATIONS	75
7.1 Impact of Spectra Variations	75
7.2 Estimate of Range of Crack Growth that can Occur in a Fleet	92
7.3 Recommendations for Formulating Spectra	101
8. REFERENCES	103
APPENDIX - EXPERIMENTAL DATA	107

# LIST OF FIGURES

<u>Figure</u>	<u>Title</u>	<u>Page</u>
1	F-15 Mission Segment Positive and Negative Peak Exceedance Curves	4
2	Baseline Load Factor Spectra	5
3	Comparison of Air-to-Air Exceedance Curves	6
4	Comparison of Air-to-Ground Exceedance Curves	8
5	Comparison of Composite Exceedance Curves	9
6	Percent Design Limit Stress vs Normal Load Factor	10
7	Baseline Stress Spectra	11
8	F-15 Wing Lower Skin Selected as Study Base	12
9	Gaussian Random Noise Histories	14
10	Power Spectral Density vs Frequency	14
11	Typical Gaussian Exceedance Curves	16
12	Computations for Power Spectral Density	17
13	Power Spectral Density vs Frequency Air-to-Air Training Data	18
14	Power Spectral Density vs Frequency Air-to-Ground Training Data	18
15	Power Spectral Density Used in Random Stress History Generation	19
16	Comparison of Exceedance Curves	22
17	Effect of Rise and Fall Requirement for Peak and Valley Counting	24
18	Willenborg Model Correlation with Constant Amplitude Test Data	30
19	Contact Stress Model Correlation with Constant Amplitude Test Data	34
20	Contact Stress Model II Correlation with Constant Amplitude Test Data	34
21	Comparison of Analysis Variations of the Willenborg Model with Spectrum Test Data	36



# LIST OF FIGURES (Continued)

<u>Figure</u>	<u>Title</u>	<u>Page</u>
22	Correlation of Calibrated Models with Spectrum Test Data	38
23	Open Hole Specimen	42
24	Starter Crack Details - Open Hole Specimen	43
25	Center Crack Panel Specimen	44
26	Crack Growth Rate Data for 7075-T73 ( $R = 0.02$ )	46
27	Crack Growth Rate Data for 7075-T73 ( $R = 0.5$ and $R = 0.3$ )	47
28	Elastic Stress Intensity Changes Rapidly at Short Crack Length	50
29	Crack Growth Analysis Curves for 102 Spectra Variations Have Very Similar Shapes	51
30	Time to Grow Crack From 0.05 to 0.5 Inches is Sufficient to Characterize the Spectrum Variations	52
31	Willenborg Analysis of Subsequent Small Peak	56
32	Variation in Irregularity Factor with Shape of Power Spectral Density Curve	70
33	Comparison of Air-to-Air Power Spectral Density Curve to Rectangular Shape	71
34	Comparison of Air-to-Ground Power Spectral Density Curve to Rectangular Shape	71
35	Reordering Loads Within a Mission	77
36	Sequence of Missions	78
37	Mission Mix	78
38	Mission Mix	79
39	Individual Flight Length	80
40	High and Low Load Truncation	80
41	High and Low Load Truncation	81
42	High and Low Load Truncation	82
43	Compression Loads	83
44	Compression Loads	84

# LIST OF FIGURES (Continued)

<u>Figure</u>	<u>Title</u>	<u>Page</u>
45	Exceedance Curve Variations	85
46	Exceedance Curve Variations	85
47	Coupling of Peaks and Valleys	86
48	Coupling of Peaks and Valleys	87
49	Effect of Stress Level on Crack Growth Prediction with Willenborg Model	88
50	Effect of Stress Level on Crack Growth Prediction with Contact Stress Model	89
51	Test Limit Stress	90
52	Effect of Stress Level on Crack Growth Prediction with Contact Stress Model II	91
53	4G Usage Severity Scatter vs Flight Hours for Air Force F-4 Aircraft Reporting Counting Accelerometer Data	93
54	6G Usage Severity Scatter vs Flight Hours for Air Force F-4 Aircraft Reporting Counting Accelerometer Data	94
55	Fleet Usage Scatter at 1000 Flight Hours	95
56	Fleet Usage Scatter at 2000 Flight Hours	96
57	Range of Crack Growth Predicted by Willenborg Model Due to Fleet Usage Scatter	97
58	Range of Crack Growth Predicted by Contact Stress Model Due to Fleet Usage Scatter	98
59	Variation of Crack Growth Scatter Factor with Fleet Flight Time	100

# LIST OF TABLES

<u>Table</u>	<u>Title</u>	<u>Page</u>
1	Chronological Summary of Spectrum Crack Growth Models	28
2	Test Program Summary	40
3	Mechanical Property Test Results	41
4	Chemical Analysis	41
5	Summary of Spectra Variations, Crack Growth Analyses, and Test Results	49
6	Summary of Analyses and Test Results for Baseline Spectra	54
7	Reordering of Loads Within a Mission	57
8	Sequence of Missions	58
9	Variation in Percentage of Flight Time Spent in Different Missions	59
10	Variation in Mission Sequence	60
11	Variation in Mission Severity	61
12	Individual Flight Length	63
13	Truncation Variations	64
14	Compression Loads Variations	67
15	Exceedance Curve Variations	68
16	Coupling of Peaks and Valleys	72
17	Combined Variations	73
18	Test Limit Stress Level Variations	74
19	Effect of Spectra Variations on Crack Growth	75
20	Effect of Spectra Variations on Crack Growth Life Prediction Accuracy	76
21	Summary of Crack Growth Predictions of Fleet Usage Effects	99
A-1	Constant Amplitude Crack Growth Data, $R = 0.02$	109
A-2	Constant Amplitude Crack Growth Data, $R = 0.5$	110

# LIST OF TABLES (Continued)

<u>Table</u>	<u>Title</u>	<u>Page</u>
A-3	Constant Amplitude Crack Growth Data, $R = -0.3$	112
A-4	Preliminary Air-to-Air Baseline Spectrum Crack Growth Data	113
A-5	Preliminary Air-to-Air Baseline Spectrum Crack Growth Data	114
A-6	Air-to-Air Baseline Spectrum Crack Growth Data	115
A-7	Air-to-Ground Baseline Spectrum Crack Growth Data	116
A-8	Air-to-Ground Baseline Spectrum Crack Growth Data	117
A-9	Instrumentation and Navigation Baseline Spectrum Crack Growth Data	118
A-10	Composite Baseline Spectrum Crack Growth Data	123
A-11	Composite Baseline Spectrum Crack Growth Data	124
A-12	Sequence of Missions Variation 6 Crack Growth Data	125
A-13	Mission Mix Variation 3 Crack Growth Data	126
A-14	Mission Mix Variation 21 Crack Growth Data	127
A-15	Mission Mix Variation 28 Crack Growth Data	128
A-16	Flight Length Variation 4 Crack Growth Data	129
A-17	Truncation Variation 5 Crack Growth Data	130
A-18	Truncation Variation 6 Crack Growth Data	131
A-19	Truncation Variation 8 Crack Growth Data	133
A-20	Truncation Variation 14 Crack Growth Data	134
A-21	Truncation Variation 18 Crack Growth Data	135
A-22	Compression Loads Variation 4 Crack Growth Data	137
A-23	Compression Loads Variation 7 Crack Growth Data	138
A-24	Compression Loads Variation 10 Crack Growth Data	139
A-25	Exceedance Curve Variation 2 Crack Growth Data	140
A-26	Exceedance Curve Variation 5 Crack Growth Data	141

# LIST OF TABLES (Continued)

<u>Table</u>	<u>Title</u>	<u>Page</u>
A-27	Exceedance Curve Variation 6 Crack Growth Data	142
A-28	Coupling of Peaks and Valleys Variation 5 Crack Growth Data	143
A-29	Coupling of Peaks and Valleys Variation 7 Crack Growth Data	144
A-30	Combined Variation 3 Crack Growth Data	145
A-31	Combined Variation 4 Crack Growth Data	146
A-32	Composite Baseline Spectrum at 19.8 KSI Crack Growth Data	147
A-33	Composite Baseline Spectrum at 40.2 KSI Crack Growth Data	150

## 1. INTRODUCTION

Variations in applied load spectra have been shown to significantly affect crack propagation behavior. It is important, therefore, to evaluate and quantify load spectra effects to improve crack propagation prediction capability and aid in the formulation of design, analysis, and test spectra. The purpose of this program was to systematically evaluate the effect of variations in flight stress spectra on crack propagation using current analysis techniques in conjunction with experimental correlations. The study was performed in four phases.

In Phase I, Spectrum Generation, 102 variations were generated, derived from four baseline load factor spectra for the F-15 aircraft. These baseline spectra are Air-to-Air, Air-to-Ground, Instrumentation-and-Navigation, and a combination of these, the Composite. In order to generate a spectrum for analysis and test, it is necessary to convert load factor to stress; the lower wing skin of the F-15 aircraft was used as the basis for performing the conversion. The resulting stress exceedance curves were used to develop the baseline stress spectra for this study. Cycle by cycle stress histories were generated using techniques based on random noise theory to obtain realistic coupling of peaks and valleys. Random stress histories were generated for the baseline spectra and modified to create the spectra variations. The spectra variation types considered were (a) Reordering of loads within a mission, (b) Sequence of missions, (c) Mission mix, (d) Individual flight length, (e) High and low load truncation, (f) Compression loads, (g) Exceedance curve variations, (h) Coupling of peaks and valleys, and (i) Test limit stress. The techniques for generating random stress histories were implemented in a computer program, described in Reference 1. The combinations and modifications of these random time histories, performed to create the spectra variations, were developed using another computer program, described in Reference 2.

In Phase II, Crack Propagation Analysis, crack growth was predicted for each baseline spectrum, and spectra variation. The Willenborg Model was the primary method of crack growth analysis. Additionally, predictions were made using a model based on analyses of crack surface contact. This model, the Contact Stress Model, was used to evaluate the effects of spectra variations which were believed to be incompletely evaluated by the Willenborg Model. All predictions with these two models were made prior to the test

verification, with the exception of constant amplitude tests, and tests of one spectrum used for calibration of the models thru the choice of plastic zone size.

In Phase III, Experimental Verification, three constant amplitude and thirty spectrum tests were performed. The purposes of the test program were to verify the predictions of the analysis methods, to evaluate the effects of spectra variations, and to provide data useful for defining guidelines for structural verification of future aircraft.

Subsequent to the testing, data trends implied that model improvements would enhance test and analysis correlation. These improvements were incorporated in the Contact Stress Model and the resulting Contact Stress Model-II was used to analyze the more significant spectra.

In Phase IV, Data Presentation and Guidelines, the experimental data was evaluated and summarized, and recommendations and guidelines were developed for deriving design, analysis and test spectra for multi-mission tactical fighter aircraft.

## 2. BASELINE EXCEEDANCE DATA

### 2.1 Load Factor Exceedance Curves

Missions of the F-15 aircraft were selected as the basis for generating fatigue spectra. The mission mix in the fatigue spectrum included 365 air to air missions, 355 air to ground missions, and 96 instrumentation and navigation training missions per 1000 hours; this is a typical distribution for a fighter aircraft. There were four different Air-to-Air (A-A) missions, two different Air-to-Ground (A-G) missions, and one Instrumentation and Navigation (I&N) training type of flight. Each of these missions was further subdivided into mission segments, viz., ascent, cruise, combat, descent, and loiter. Schematic exceedance curves for these mission segments are shown in Figure 1. The exceedance data are presented in terms of peaks per hour of time spent in a given segment. For each of the seven basic F-15 missions, the time in each mission segment was determined by mission analyses. This time estimate was based on mission range requirements with optimized fuel consumption through choice of speed and altitude. The mission segment times were multiplied by the appropriate exceedance data in Figure 1 to obtain the total number of peaks for the segments in each mission. Combat maneuvering is considerably more severe than any of the other mission segments; when the actual number of peaks are compared for the F-15 design spectrum, 87% of all peaks exceeding 2 g's and 99% of all peaks exceeding 4 g's are recorded in the combat segments.

The four baseline spectra selected for the program are presented in Figure 2. The A-A load factor exceedance curve is the combined average exceedance curve for the four A-A missions. Similarly, the A-G curve is the combined average load factor exceedance curve of the two A-G missions. The Composite spectrum, in terms of load factor exceedances, is also given in Figure 2. It is based on 475 hours of A-A, 325 hours of A-G, and 200 hours of I&N. The Composite spectrum was selected as a baseline spectrum since it represents a realistic lifetime experience of an operational aircraft. The other three spectra represent extremes of single-purpose usage as well as providing a means of defining spectrum variation via mission mix.

The general applicability of these spectra definitions to any multi-mission tactical fighter is demonstrated by the fact that F-4 Phantom II load factor exceedance data correlate reasonably well with the F-15 curves. Load factor exceedance data from A-A missions studied during the F-4C/D and F-4E (S) ASIP programs, are compared to the F-15 A-A load factor exceedance curves in Figure 3. Because of the better maneuvering capability



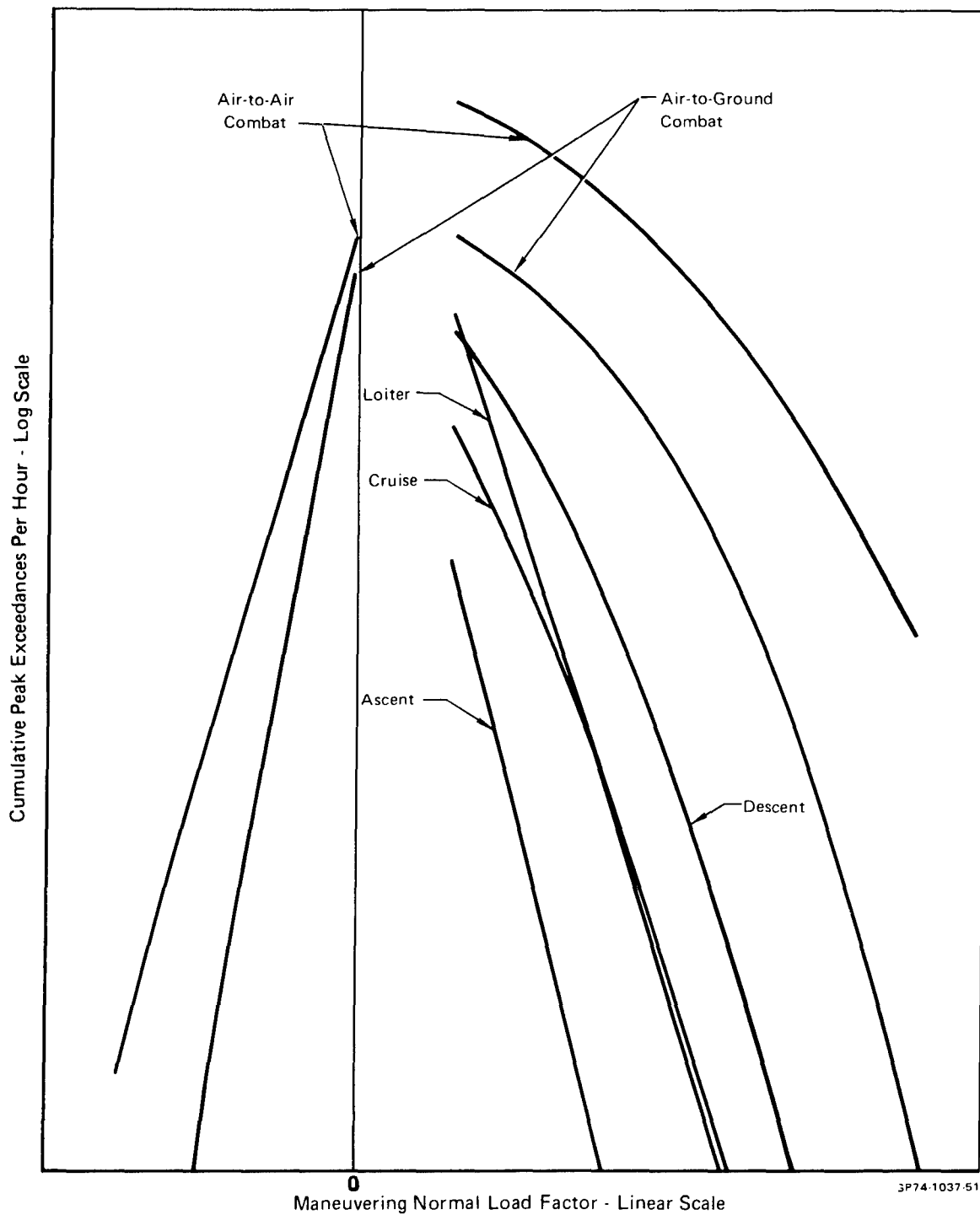


**FIGURE 1. F-15 MISSION SEGMENT POSITIVE AND  
NEGATIVE PEAK EXCEEDANCE CURVES**

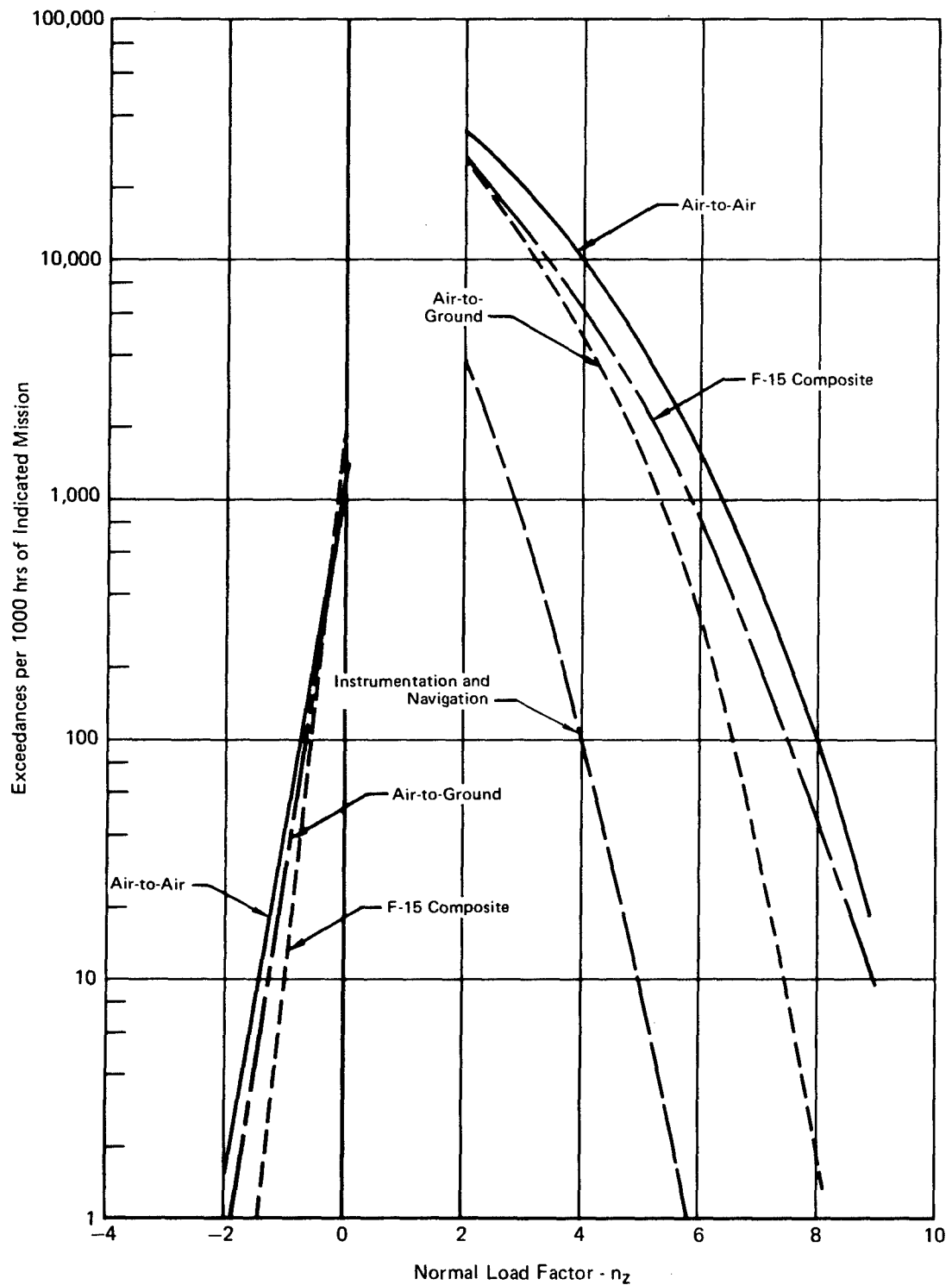


FIGURE 2. BASELINE LOAD FACTOR SPECTRA

GP75-0162-38

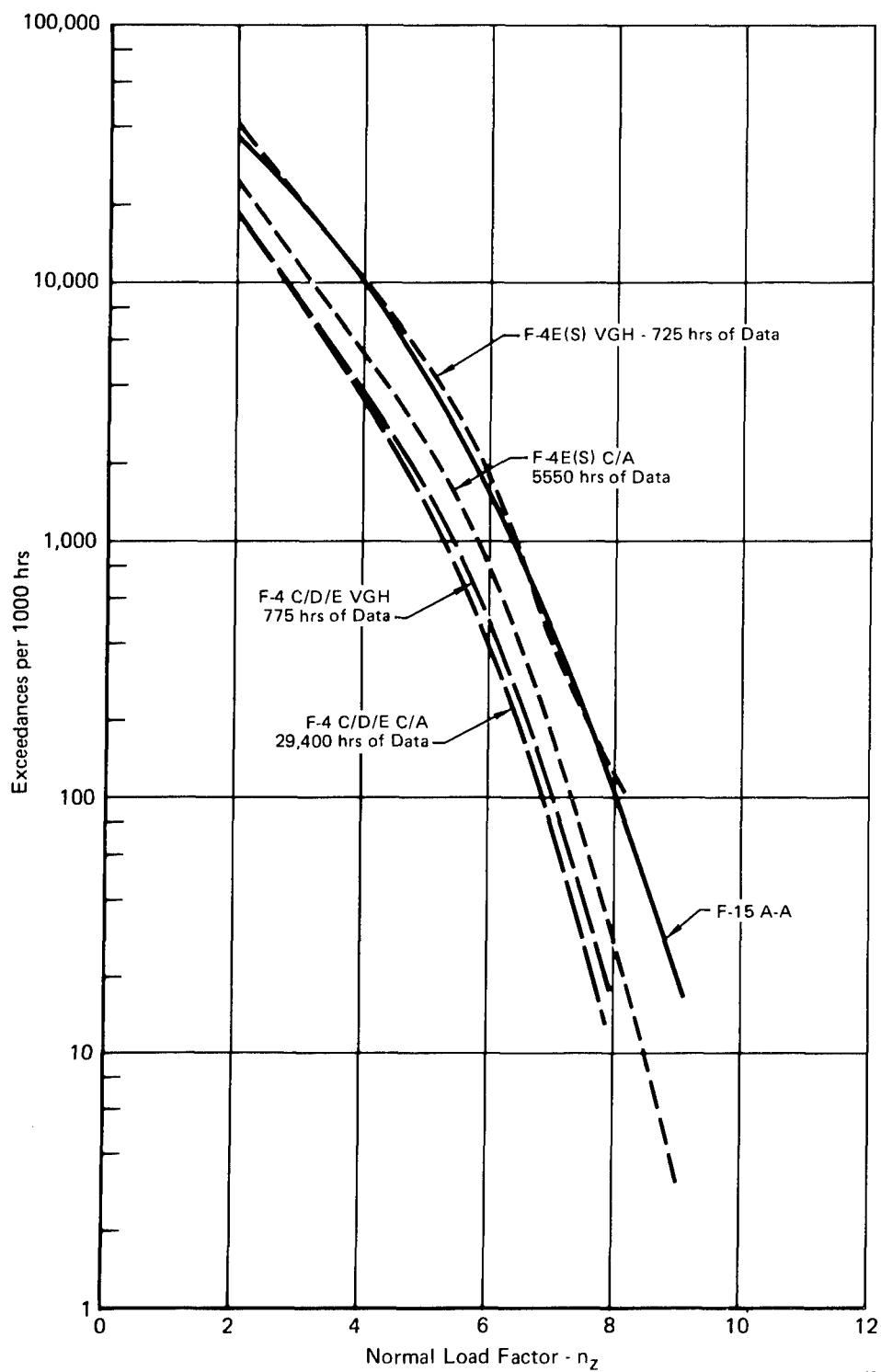


FIGURE 3. COMPARISON OF AIR-TO-AIR EXCEEDANCE CURVES

of the F-4E(S), its load factor frequency of occurrence is higher for A-A than for F-4C/D. The F-4E(S) data tends to approach the F-15 A-A curve. Load factor exceedance data from A-G missions also studied during the F-4C/D and the F-4E(S) ASIP programs are compared to the F-15 A-G load factor exceedance curves in Figure 4. All three aircraft have **similar load factor** exceedance curves for A-G where maneuvering capabilities would not be very important. The overall average curves for the three aircraft are compared in Figure 5.

## 2.2 Stress Exceedance Curves

In order to generate a spectrum for analysis and test, it is first necessary to convert load factor to stress at critical locations. Varying external loading distributions were defined for each flight condition by speed, altitude, gross weight, and airplane configuration with both symmetric and asymmetric maneuvers considered. These loading distributions were used with finite element models of the structure to predict stress at critical locations as a function of load factor for the different flight conditions. A typical prediction of stress for the lower wing skin is shown in Figure 6. Such data together with load factor frequencies were used to develop the baseline stress spectra for this study (Figure 7).

The baseline spectra and their variations generated for this program were defined by stresses at fatigue and fracture critical locations of the F-15 lower wing skin outboard of the manufacturing splice at B.L. 155, shown in Figure 8. The skin thicknesses in these areas range between .11 to .44 inches. The test specimens in this program have a .25 inch thickness. The alloy selected for this study was 7075-T73 because of its common use in the industry, ready availability, and availability of data required for crack growth analyses. The stress spectra developed for critical areas in the outer wing lower skin would be very nearly the same as stress spectra developed for an aluminum inner wing lower skin, spar, carrythrough bulkhead, etc.

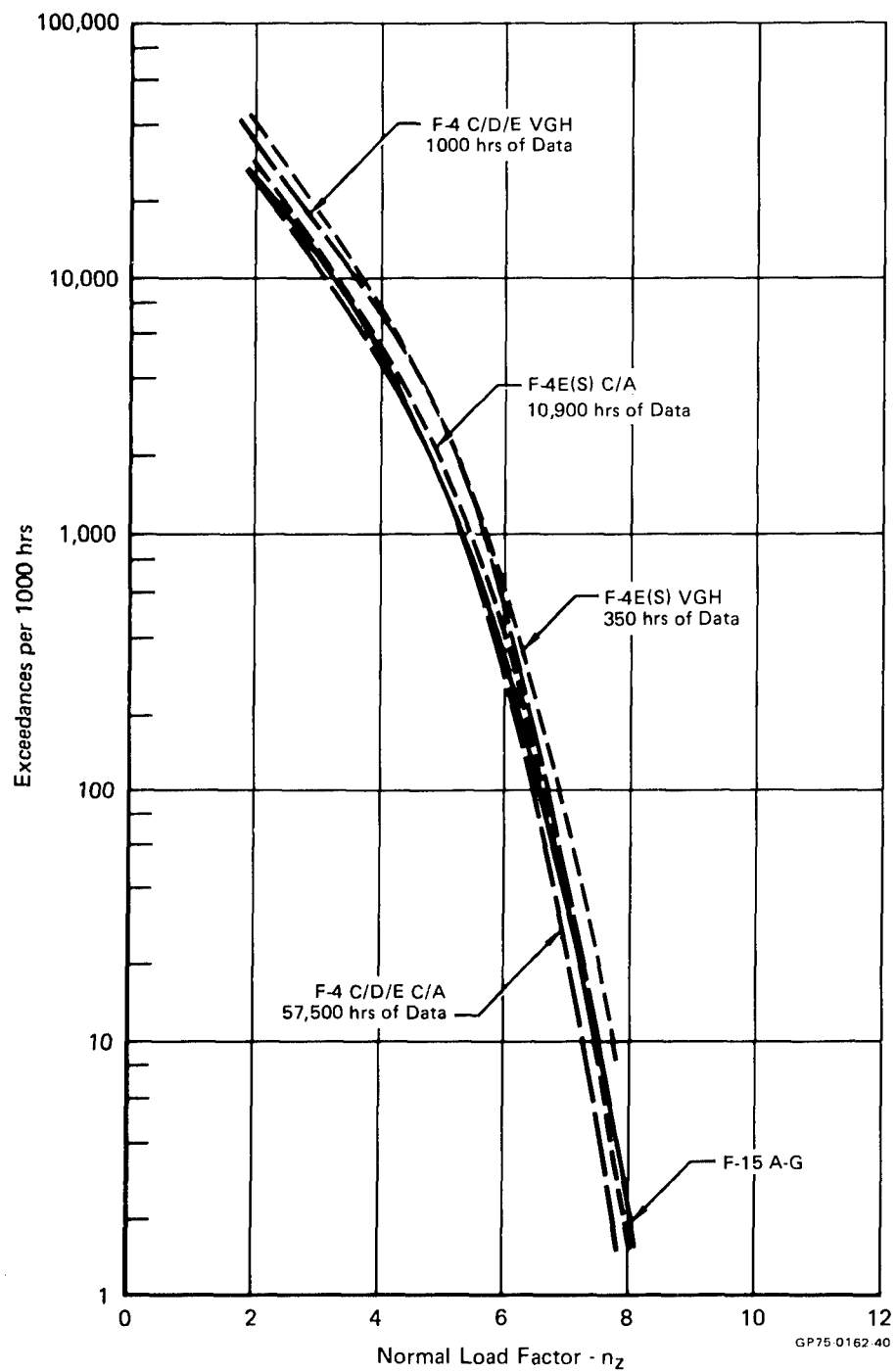


FIGURE 4. COMPARISON OF AIR-TO-GROUND EXCEEDANCE CURVES

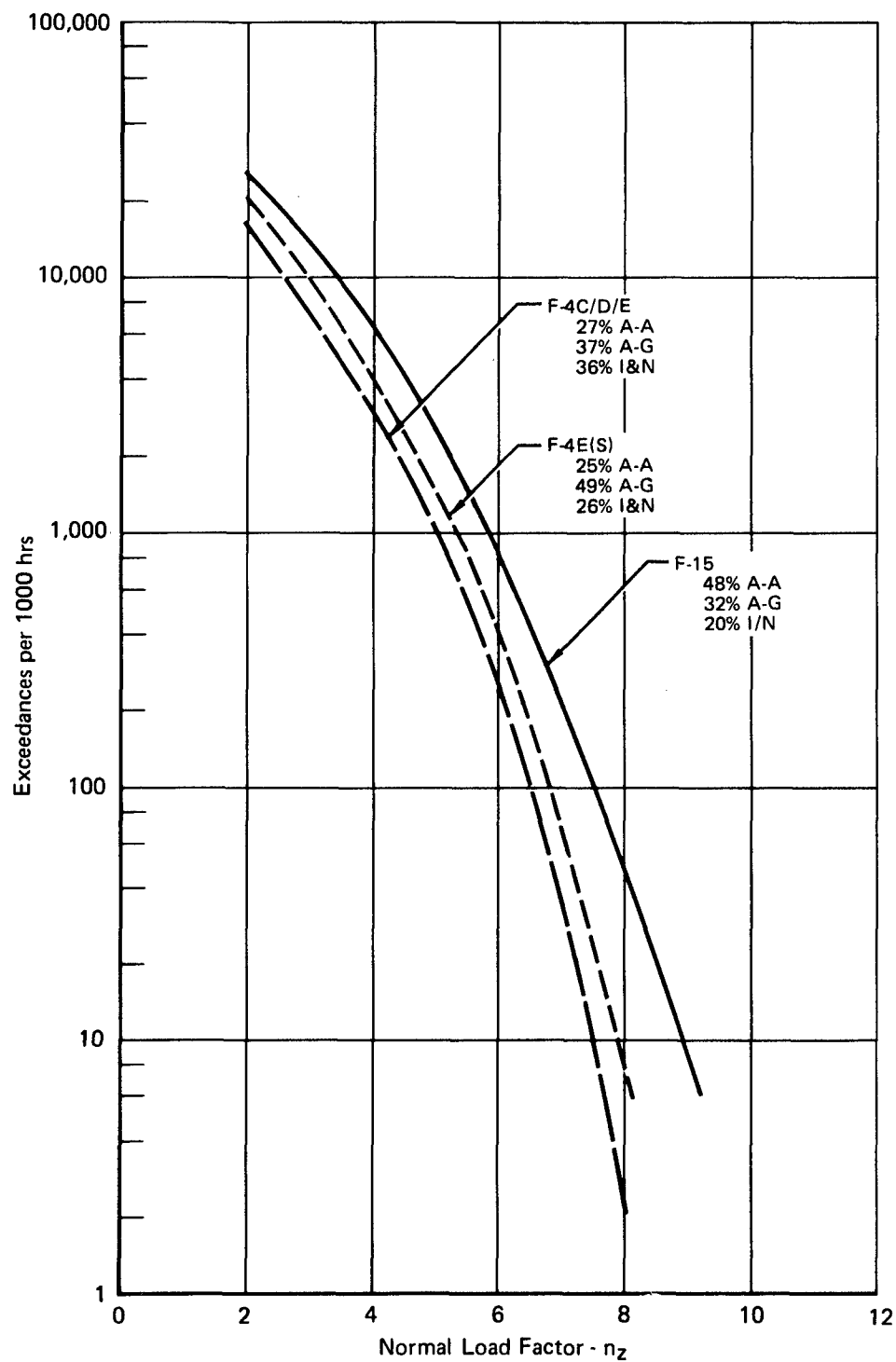
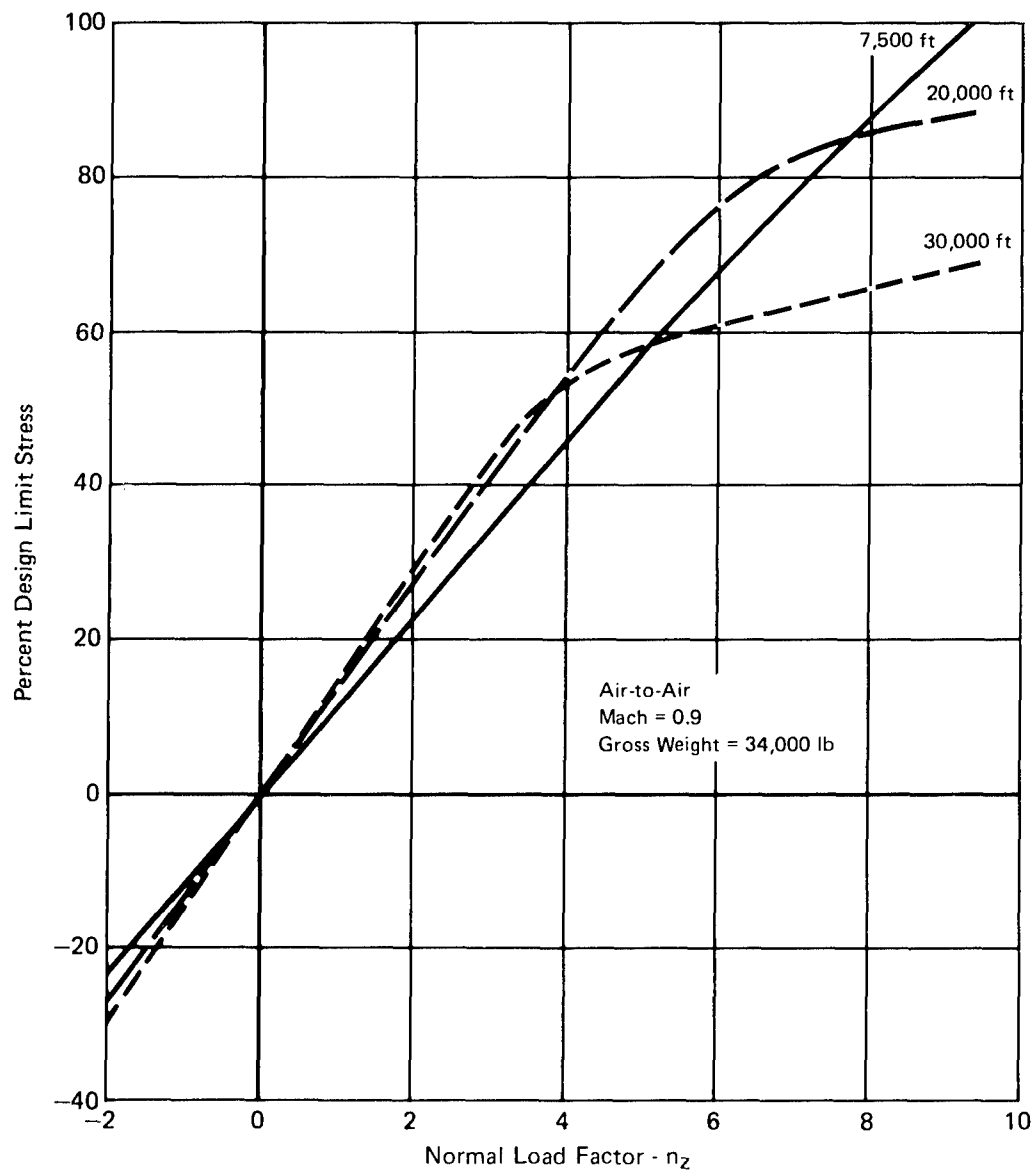


FIGURE 5. COMPARISON OF COMPOSITE EXCEEDANCE CURVES



GP75 0162 42

FIGURE 6. PERCENT DESIGN LIMIT STRESS vs NORMAL LOAD FACTOR

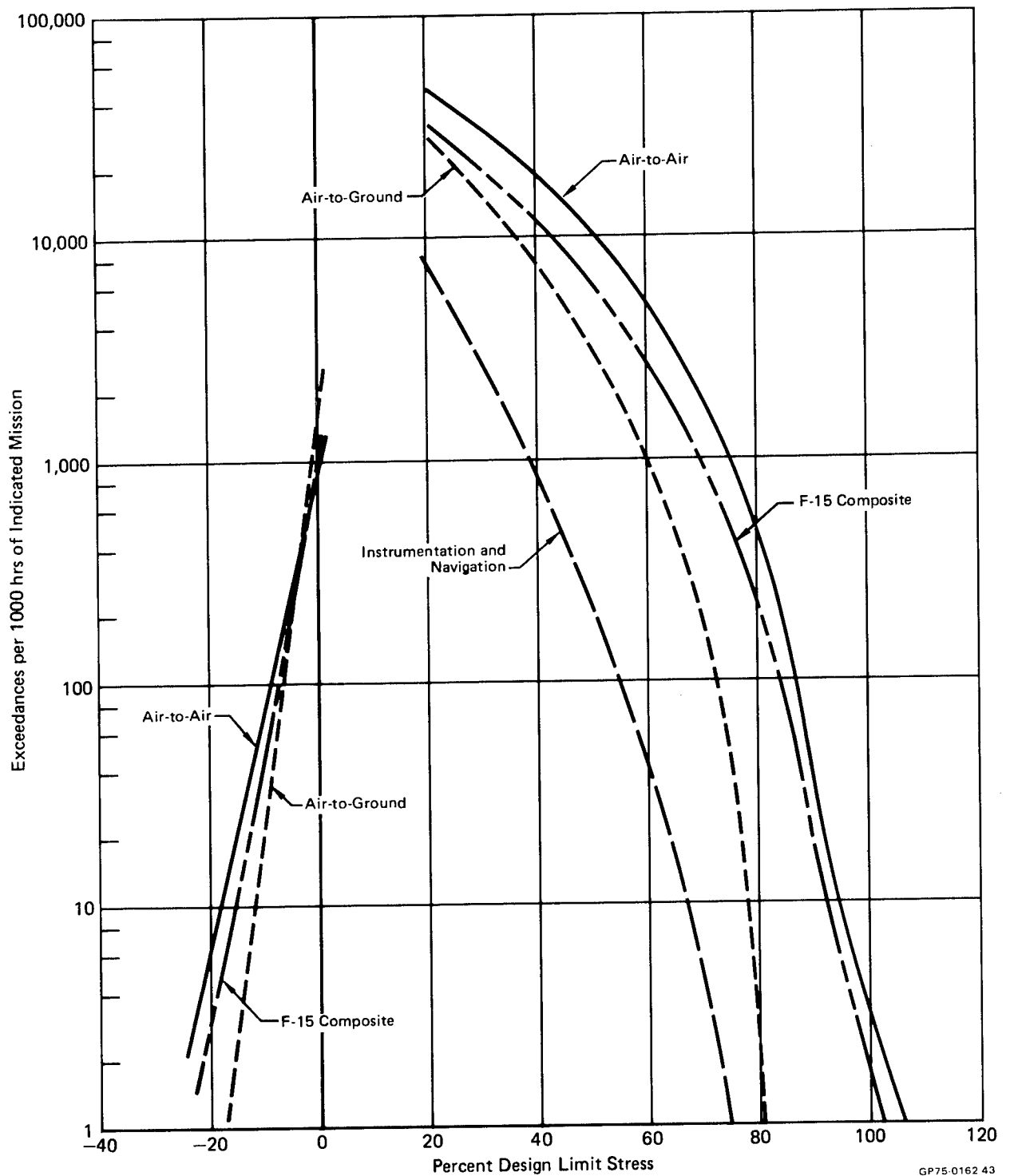
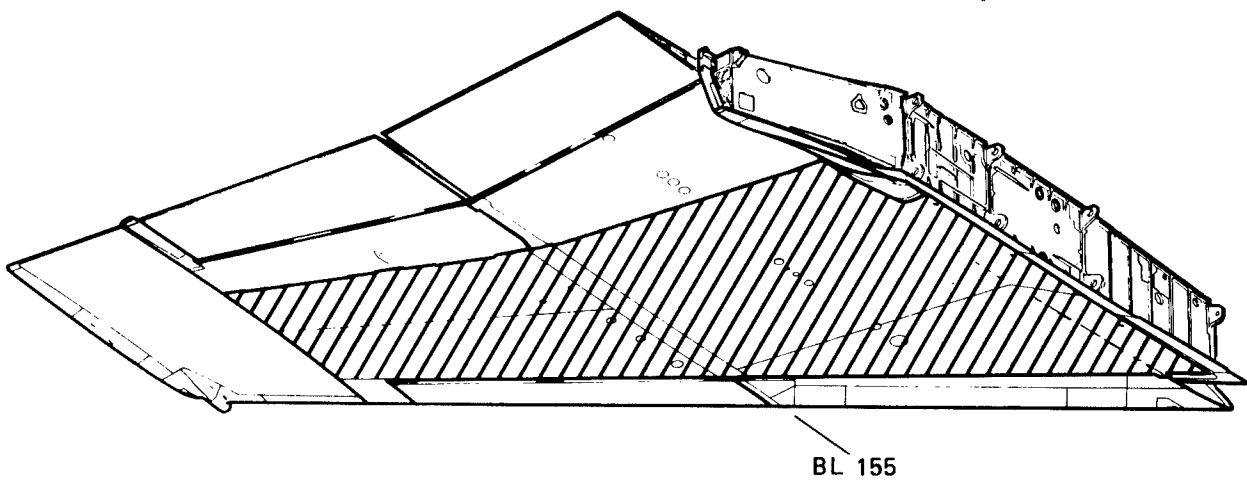


FIGURE 7. BASELINE STRESS SPECTRA





GP75-0162-44

**FIGURE 8. F-15 WING LOWER SKIN SELECTED AS STUDY BASE**

### 3. SPECTRUM DEVELOPMENT USING RANDOM NOISE THEORY

A common fault of arbitrary stress history simulation is unrealistic coupling of peaks and valleys. An advantage of the power spectral density (PSD) approach is that both the desired exceedance content and frequency content are preserved. The preservation of the frequency content assures that proper coupling of peaks and valleys is attained. Stress history simulations developed using the PSD approach appear similar to measured histories. The techniques used in developing stress history simulations using random noise theory are described in this section. The spectrum generation procedures are incorporated into two computer programs. The first program generates random histories for Air-to-Air, Air-to-Ground, and Instrumentation-and-Navigation baseline missions. The theory for this program is described in this section, and the program is described in Reference 1. The second program combines the appropriate histories, inserts the ground loads between missions, and perform the data management operations required to develop the Composite Baseline spectrum, and the spectra variations. This program is described in Reference 2.

#### 3.1 Random Noise Theory

If it is assumed that the  $x(t)$  on a given structural element is a stationary random function of time, the probability density function of  $x(t)$  is independent of time and defined as the probability that  $x(t)$  will fall within the range of  $x$  to  $x + dx$  at any instant in time. The shape of the history is governed by the frequency distribution of  $x(t)$ . The shape called narrow band in Figure 9 consists of variable amplitude cycles of very nearly the same frequency. The term narrow band refers to the limited frequency bandwidth existing in the history of  $x(t)$ . Similarly, the shape called wide band in Figure 9 also consists of variable amplitude cycles, but with a significant spread in the cyclic frequency. The term wide band refers to the generally unlimited frequency bandwidth existing in the history of  $x(t)$ .

The frequency distribution of  $x(t)$  which governs the shape of the history is specified by  $S(\omega)$ , the power spectral density of  $x(t)$ . It quantitatively defines the density of the mean square value of  $x(t)$  at any given frequency. The integration of this density, therefore, over the entire range of frequencies yields the mean square of  $x(t)$ . The power spectral densities for the histories in Figure 9 are presented in Figure 10. The mean square value of  $x(t)$  is given by the area under the Figure 10 curves. The square root of this area is the root mean square (RMS) value for  $x(t)$ . The mean square value of  $x(t)$  is called the autocorrelation function  $R(\tau)$  at  $\tau = 0$ . The autocorrelation function is determined from  $x(t)$  as follows:

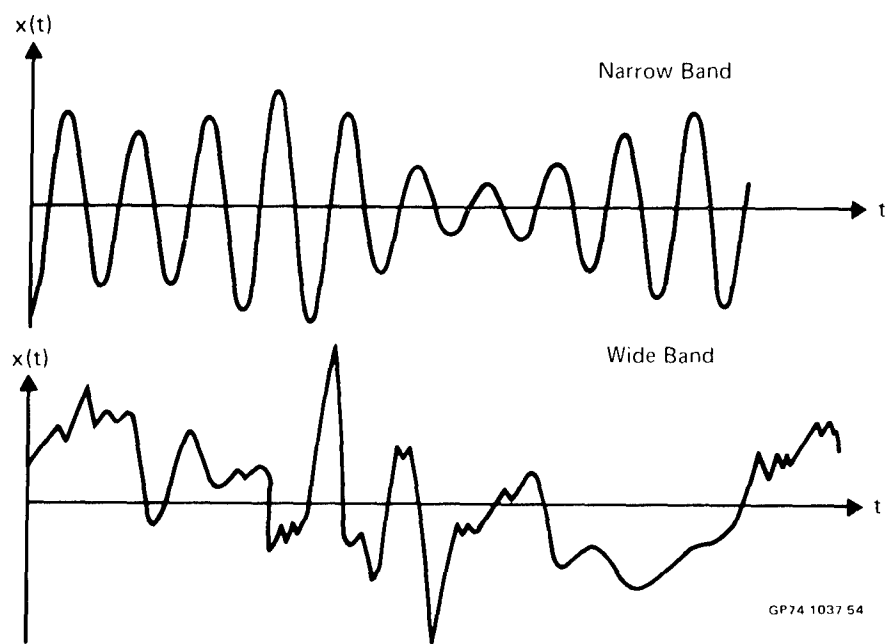


FIGURE 9. GAUSSIAN RANDOM NOISE HISTORIES

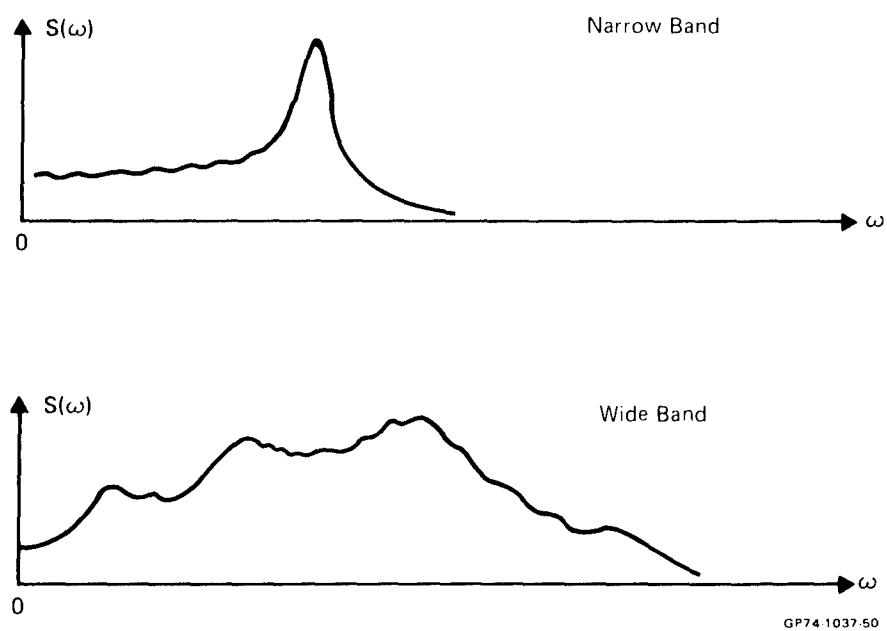


FIGURE 10. POWER SPECTRAL DENSITY vs FREQUENCY

$$R(\tau) = \lim_{T \rightarrow \infty} \frac{1}{T} \int_0^T x(t) x(t + \tau) dt \quad (1)$$

It follows from the equation above that  $R(\tau)$  evaluated at  $\tau = 0$  gives the mean square value of  $x(t)$ . The autocorrelation function and the power spectral density are related by the Fourier inversion formulae:

$$S(\omega) = 4 \int_0^\infty R(\tau) \cos(2\pi\omega\tau) d\tau$$

$$R(\tau) = \int_0^\infty S(\omega) \cos(2\pi\omega\tau) d\omega \quad (2)$$

If  $\tau$  is set equal to zero in the second equation above, it reduces to the integration of the power spectral density over the entire range of frequencies which is the mean square value of  $x(t)$  as stated above.

If the probability distribution of  $x(t)$  is Gaussian, the probability distribution of the maxima or peaks of  $x(t)$  will either be Gaussian, Rayleigh, or somewhere in between depending on the power spectral density of  $x(t)$ . In particular for a narrow band process, the probability density of the peaks is Gaussian. In terms of structural fatigue design criteria, the distribution of peaks is usually defined by cumulative peak exceedance curves. For a frequency distribution between the two extremes of narrow and wide band random noise, the cumulative peak exceedance  $N_x$  is given as follows:

$$N_x = N_p P(x/a\sigma) + N_o [1 - P(x/b\sigma)] e^{-x^2/2\sigma^2} \quad (3)$$

- where  $N_p$  = total number of peaks per unit time  
 $N_o$  = total number of zero (or mean level) crossings per unit time with positive slope  
 $P(x/a\sigma)$  = probability of exceeding  $x/a\sigma$  determined from a standard normal probability table  
 $\sigma$  = root mean square (RMS) of  $x(t)$   
 $a$  =  $\sqrt{1 - (N_o/N_p)^2}$   
 $b$  =  $a/(N_o/N_p)$

Typical theoretical exceedance curves developed using the equation above are shown in Figure 11. The curves are symmetrical about the mean. Actual exceedance curves are not symmetrical about the mean, therefore, the results

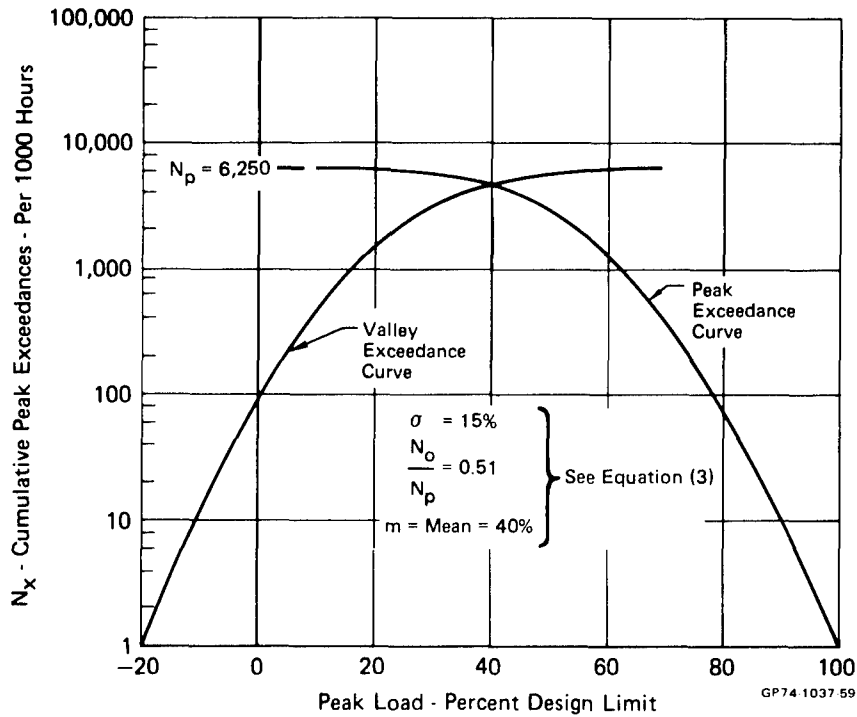


**FIGURE 11. TYPICAL GAUSSIAN EXCEEDANCE CURVES**

of the Gaussian generation process are modified to match the actual exceedance curves. This modification is described in Section 3.3.

The ratio  $N_o/N_p$  is sometimes called the irregularity factor. For  $N_o/N_p = 1$ ,  $a = b = 0$  and therefore  $P(x/a) = P(x/b) = 0$  which gives

$$N_x = N_p e^{-x^2/2\sigma^2} \quad (4)$$

which is the Rayleigh distribution; this distribution represents a narrow band process. Figure 9 demonstrates this since it is apparent that the number of peaks equals the number of zero crossings (with positive slope) for the narrow band history. For  $N_o/N_p = 0$ ,  $a = 1$  and  $b \rightarrow \infty$  and therefore  $P(x/b\sigma) = 1$  which gives

$$N_x = N_p P(x/\sigma) \quad (5)$$

which is the Gaussian distribution; this distribution represents a broad band process. Figure 9 also demonstrates this since it is apparent that the number of peaks is much greater than the number of zero crossings (with positive slope) for the broad band history. The calculation of  $N_o/N_p$  is based on the following equations:

$$N_o^2 = \frac{\int_0^{\infty} \omega^2 S(\omega) d\omega}{\int_0^{\infty} S(\omega) d\omega} \quad (6)$$

$$N_p^2 = \frac{\int_0^{\infty} \omega^4 S(\omega) d\omega}{\int_0^{\infty} \omega^2 S(\omega) d\omega} \quad (7)$$

The frequency distribution which governs the shape of the history is specified by the curve of power spectral density (PSD) versus frequency. In order to determine appropriate PSD versus frequency curves for fighter aircraft, actual load factor histories from F-4's were analyzed. A total of 5,658 seconds of air combat maneuvering training data and 15,675 seconds of air to ground combat maneuvering training data were included in the calculations. These data were digitized and then numerical techniques used to perform the integration specified in Figure 12 where  $x(t)$  represents a typical load factor history. The resulting PSD versus frequency curves for air to air maneuvering and air to ground maneuvering are shown in Figures 13 and 14, respectively.

#### Autocorrelation Function

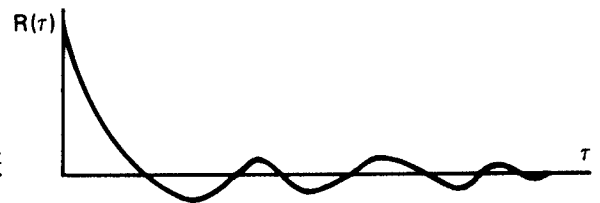
$$R(\tau) = \lim_{T \rightarrow \infty} \frac{1}{T} \int_0^T x(t) x(t + \tau) dt$$



Note: x is Variation from Mean

#### Power Spectral Density - PSD - G(f)

$$S(\omega) = 4 \int_0^{\infty} R(\tau) \cos 2\pi\omega\tau d\tau$$



GP74-1037-55

FIGURE 12. COMPUTATIONS FOR POWER SPECTRAL DENSITY

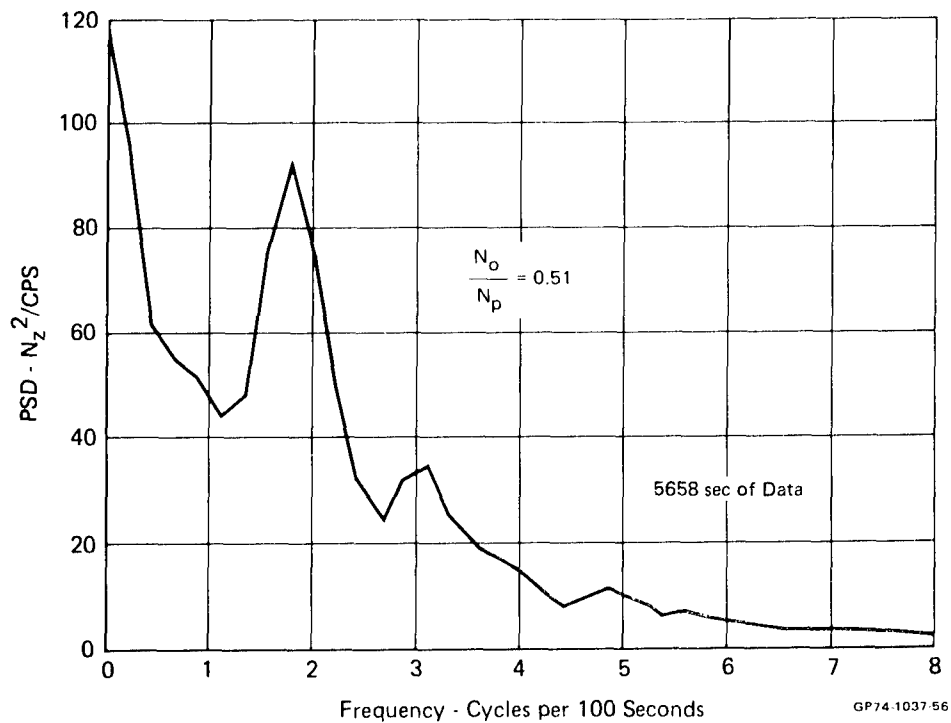


**FIGURE 13. POWER SPECTRAL DENSITY vs FREQUENCY  
AIR-TO-AIR TRAINING DATA**

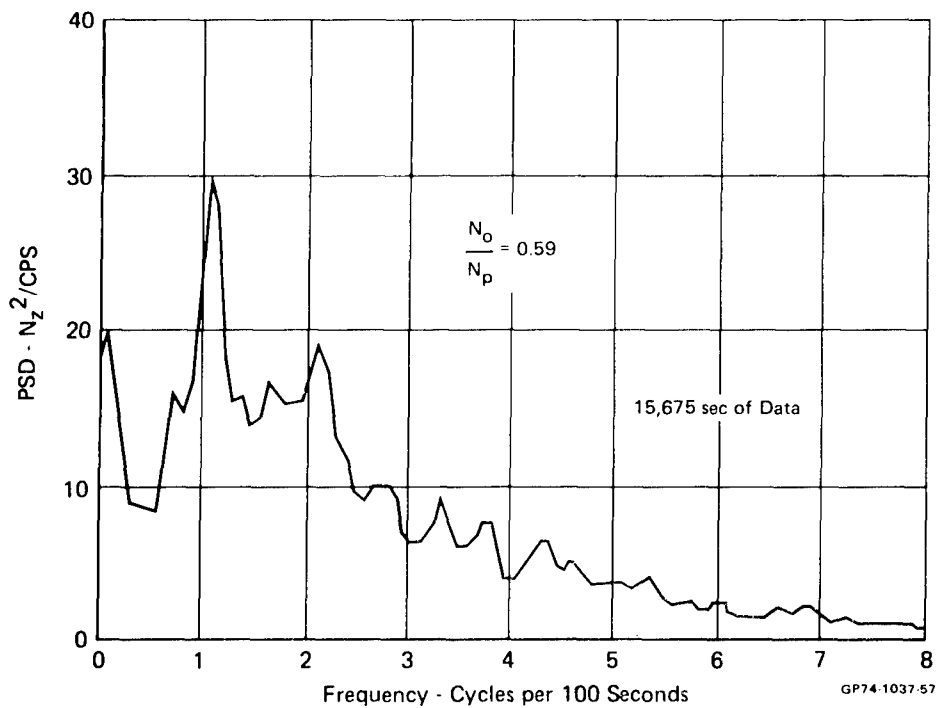


**FIGURE 14. POWER SPECTRAL DENSITY vs FREQUENCY  
AIR-TO-GROUND TRAINING DATA**

### 3.2 Gaussian Process Simulation

The basic equation used in forming the random load history is

$$x(t) = \sqrt{2} \sum_{K=0}^{N-1} D_K \cos (2\pi\omega_K t + B_K) \quad (8)$$

where  $x(t)$  = Stress, a function of time

$D_K$  = Amplitude of cosine series term, defined in Figure 15.

$\omega_K$  =  $K\Delta\omega$

$N$  =  $\omega_U/\Delta\omega$ ,  $\omega_U$  = Upper limit of frequency of PSD

$B_K$  = Random number uniformly distributed between 0 and  $2\pi$

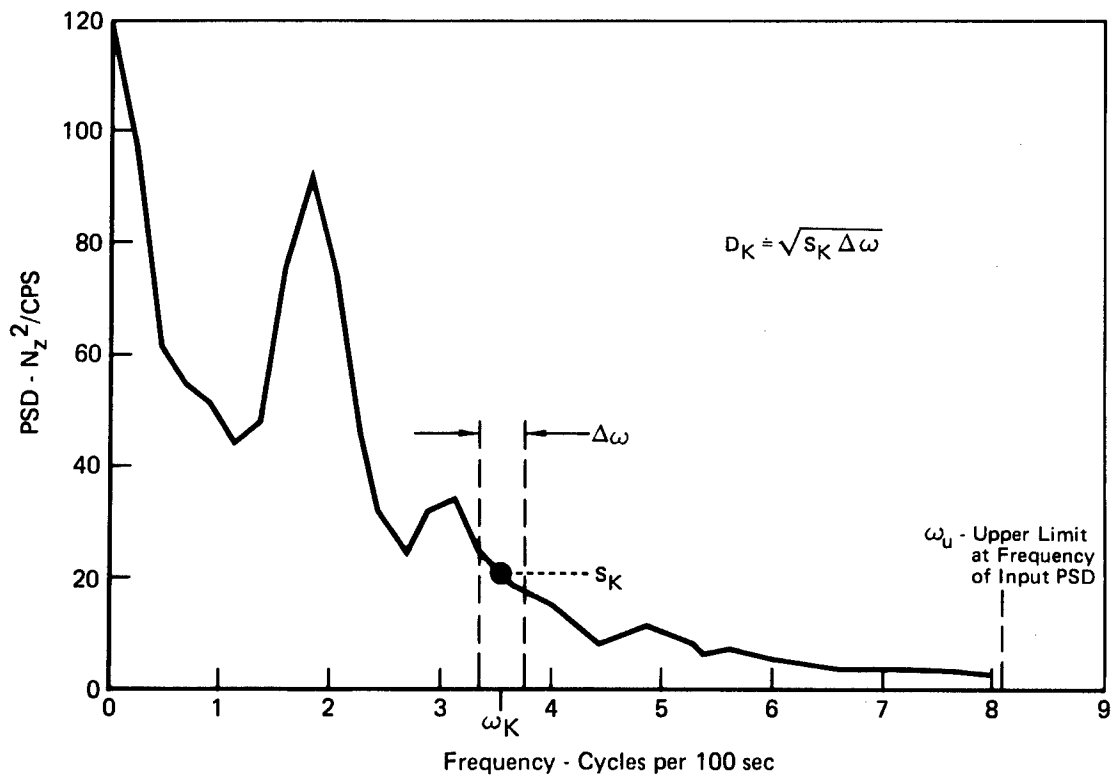


FIGURE 15. POWER SPECTRAL DENSITY USED IN RANDOM STRESS HISTORY GENERATION



Making the substitution  $D_K = \sqrt{S_K \Delta \omega}$ , and assuming  $\Delta \omega$  is constant throughout the summation described by Equation (8), that equation can be re-written

$$x(t) = \sqrt{2\Delta\omega} \sum_{K=0}^{N-1} \sqrt{S_K} \cos(2\pi \omega_K t + B_K) \quad (9)$$

Rather than solving this equation directly, considerable efficiency is attained by use of the Fast Fourier Transform (FFT) as outlined in Reference 3. In order to use the FFT, Equation (9) is expressed in complex notation.

$$x(t) = \sqrt{2\Delta\omega} \operatorname{Re} \sum_{K=0}^{N-1} \sqrt{S_K} e^{iB_K} e^{i2\pi \omega_K t} \quad (10)$$

The FFT computes  $N$  points in the random history for  $N$  input values of  $A_K$ , as described by Equation (11),

$$x_J = \sum_{K=0}^{N-1} A_K e^{\frac{2\pi i}{N} JK} \quad J = 0, 1, \dots, N-1 \quad (11)$$

$J$  represents time,  $t$

$K$  represents frequency,  $\omega_K$

$$t = \text{time} = J/\omega_u \quad J = t \times \omega_u \quad (12)$$

$$\omega_K = \text{frequency} = \frac{K \times \omega_u}{N} \quad K = \frac{\omega_K}{\omega_u} \times N \quad (13)$$

$$\text{Total time} = N/\omega_u \quad (14)$$

In terms of the PSD input

$$\operatorname{Re} A_K = \sqrt{2\Delta\omega} S_K \cos B_K \quad (15)$$

$$\operatorname{Im} A_K = \sqrt{2\Delta\omega} S_K \sin B_K \quad (16)$$

where  $\Delta\omega = \omega_u/N$

In summary,

- o "N" values of PSD ( $S_K$ ) are determined from the PSD curve corresponding to  $K = 0, 1, \dots, N-1$
- o "N" random phase angles ( $B_K$ ) between 0 and  $2\pi$  are generated.
- o An array of  $N$  complex coefficients,  $A_K$ , are calculated as shown in Equations (15) and (16)
- o The Fast Fourier Transformation is used to generate a history of  $N$  values of stress  $x_t$ , as defined by Equation (11).

Random Number Generation - The generation of the random stress history requires the generation of random numbers uniformly distributed between 0 and  $2\pi$ , as described by Equations (15) and (16). This can be accomplished by using the power residue method, as outlined in Reference 4. In simplest terms, the method uses the remainder of a division as the next random number, as outlined by Equation (17).

$$\frac{2^K}{S \times \text{Random Number}_I} = \text{Quotient} + \text{Remainder} \quad (17)$$

$$\text{Random Number}_{I+1} = \text{Remainder}$$

where S and K are integers.

A sequence generated in this manner will be uniformly randomly distributed over the interval 1 to  $2^K$ . The procedure for generating the random numbers is as follows.

- (a) Choose for a starting value any odd integer  $N_1$
- (b) Choose as a constant multiplier an integer S of the form

$$S = 8T + 3$$

where T is any integer. A value of T close to  $2^{K/2}$  is a good choice.

- (c) Compute  $S \times N_1$
- (d) Find the remainder of  $2^K / (S \times N_1)$
- (e) Random number  $N_2$  = remainder from the subsequent step (d). Return to step (c), replacing  $N_1$  with  $N_2$ .

In the computer program described in Reference 1,  $K = 20$  and  $S = 1029$ . The value of  $2^{20} = 1,048,576$ . Equation (17) then becomes

$$\frac{1,048,576}{1,029 \times \text{Random Number}_I} = \text{Quotient} + \text{Remainder} \quad (18)$$

$$\text{Random Number}_{I+1} = \text{Remainder}$$

The random number generated is uniformly distributed between 1 and 1,048,576, to acquire a random number uniformly distributed between 0 and  $2\pi$ , the random number generated by Equation (18) is multiplied by  $2\pi/1,048,576 = 1/166886$ . This procedure will produce  $2^{K-2} = 262,144$  terms before repeating and can be used on any computer with the capability of storing a number equal to  $2^{31}$  or larger.

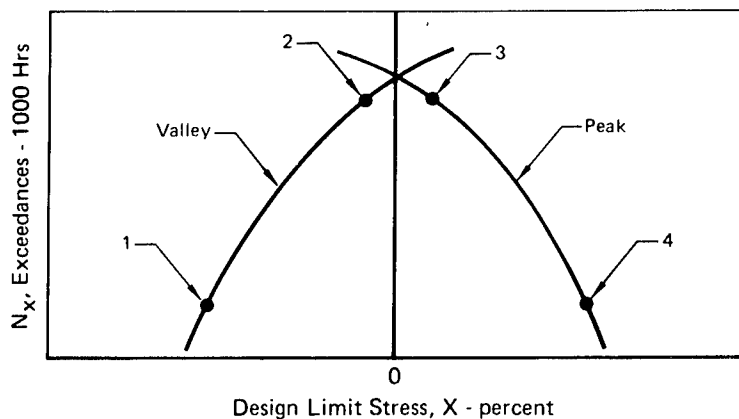
### 3.3 Mapping of Gaussian History to Real History

The exceedance curve for a Gaussian random history is symmetrical with zero mean, as depicted in Figure 16. Actual exceedance curves are **asymmetrical** with a non-zero mean. Gaussian random histories are adjusted so that exceedance curves are matched. This is accomplished using the transformations:

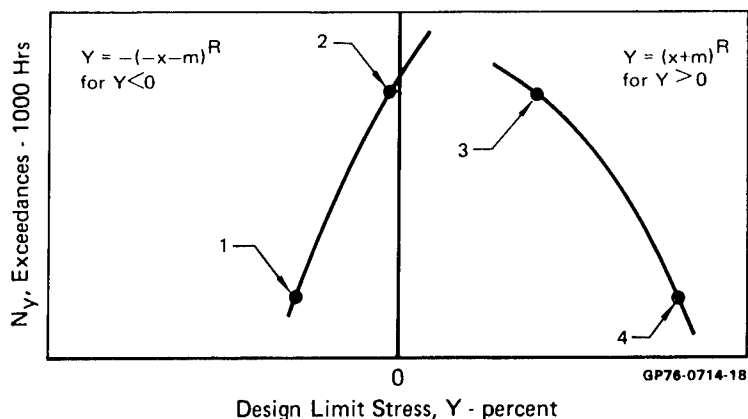
$$y = (x + M)^R \quad \text{for positive } x + M \quad (19)$$

$$y = -(-x - M)^R \quad \text{for negative } x + M \quad (20)$$

Numbered points are used to transform the Gaussian data to the actual process



Exceedance Curve for Gaussian Random Time History is Symmetrical with a Zero Mean



Actual Exceedance Curves are Non-Symmetrical with a Non-Zero Mean

FIGURE 16. COMPARISON OF EXCEEDANCE CURVES

$$\text{and conversely, } x = y^{1/R} - M \quad \text{for positive } y \quad (21)$$

$$x = -(-y)^{1/R} - M \quad \text{for negative } y \quad (22)$$

where  $x$  = load factor for Gaussian process

$y$  = load factor for actual process

$M$  = Mean level for actual curve

$R$  = Transformation coefficient

Equation (3) describes the exceedance curve for the Gaussian process. This equation also describes the exceedance curve for the actual process when the substitutions indicated by Equations (21) and (22) are performed. The values  $M$ ,  $R$ ,  $N_p$  and  $\sigma$  are unknowns, and are determined by a trial and error process. Using the actual exceedance curves, two points on the valley curve and two points on the peak curve are selected. This results in four sets of values of  $N$  and  $y$ . By using Equation (3) in combination with Equations (21) and (22), four non-linear simultaneous equations can be written, relating  $N$  and  $y$  with  $M$ ,  $R$ ,  $N_p$ , and  $\sigma$  as the unknowns.

### 3.4 Rise and Fall Counting

Counting accelerometers and VGH recorders are the primary instruments for measuring the load experience of fighter aircraft, summarized in exceedance tables. This exceedance data, obtained from measured flight accelerations, has a rise and fall counting criterion applied. For example, VGH recorders require from .4g to 1.2 g's rise and fall, depending on the g level, before the peak or valley is counted. The significance of the rise and fall counting requirement is indicated in Figure 17. Peaks and valleys were counted with no rise and fall requirement, and with a 10% Design Limit Stress (DLS) rise and fall requirement for the Air-to-Air Baseline spectrum generated in this program, using the PSD generation process. Figure 17 indicates there is a significant number of very small amplitude cycles with a range less than 10% DLS. The F-4 data studied to obtain PSD versus frequency curves indicate that these low amplitude cycles do actually occur in flight. One spectra variation studied in this program was the inclusion of numerous low load levels to the Air-to-Air and Composite Baseline spectra; analysis indicates there is little effect on crack growth with the addition of these load levels.

All of the spectra generated in this program were developed with a 10% DLS rise and fall requirement, with the previously noted exceptions.

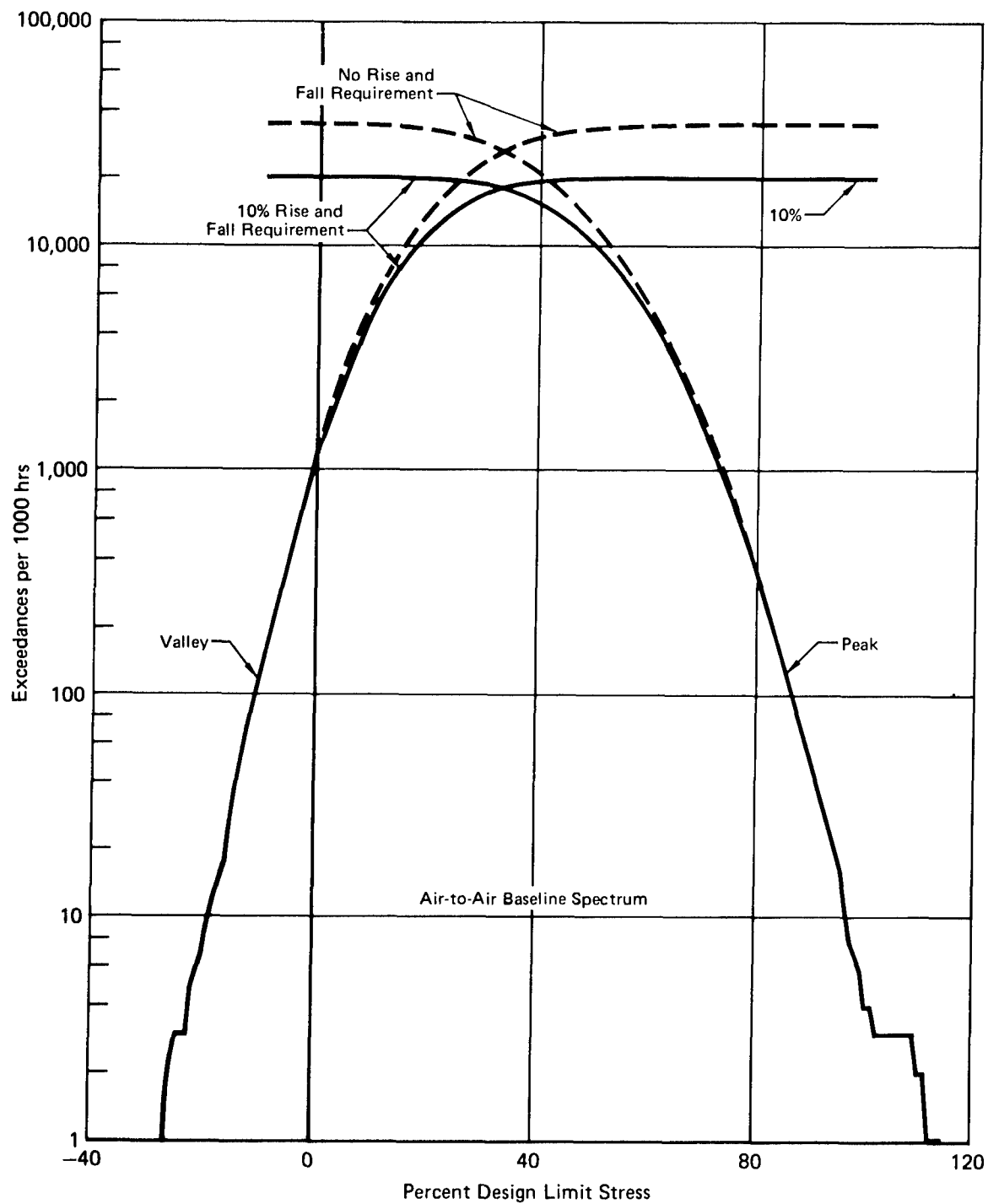
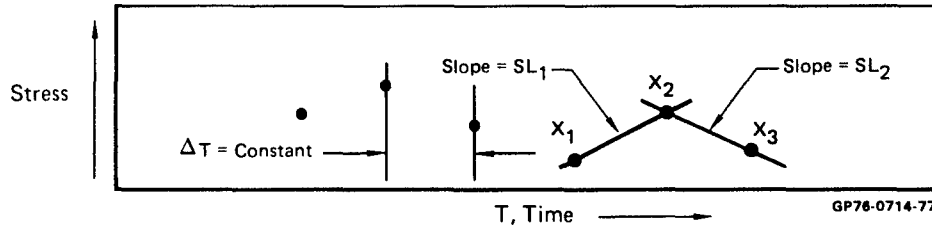


**FIGURE 17. EFFECT OF RISE AND FALL REQUIREMENT  
FOR PEAK AND VALLEY COUNTING**

### 3.5 Search for Peaks and Valleys

The history generated by Fast Fourier Transform, outlined in Reference 3, results in a series of stress values at constant time intervals, as depicted in the following sketch. The presence of a peak or valley is



detected when there is a difference in sign of slope between two consecutive sets of values. The value of the peak or valley is determined by assuming a quadratic relation of the form,

$$x = a + bt + ct^2 \quad (23)$$

Setting  $\Delta t = \text{unity}$  and using known values of  $x_1$ ,  $x_2$  and  $x_3$ , three equations can be written

$$x_1 = a \quad (24)$$

$$x_2 = a + b + c \quad (25)$$

$$x_3 = a + 2b + 4c \quad (26)$$

Solving for  $a$ ,  $b$ , and  $c$

$$a = x_1 \quad (27)$$

$$b = \frac{-3}{2} x_1 + 2 x_2 - \frac{1}{2} x_3 = \frac{1}{2} (3SL_1 - SL_2) \quad (28)$$

$$c = \frac{1}{2} x_1 - x_2 + \frac{1}{2} x_3 = \frac{1}{2} (SL_2 - SL_1) \quad (29)$$

The peak (or valley) is determined from

$$dx/dt = b + 2ct = 0$$

$$t_{\text{peak or valley}} = \frac{-b}{2c} = \frac{SL_2 - 3SL_1}{2SL_2 - 2SL_1} \quad (30)$$

$$x_{\text{peak or valley}} = a - \frac{b^2}{2c} + \frac{b^2 c}{4c^2} = a - \frac{b^2}{4c} \quad (31)$$

where a, b and c are obtained from Equations (27), (28), and (29).

The stress history generated with this procedure contains the sequence of peak and valley stresses and the time at which each peak and valley occurs. For this study, the effects of the sequence of peaks and valleys were of interest and the generated times were not used.

#### 4. CRACK PROPAGATION ANALYSIS METHODS

##### 4.1 Selection of Analysis Method

Since the advent of Wheeler's model for computing load interaction effects on crack growth behavior, Reference 5, many models have been proposed to predict spectrum crack growth; Willenborg, et al, Reference 6, Vroman, Reference 7, Porter, Reference 8, Elber, Reference 9, Generalized Closure (Grumman), Reference 10, and Contact Stress, Reference 11. These models fall into two general categories: yield zone models, which assume that the residual stress field ahead of the crack tip controls load interaction effects, and closure models, which assume that stresses arising from crack surface contact control the load interaction effects. The grouping of the models into these categories is shown in Table 1. The Wheeler, Porter and Generalized Closure Models are all semi-empirical, and require substantial spectrum testing in order to obtain accurate predictions. These models were therefore considered unacceptable for performing this program.

The Willenborg, et al, Model as generalized by Gallagher and Hughes, Reference 12, was the primary model used for crack propagation analysis and test spectrum selection. This model represents advanced state-of-the-art in yield zone models and accounts for cycle-by-cycle load interaction effects such as overall crack growth retardation following a single overload, and cessation of crack growth following severe overloads. Results obtained from the Willenborg Model are equivalent or superior to those obtained from other published yield zone models. However, this model does not adequately account for interaction effects of compressive loads with overloads, effects of sequenced blocks, i.e., low-high, high-low, delayed retardation, and increased retardation following multiple overloads, as described in References 13 and 14. The Contact Stress Model can account for these effects as discussed in Reference 11. Therefore, the Contact Stress Model was used in support of the generalized Willenborg Model to evaluate spectra in which these effects were expected to dominate crack growth behavior and to provide additional insight for test spectrum selection and justification. The Contact Stress Model is being continuously developed, and early predictions were made with a preliminary model. During the performance of this study, an improved version of the Contact Stress Model was developed which was shown to accurately account for compression load interactions, Reference 15, and to be cost competitive with the Willenborg Model. Analyses performed with this model, Contact Stress Model II, showed that a closure model could provide good correlation with the test results. Descriptions of these models are provided in the following sections.



**TABLE 1. CHRONOLOGICAL SUMMARY OF SPECTRUM CRACK GROWTH MODELS**

Yield Zone Models		Closure Models	
Model	Approx Date	Model	Approx Date
Wheeler*	1970	Elber	1969
Willenborg, Engle, Wood	1971	Generalized* Closure	1974
Vroman	1971	Contact Stress	1975
Porter*	1971		
Gray (Generalized Wheeler)*	1973		
Gallagher and Hughes (Generalized Willenborg)	1974		

\* These models are semi-empirical.

GP75 0162 45

#### 4.2 Willenborg Model

The original Willenborg Model was developed to describe crack growth retardation following high-low block loadings. It is based on observations of the following phenomena:

- (1) retarded crack growth occurs whenever the maximum applied stress intensity is reduced,
- (2) such retardation is directly related to the reduction in maximum stress intensity,
- (3) the length over which crack growth is retarded, i.e., load interaction zone, is proportional to the plastic zone created by the maximum stress intensity,
- (4) there is no retardation of growth if the current maximum stress creates a load interaction zone which extends out to or beyond a previously established interaction zone.

Based on these observations, Willenborg, et al, assumed that the load interaction effects were caused by variations in local stress intensity as the crack grows through the residual stress field produced by the overload(s).

Mathematically, the effective stress intensity is defined by Willenborg in Reference 6 as:

$$K_{eff} = K^{\infty} - K_{RED} \quad (32)$$

$$K_{RED} = K_{max}^{OL} \left(1 - \frac{\Delta a}{z_{OL}}\right)^{1/2} - K_{max}^{\infty} \quad (33)$$

where  $K^\infty$  is the applied stress intensity,  $K_{RED}$  is the additional stress intensity required to extend the current interaction zone to that created by the overload,  $\Delta a$  is the growth following the overload, and  $z_{OL}$  is the overload interaction zone size. The effective stress intensity range and stress ratio are computed as,

$$\Delta K_{eff} = K_{eff}^{max} - K_{eff}^{min} = K_{max}^\infty - K_{RED} - (K_{min}^\infty - K_{RED}) = \Delta K^\infty \quad (34)$$

$$R_{eff} = \frac{K_{eff}^{min}}{K_{eff}^{max}} = \frac{K_{min} - K_{RED}}{K_{max} - K_{RED}} \quad (35)$$

Thus, as noted by Gallagher in Reference 16, the Willenborg Model predicts retardation by depressing the effective stress ratio below that remotely applied while leaving the stress intensity range intact. Since  $K_{RED}$  decreases as the crack grows through the overload interaction zone, the Willenborg Model predicts that the maximum retardation will occur just after the overload and that the growth rate will return to constant amplitude when the current interaction zone extends to the end of the overload interaction zone.

Due to the dependence of the Willenborg retardation on effective stress ratio and because the model does not inherently account for stress ratio effects, a crack growth rate equation which interrelates the influence of stress ratio with stress intensity range must be used. In this study, the Forman equation, Reference 17, was used to correct constant amplitude data obtained with a zero stress ratio. This equation can be written as,

$$\frac{da}{dN} = \left. \frac{da}{dN} \right|_{R=0} \times \left[ \frac{K_C - \Delta K^\infty}{(1-R) K_C - \Delta K^\infty} \right] \quad (36)$$

This equation was used in obtaining the results presented in Figure 18, the results indicate the equation accurately predicts constant amplitude stress ratio effects.

The Willenborg Model predicts zero maximum stress intensity, or shut off, when the overload ratio (ratio of overload stress intensity to maximum constant amplitude stress intensity) is two, that is, when  $K_{RED}$  equals  $K^\infty$  in Equation (32). This can be shown by rewriting (32) for the maximum effective stress intensity as,

$$K_{max}^{eff} = K_{max}^\infty - \left[ K_{max}^{OL} \left( 1 - \frac{\Delta a}{z_{OL}} \right)^{1/2} - K_{max}^\infty \right] \quad (37)$$

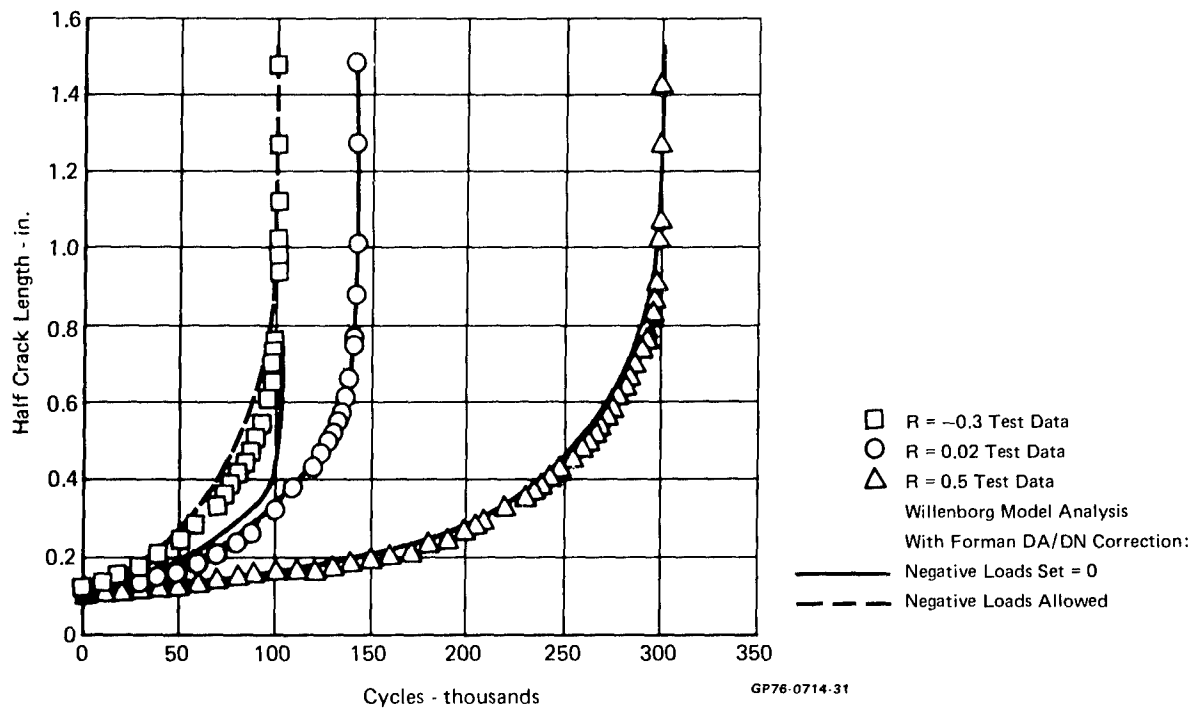


FIGURE 18. WILLENBORG MODEL CORRELATION  
WITH CONSTANT AMPLITUDE TEST DATA

where  $K_{\max}^{OL}$  is the maximum overload stress intensity,  $\Delta a$  is growth following overload and  $z_{OL}$  is overload interaction zone size. Immediately following the overload,  $\Delta a$  is usually very close to zero so that  $K_{\max}^{eff}$  is zero when  $K_{\max}^{OL}$  is twice  $K_{\max}$ . Test results obtained by several investigators, References 12, 18, and 19, show that the actual crack growth shut-off ratio can be somewhat greater than two.

Gallagher and Hughes, Reference 12, generalized the Willenborg, et al, Model to correct prediction of the overload to maximum load ratio required to produce cessation of crack growth. They proposed modifying Equation (37) so that for  $R = 0$ ,

$$K_{\max}^{eff} = K_{\max}^{\infty} - \phi_1 \left[ K_{\max}^{OL} \left( 1 - \frac{\Delta a}{z_{OL}} \right)^{1/2} - K_{\max}^{\infty} \right] \quad (38)$$

When shut-off occurs,  $\Delta a = 0$  and  $K_{\max}^{eff} = K_{\max TH}^{eff}$  (threshold stress intensity) so that,

$$\phi_1 = \frac{1 - \frac{K_{\max TH}}{K_{\max}^{\infty}}}{\frac{K_{\max}^{OL}}{K_{\max}^{\infty}} - 1} \quad (39)$$

where the shut-off overload ratio must be obtained from test for given material and thickness.

Gallagher and Hughes used the generalized model quite successfully to predict the number of cycles required to return to constant amplitude growth rate following an overload in two steels having different yield strengths. Gallagher and Stalnaker, Reference 20, also used the generalized model to predict magnitude and trends of crack growth rate data generated under transport-wing simulation loading. The correlation of test and analysis was significantly improved over that of the original model.

The generalized Willenborg Model, including a Forman-type crack growth rate equation, represents the advanced state-of-the-art in development of yield zone models. While significantly improved by recent developments, it does not account for

- delayed retardation following single and multiple overloads,
- increased retardation following multiple overloads as compared with single overload, and
- interaction effects of compression loads.

The computer routine for the generalized Willenborg Model was extracted from the Air Force's CRACKS II computer program, Reference 21. The stress intensity range in that routine was redefined to be that from  $K_{\min}^{eff}$  to  $K_{\max}^{eff}$ , the effective loading range. The applied stress intensities included both finite width effects and effects of single crack growth from a hole. The finite width correction included the effect of eccentricity caused by crack growth from one side of the hole. The stress intensity factors were computed according to the following equations.

$$K = \lambda_1 \lambda_2 \sigma \sqrt{\pi a} \quad (40)$$

where  $\sigma$  is the remote stress,  $a$  is the crack depth from the hole,  $\lambda_1$  is the finite width correction, and  $\lambda_2$  is the Bowie single crack correction. Then,

$$\lambda_1 = \left[ \left( \frac{W(W-a)}{2a(d+a)} \right) \cos \left( \frac{\pi r}{W} \right) \sec \left( \frac{(d+a)}{2(W-a)} \right) \sin \left( \frac{2a(d+a)}{W(W-a)} \right) \right]^{1/2} \quad (41)$$

and

$$\lambda_2 = 0.6762062 + (0.8733015 / (0.3245442 + \frac{a}{r})) \quad (42)$$

where  $r$  is the hole radius,  $d$  is the hole diameter, and  $W$  is the plate width.

#### 4.3 Contact Stress Model

Since Elber first measured crack closure at stress levels greater than the minimum applied stress, Reference 9, and hypothesized that this effect was due to permanent deformation of the crack surfaces during crack growth, many investigators have verified the existence of residual deformations and closure or have used closure concepts to explain crack growth phenomena, References 18, 22 thru 31. The Contact Stress Model was developed to evaluate the effect of residual deformations of the crack surface on the stress intensity range effective in propagating the crack. The model is used to determine the effect of crack surface contact on the stress intensity range felt by the crack tip rather than to compute either closure, i.e., the stress level at which the crack surfaces first come into contact during unloading, or opening, i.e. that stress level at which the surfaces become free of contact during the loading cycle.

The Contact Stress Model predictions are based on evaluations of the effective maximum and minimum stress intensity factors occurring during a load cycle. An analysis of crack tip displacements during loading and unloading is used to determine the permanent plastic deformation left in the wake of a growing crack. Contact stresses caused by interference of these permanent deformations at maximum and minimum loads are determined by treating the interference as a wedge between the crack surfaces and performing an elastic-plastic analysis of stresses caused by the wedge. The effective stress intensity factor is the sum of the applied stress intensity factor and the stress intensity factor due to these contact stresses. Because the permanent deformations left in the wake of the growing crack preserve a memory of all previous load cycles, the interference, and consequently the effective stress intensity factor range, contains the effects of the total load history. Thus, analyses of crack surface contact can account for many of the observed details of crack growth behavior.

Comparison with test and a more detailed description of the model are included in Reference 11. The comparisons therein show that the Contact Stress Model can accurately account for the effects of stress ratio, delayed retardation, increased retardation following multiple high loads, and acceleration during high loads.

#### 4.4 Contact Stress Model-II

Improvements were made on the Contact Stress Model, resulting in Contact Stress Model-II. These improvements include the use of a linear effective stress intensity curve, analyses of residual stresses and residual stress intensities caused by yielding near holes, large scale yielding solutions for COD and plastic zone size, and rain-flow cycle counting of the spectra. These improvements are described in the following paragraphs.

To enhance correlation of the Contact Stress Model with constant amplitude  $R = -.3$  data, as shown in Figure 19, and with compression loads variations, improvements described in Reference 15 were made. The Contact Stress Model-II is based on a linear effective stress intensity curve which not only provided better correlation with compression loads data, as shown in Reference 15 and in Figure 20, but reduced computational time by a factor of two. This makes the model cost competitive with the Willenborg Model. The Contact Stress Model-II was used to analyze the spectra selected for test and several other spectra to evaluate the correlation afforded by this model.

As this improved model became available, the testing phase of the study was completed. These test results showed that prediction error with both the Contact Stress Model and the generalized Willenborg Model was a function of the highest stress level attained in a spectrum. This correlation was attributed to the presence of residual stresses near the hole caused by local plasticity during high stress level applications. A solution scheme for computation of residual stress intensity, similar to that suggested by Grandt and Gallagher, Reference 32, was incorporated into the Contact Stress Model-II. In addition, large scale yielding solutions for Dugdale plastic zone size and COD, Reference 33, were included in the model to better account for plasticity caused by high stresses.

As discussed in Section 6.3, differences were measured in crack growth rates between the Preliminary Air-to-Air Baseline and Air-to-Air Baseline spectra. The difference in these two spectra is that the largest peaks were left unchanged but peaks with small ranges were added. The increase in crack growth with the addition of these peaks with small ranges indicated that cycle counting the spectra would be necessary to account for the actual loading ranges felt by the crack. A rain-flow cycle counting method was developed which retained the peak load sequence in the spectrum but associated each peak with the most appropriate valley. Each spectrum analyzed with the Contact Stress Model-II was counted by this method.

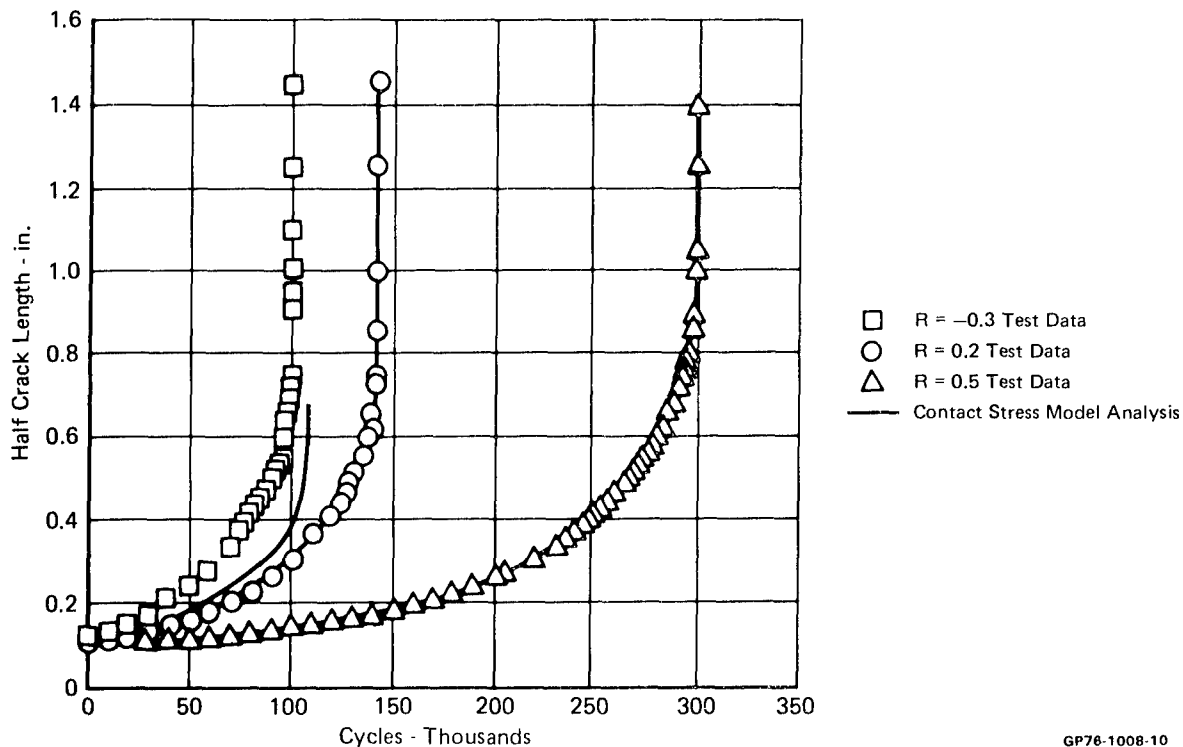


FIGURE 19. CONTACT STRESS MODEL CORRELATION WITH  
CONSTANT AMPLITUDE TEST DATA

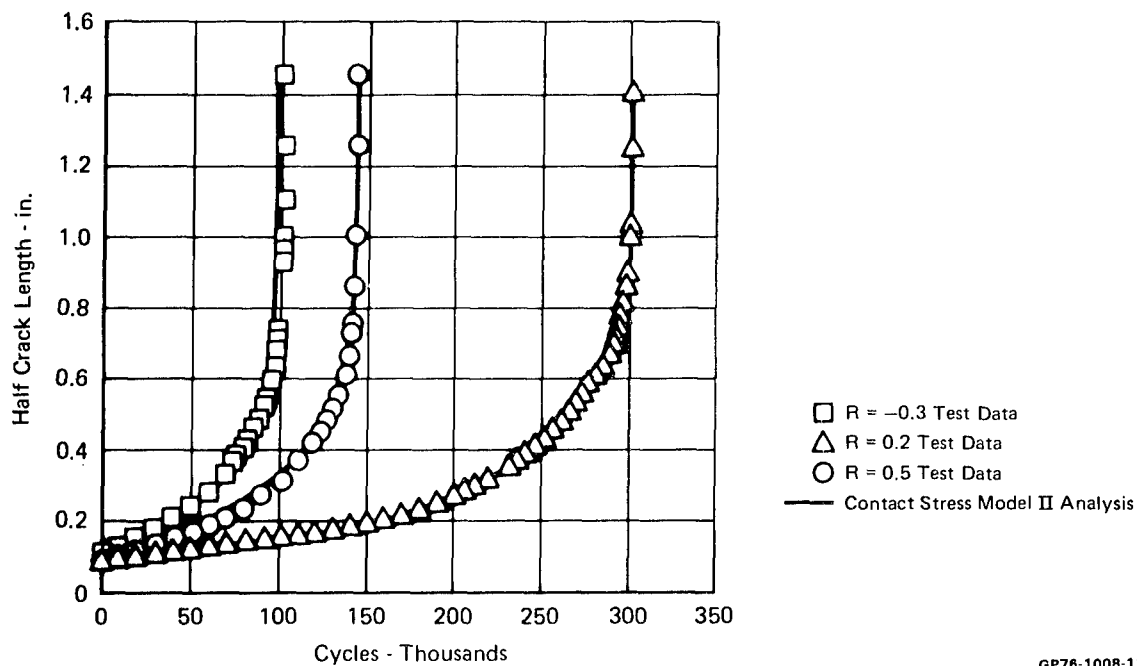


FIGURE 20. CONTACT STRESS MODEL II CORRELATION  
WITH CONSTANT AMPLITUDE TEST DATA

The test results also showed in a few cases that appreciable crack growth occurred at the side of the hole opposite the intended flaw before the intended flaw reached 0.5 inches length. This growth was not anticipated in earlier analyses. However, to assess the impact of such growth, the stress intensity solution was modified in the improved model to account for such growth when it occurred in test.

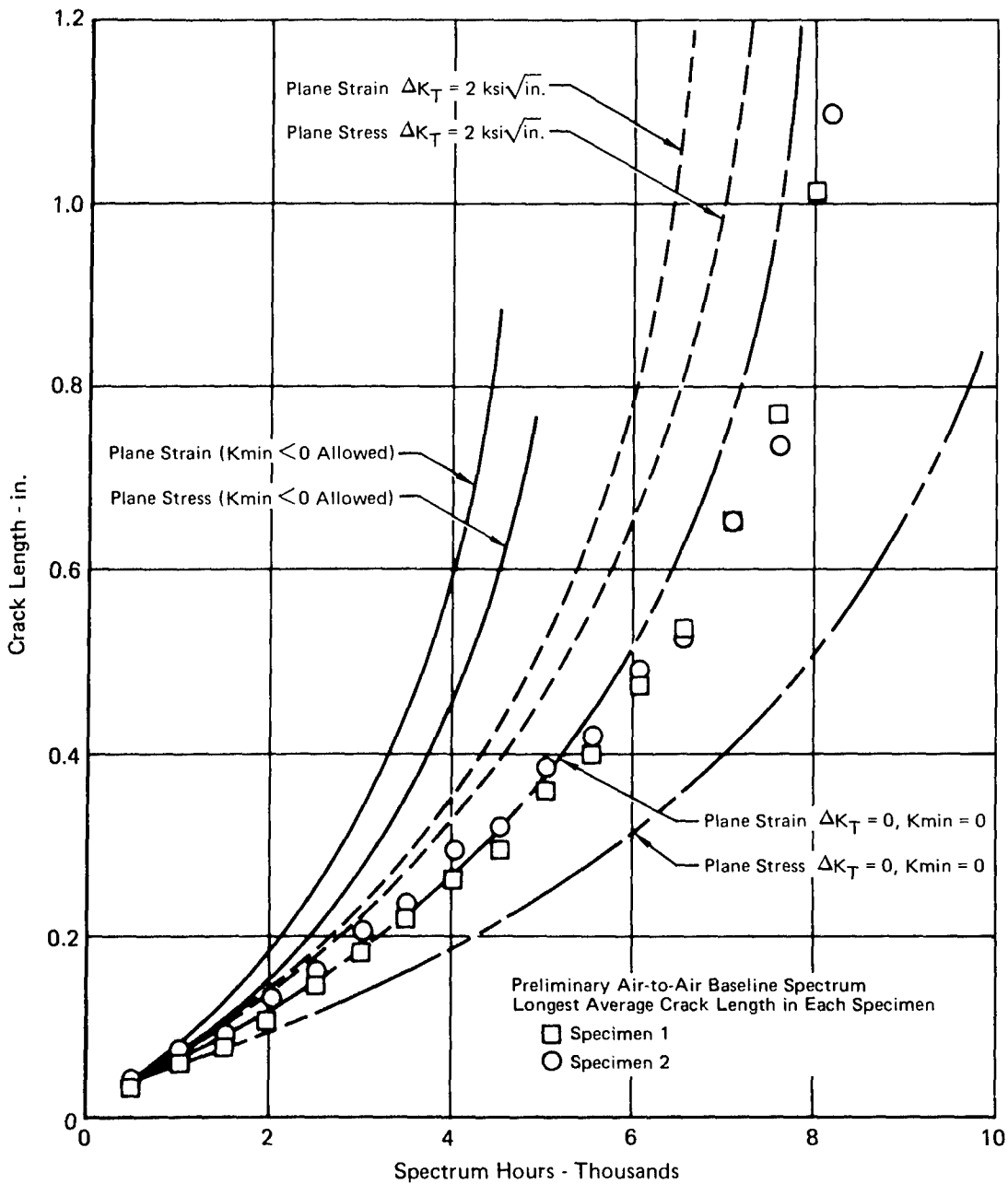
Results of analyses with the Contact Stress Model-II show the anticipated trends; a reduced effect of stress level on prediction accuracy, although the dependence has not been completely eliminated, and a reduced scatter band indicating more consistently accurate predictions. It should be pointed out that one analysis involving very high stress levels shows greater scatter than the preliminary model. These results indicate that still more work is desirable to obtain accurate prediction spectrum crack growth.

If the residual stress intensity solution, stress intensity modifications for crack emanating from the opposite side of the hole, cycle counting, compressive load analyses, and plasticity corrections were implemented into the Willenborg Model, it is reasonable to expect analysis accuracy comparable to the Contact Stress Model-II.

#### 4.5 Model Calibration

Willenborg Model - Attempts to calibrate the generalized Willenborg Model showed that the model is extremely sensitive to the choice of threshold stress intensity and to negative stress intensities. As summarized in Figure 21, analyses using a threshold  $\Delta K$  of 2 ksi  $\sqrt{\text{in}}$  or allowing negative stress intensities resulted in crack growth rates substantially higher than those recorded in test even when a plane stress plastic zone condition was assumed, and the differences in crack growth rates between plane stress and plane strain conditions were greatly reduced. This means that the plastic zone size assumption required to provide correlation with the test results would have to be far larger than the usual plane stress limit. In order to use a plastic zone size assumption consistent with those used in previous work with the Willenborg Model, the threshold  $\Delta K$  was assumed to be zero and effective stress values were not allowed to be negative. The results of analyses performed with these assumptions are also shown in Figure 21. These predictions, based on plane stress and plane strain assumptions, bound the test data obtained in this study for the Preliminary Air-to-Air Baseline spectrum. This spectrum data was used to calibrate the models for subsequent analyses. Calibration of the generalized Willenborg Model with the test data from the Preliminary





GP78-1008-12

**FIGURE 21. COMPARISON OF ANALYSIS VARIATIONS OF THE WILLENBORG MODEL WITH SPECTRUM TEST DATA**

Air-to-Air Baseline spectrum was obtained with a plastic zone size assumed to be 45 percent of the plane stress zone size corresponding to this model. This assumed zone size is

$$\omega = .0716 \left( \frac{K^{\infty}}{f_y} \right)^2 \quad (43)$$

where  $K^{\infty}$  is the applied stress intensity and  $f_y$  is the material tensile yield stress. The calibrated analysis results are shown in Figure 22, compared to the spectrum crack growth results.

The impact of not allowing negative effective stresses in analyses using the generalized Willenborg Model is two-fold. The effect of retardation as predicted by the generalized Willenborg Model is to reduce both peak and valley stress intensities, tending to drive all the valley stress intensities less than zero. By truncating the effective stress intensities at zero, the effect of retardation on the model is not only to reduce the effective stress ratio but to reduce directly the effect of stress range since  $K_{\max}^{\text{eff}}$  is reduced but  $K_{\min}^{\text{eff}}$  is not permitted to be less than zero. This truncation of effective stress intensities at zero allows a reasonable plastic zone size assumption, but does not allow the model to accurately analyze the effects of compression loads. Figure 18 presents data obtained from the constant amplitude tests performed in this study. The generalized Willenborg Model, with the Forman stress ratio correction included, accurately predicts the  $R = 0.5$  test data. The model also accurately predicts the  $R = 0.3$  test data with negative loads allowed in the analysis; with the negative loads set to zero, the analysis accuracy is reduced.

Contact Stress Models - The applied stress intensity factor solution used with these models was the same as that used in the Willenborg Model, Equations (40) - (42). Calibration of the Contact Stress Model with Preliminary Air-to-Air Baseline spectrum test results was obtained with a plastic zone size assumed to be 39 percent of the Dugdale plane stress zone size. A value of 45 percent was assumed for the Contact Stress Model-II. These assumed zone sizes are

$$\omega = .1532 \left( \frac{K^{\infty}}{f_y} \right)^2 \quad (44)$$

$$\omega = .1767 \left( \frac{K^{\infty}}{f_y} \right)^2 \quad (45)$$

The calibrated analysis results are shown in Figure 22.

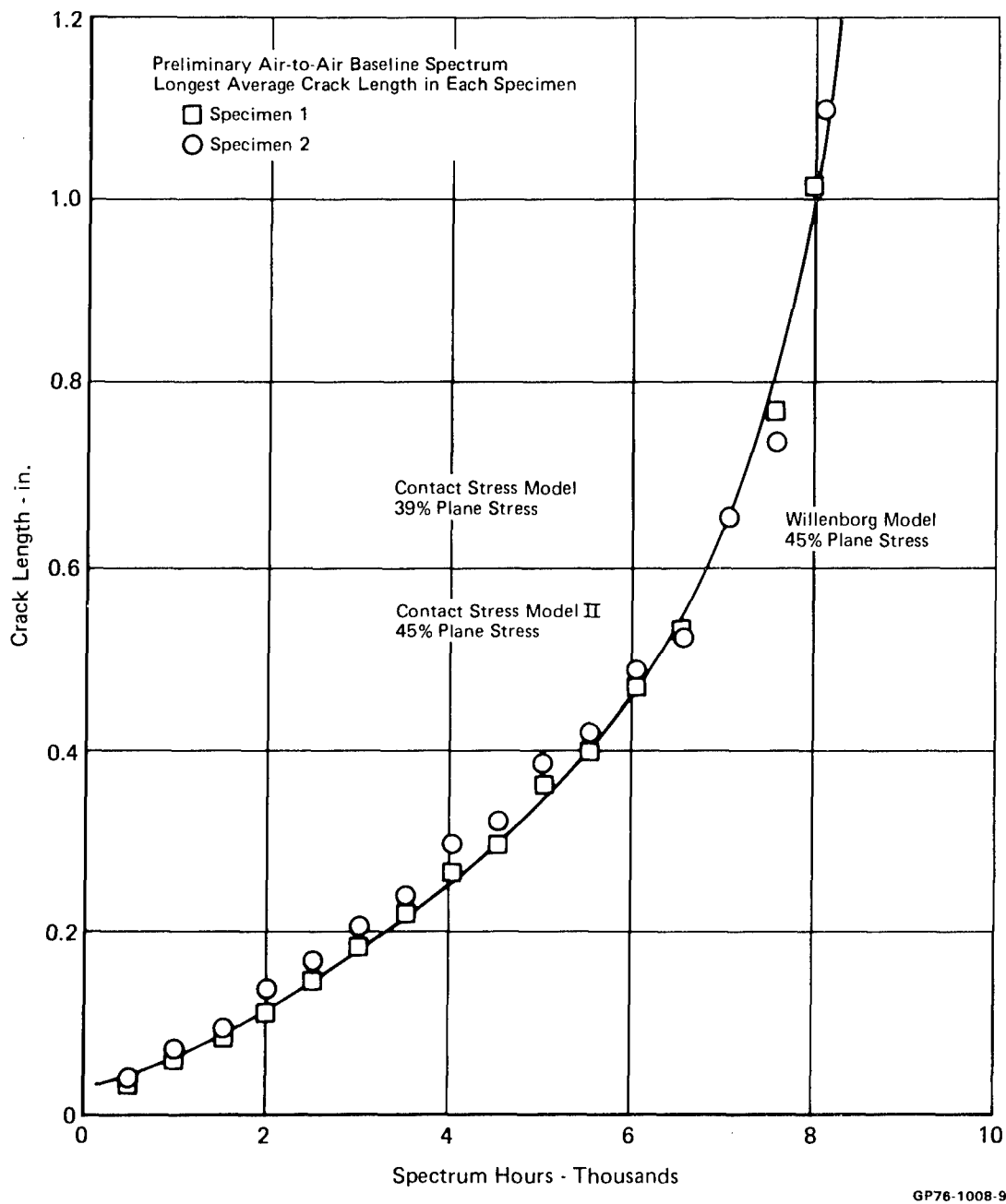


FIGURE 22. CORRELATION OF CALIBRATED MODELS WITH SPECTRUM TEST DATA

## 5. SPECIMEN DEFINITION AND TEST PROCEDURES

### 5.1 Test Program Summary

The purpose of the test program was threefold; (1) to empirically verify the predictions of advanced state-of-the-art crack growth models and thus test the analytical methods, (2) to provide data for evaluating spectrum effects on crack propagation, and (3) to provide data useful for defining guidelines for structural verification of future fighter aircraft. Spectra variations were selected for test based on their relevance to these objectives. A limited number of tests were conducted to check basic rate data for material characterization, and to support the analysis method. The specimen used for spectrum tests had a thru-thickness crack emanating from an open hole. Center crack panels were used to check basic rate data for material characterization. Thirty spectrum loading tests and three constant amplitude loading tests were performed. Results of constant amplitude tests are summarized in this section. Results of spectrum tests are summarized in Section 6.

The thirty spectrum and three constant amplitude tests are grouped into four test series as outlined in Table 2. Test Series A, C, D are spectrum tests, Series B are constant amplitude tests. Five tests (Series A and B) were performed prior to prediction of crack growth, including tests using one baseline load spectrum. Twenty-eight spectrum loading tests were performed after crack growth prediction analyses were completed.



Test Series A - The objectives of this test series were to evaluate crack growth for one baseline spectrum and to permit the analysis input parameters to be adjusted to improve correlation of test and analysis. The analysis input parameter that is adjusted within the Willenborg and Contact Stress Models is the plastic zone size assumption. This test was performed in duplicate to evaluate the effects of specimen to specimen variability.


Test Series B - The objective of these tests was to obtain constant amplitude crack growth rate data for the heat of material used in this program. These tests provided a check of the basic growth rate data that was available for the material.

Test Series C - The primary objectives of this test series were to evaluate crack growth for the three remaining baseline spectra, and to permit an evaluation of analysis method accuracy. A secondary objective was to evaluate specimen to specimen variability; therefore, duplicate specimens were tested.

Test Series D - This was the primary test series in the verification program. The objective was to evaluate crack growth for selected spectra variations and provide data to permit evaluations of analysis method accuracy.

**TABLE 2. TEST PROGRAM SUMMARY**  
**30 Spectrum Tests      3 Constant Amplitude Tests**

Test Series	Specimen Type	Figure Number	Test Purpose	Number of Specimens
A	Open-Hole	3	Evaluate crack growth for a baseline spectra. Support analysis methods.	2 
B	Center-Crack	4	Obtain constant amplitude crack growth data for the heat of material.	3
C	Open-Hole	3	Evaluate crack growth for three baseline spectra. Test analysis methods.	6 
D	Open-Hole	3	Evaluate crack growth for selected spectra variations. Test analysis methods.	22

Notes:  Duplicate specimens included in total

GP75-0162-60

## 5.2 Specimens

Material - Aluminum alloy 7075-T7351 was selected because of common usage in the industry, ready availability, and availability of  $da/dN$ ,  $K_{IC}$ , and standard mechanical data required for crack growth analyses. The alloy has been characterized in several previous investigations. All specimens were prepared from one lot of material. Three mechanical property tests and a chemical analysis of the material were performed. The results are summarized in Tables 3 and 4.

Specimen Preparation - Open Hole Specimen - Specimens containing thru-thickness cracks emanating from open holes were selected for the spectrum tests in this program. The specimen is described in Figure 23. Specimens are constant width with a reduced-thickness test section. Electrical discharge machined (EDM) starter notches were introduced at each pilot hole located as shown in Figure 24. The specimens were precracked at a stress ratio of 0.02 and peak cyclic stress of 10 ksi until the visible length of the longest of the two cracks was 0.05 inches. Subsequently, the pilot holes were reamed to a diameter of .2500 inches. The pre-crack geometry was measured and recorded. This procedure left a fatigue pre-crack of approximately .01875 inches emanating from one of the holes in the specimen.

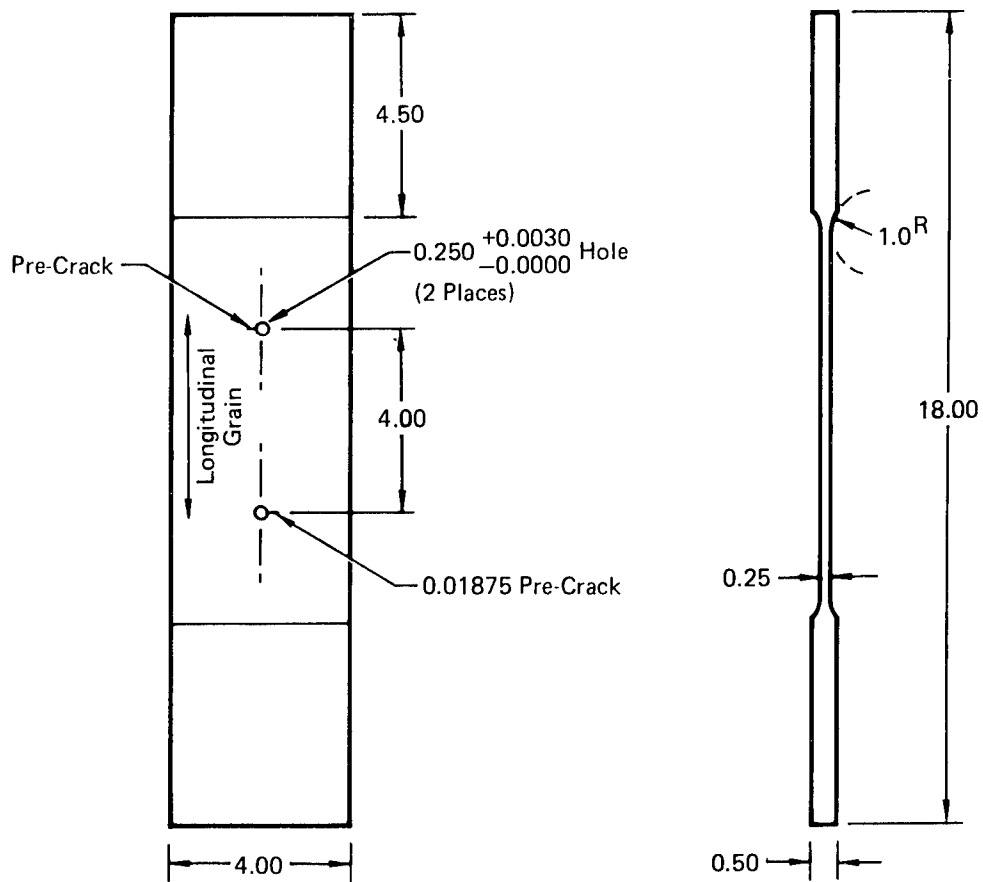
**TABLE 3. MECHANICAL PROPERTY TEST RESULTS**

Specimen No.	F <sub>ty</sub>	F <sub>tu</sub>	% EL
1	61.0	72.0	13.0
2	61.5	72.5	14.0
3	63.0	74.0	13.0
Average	61.8	72.8	13.3
Specification Min	57.0	68.0	7.0

**TABLE 4 CHEMICAL ANALYSIS**

Element	%	Specification Limits - %
Zn	5.51	5.1 - 6.1
Mg	2.60	2.1 - 2.9
Cu	1.42	1.2 - 2.0
Cr	0.22	0.18 - 0.35
H <sub>2</sub>	13.6 PPM or less	

GP76-0714-19



Note: All dimensions in inches.

GP75-0162-1

FIGURE 23. OPEN HOLE SPECIMEN

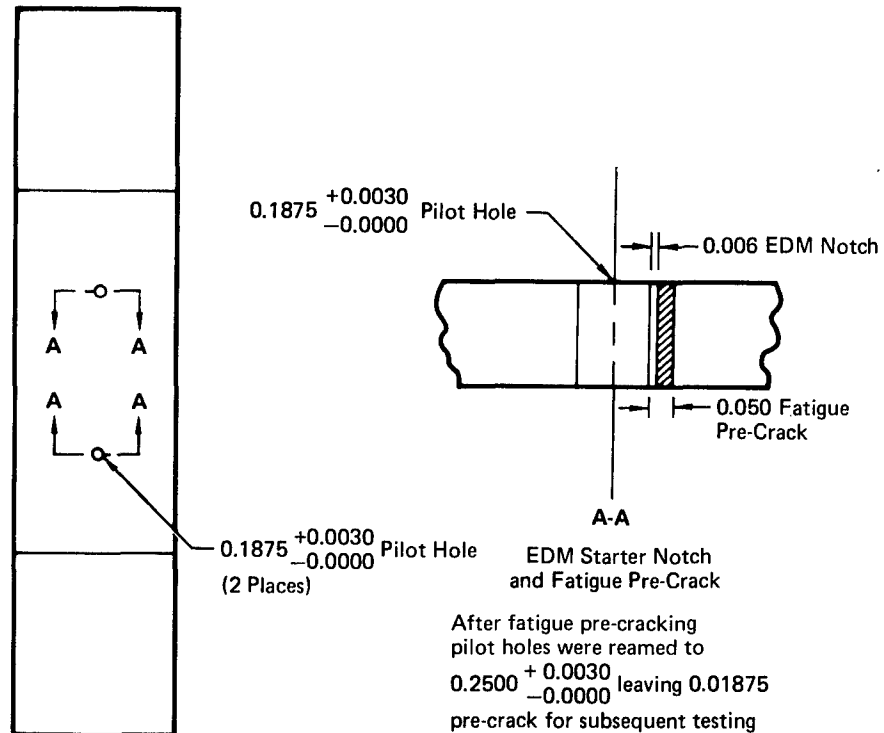


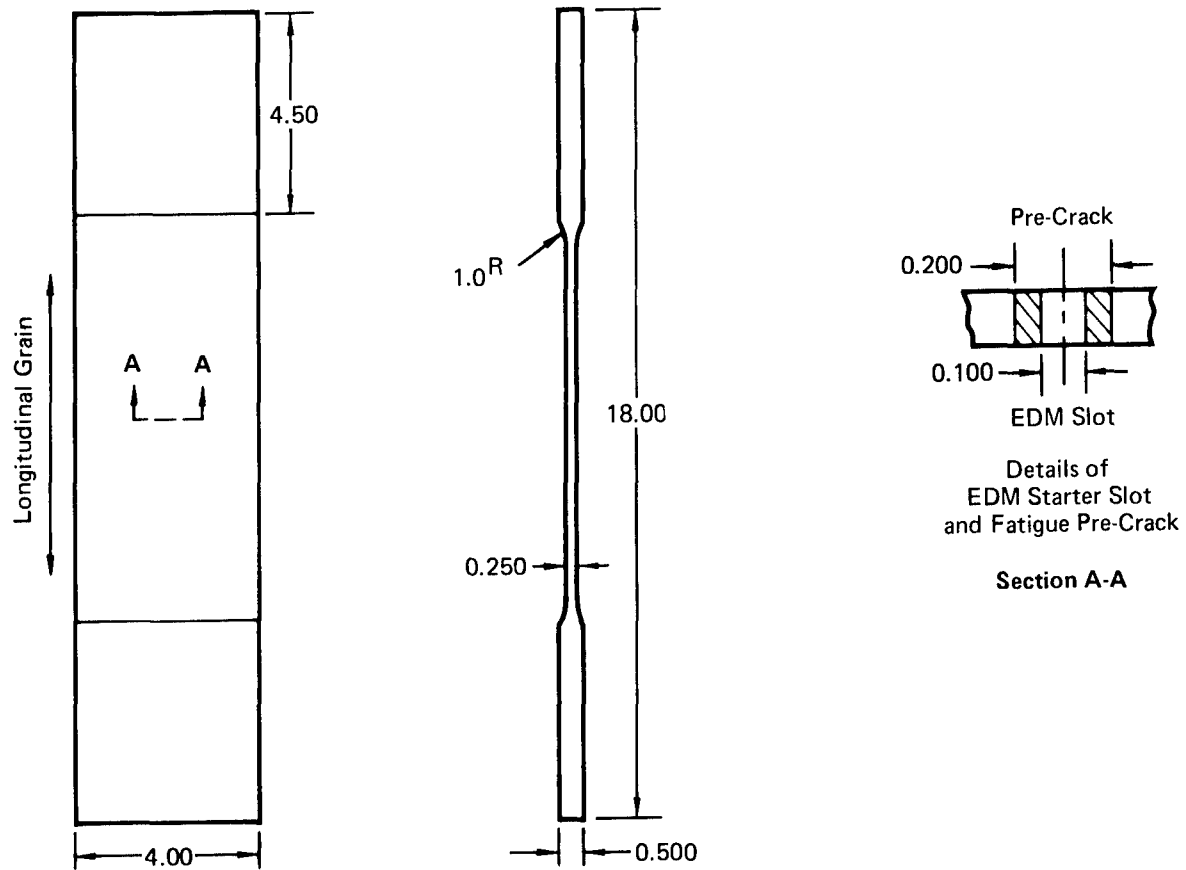
FIGURE 24. STARTER CRACK DETAILS - OPEN HOLE SPECIMEN

Specimen Preparation - Center Crack Panels - The center crack panel was selected for the constant amplitude material characterization tests in this program; the specimen is described in Figure 25. Specimens were constant width with a reduced-thickness test section. An EDM starter notch was introduced as shown in Figure 25. The specimens were pre-cracked at a stress ratio of 0.02 until the total crack length was approximately 0.20 inches. The final 0.04 inches of crack extension was performed at a load level equal to or less than that at which the subsequent crack propagation test was performed.

### 5.3 Test Procedure, Crack Growth Monitoring, and Instrumentation

All fatigue testing was performed using closed loop electrohydraulic servo machines. Each machine uses hydraulic clamp grips to insure continuous control through zero load. Individual programming systems are utilized for each testing machine and each system is programmed using either a digital punch tape or a magnetic tape. Each machine has individual servo loop controls. All load feedback signals are monitored with strip chart recorders. In addition, dynamic comparisons of feedback and programmed peak voltages are made to assure loading accuracies.





GP75-0162-2

FIGURE 25. CENTER CRACK PANEL SPECIMEN

Specimens were clamped in the machine grips and teflon roller guides were installed against the specimen surface to prevent buckling during application of compression loadings. During the testing, surface crack lengths were optically monitored. Crack length measurements were made at intervals of 500 spectrum flight hours. In addition, during one 1000 hour block of simulated flight hours on each specimen, the crack length was measured every 50 spectrum hours. The crack length measurements were used for correlation with subsequent fractographic crack growth measurements.

After completion of spectrum testing, the specimens were dissected for fractographic crack growth analyses. Both mating surfaces of the specimens were examined at up to 30X magnifications with a stereo microscope to determine which surface was most suitable for examination. The best fracture surface of each specimen was documented with a photomacrograph. Prominent fatigue striations indicative of significant crack growth that resulted from high load applications were evident, and were correlated with known high loads in the spectra to identify crack growth benchmarks.

The results of the 30 spectrum tests are reported in Section 6 and Appendix A, the results of the constant amplitude tests are discussed in the following section.

#### 5.4 Constant Amplitude Test Results

The results of the constant amplitude crack growth tests are presented in Figures 26 and 27. Figure 26 compares the results of the  $R = .02$  test to data available in the literature, and from previous MCAIR testing. Data from this program and previous data are in good agreement. These data were used to make the predictions shown in Figures 27, 18, 21 and 22. The agreement between the prediction and test data for the  $R = .02$  case shown in Figures 18, 21 and 22 indicate the faired line shown in Figure 26 is an accurate representation of the growth rate behavior.

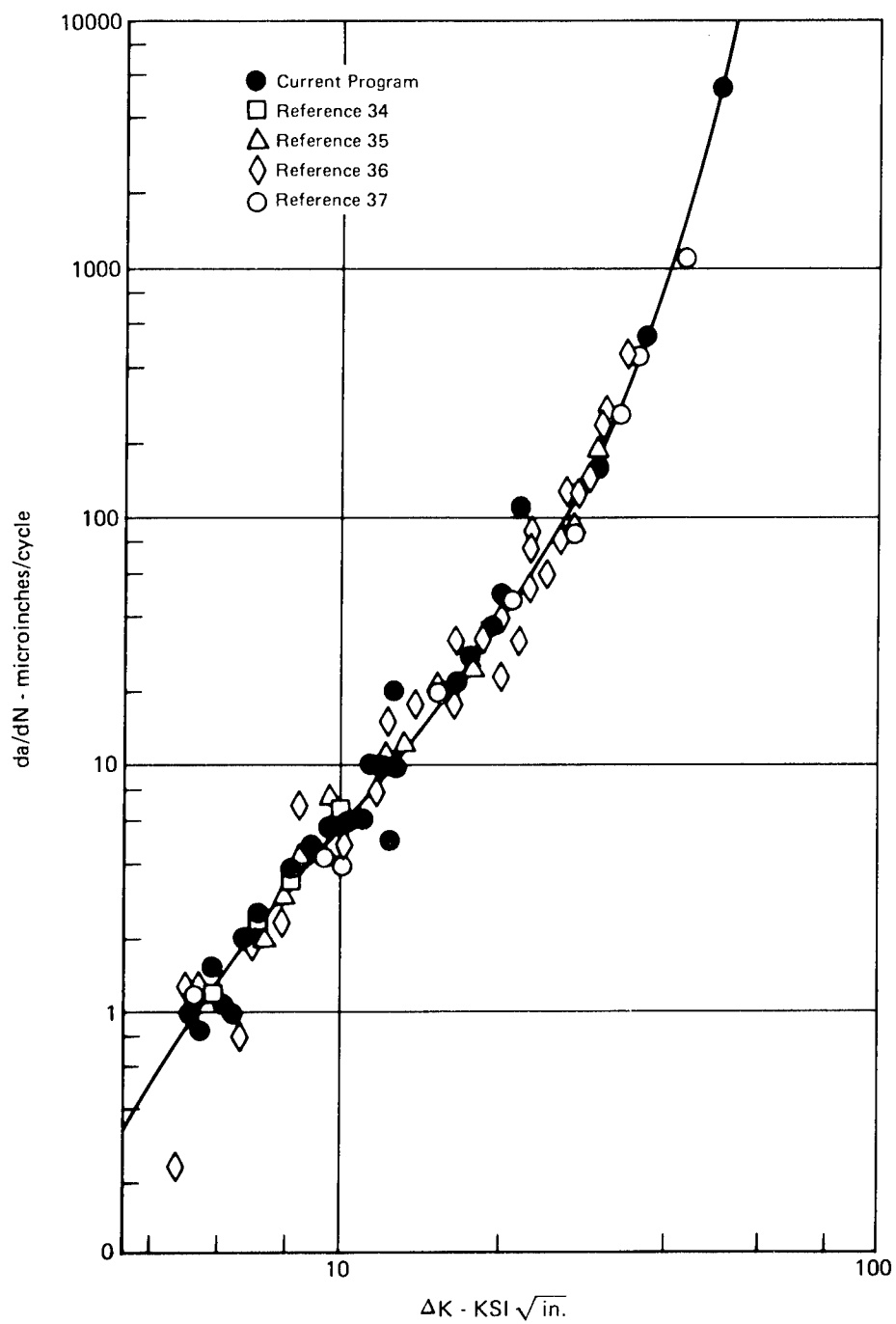


FIGURE 26. CRACK GROWTH RATE DATA FOR 7075-T73 (R = 0.02)

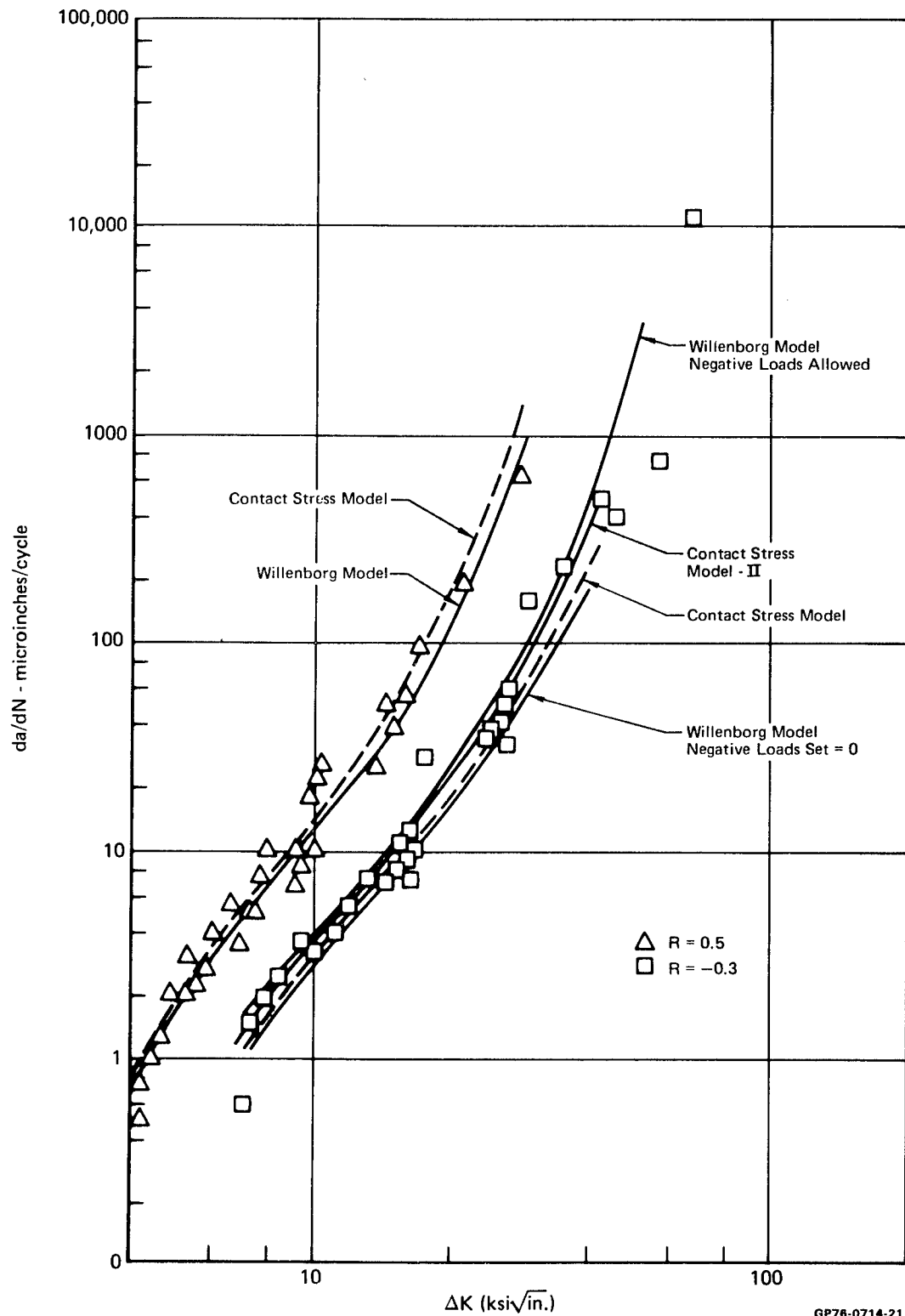


FIGURE 27. CRACK GROWTH RATE DATA FOR 7075-T73 ( $R = 0.5$  AND  $R = 0.3$ )

## 6. SPECTRA, CRACK GROWTH ANALYSIS, AND TEST RESULTS

### 6.1 Overview

This section presents definitions of the baseline spectra, describes development of 102 variations of these baseline spectra, presents crack growth prediction results, discusses test spectra selection, and presents test results.

The baseline spectra were generated with two different computer programs. The first program was used to generate the Preliminary Air-to-Air Baseline spectrum to which two specimens were tested. These test results were used to calibrate the crack growth models. Subsequently a revised program was developed which was used to produce all four of the baseline spectra. Because of a difference in the filtering techniques between these computer programs the Air-to-Air Baseline spectrum contained 2000 more load cycles than the Preliminary Air-to-Air spectrum. The revised spectrum generation program is described in Reference 1. A third computer program was used to develop the 102 spectra variations from the baseline spectra. These variations are summarized in Table 5 along with a breakdown of the analyses performed and spectra selected for test. The computer program used to develop the spectrum variations is described in Reference 2.

Linear, Willenborg, and Contact Stress Models were used to predict crack growth for the spectra variations summarized in Table 5. The Willenborg and Contact Stress Models were calibrated with the Preliminary Air-to-Air Baseline spectrum test results. Predictions were obtained using these models prior to selection of the 28 remaining test spectra. During the test program, Contact Stress Model-II became available and was used to analyze the test spectra and several of the other spectra as noted in Table 5.

Test spectra selection was based primarily on the Willenborg Model predictions and Air Force and MCAIR experience. To a lesser extent, Contact Stress Model predictions were used to support the Willenborg results for test spectrum selection. Generally the test spectra selected reflect the significance of the variation to fatigue and fracture design practices and the anticipated range of crack growth caused by the variation.

The method for presenting the analysis and test results is described in the following subsection. Subsequent sections describe the baseline spectra and spectra variations along with the corresponding analyses and test results. Correlation between test and analysis results is presented in Section 7.

**TABLE 5. SUMMARY OF SPECTRA VARIATIONS,  
CRACK GROWTH ANALYSES, AND TEST RESULTS**

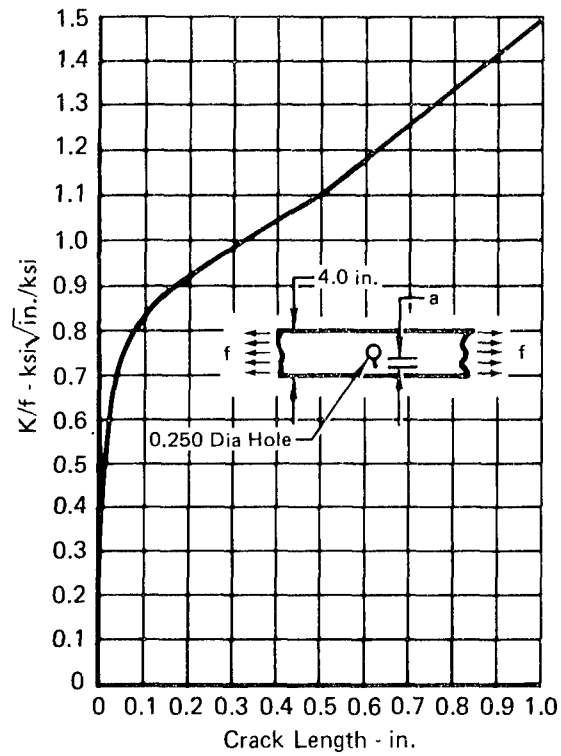
Spectrum Variation Types	Baseline Spectra				Total	Linear and Willenborg Analyses	Contact Stress Analyses	Contact Stress Model - II Analyses	Tests
	A-A	A-G	I & N	Comp					
Reordering of Loads Within a Mission	2	2	—	2	6	6	6	2	0
Sequence of Missions	2	2	—	2	6	6	6	2	1
Mission Mix	—	—	—	28	28	28	3	3	3
Flight Length Variations	2	2	2	2	8	8	1	2	1
High and Low Load Truncation	2	—	—	18	20	20	19	12	5
Compression Load Variations	1	1	1	7	10	10	10	6	3
Exceedance Curve Variations	6	—	—	—	6	6	6	6	3
Coupling of Peaks and Valleys	3	3	—	1	7	7	7	3	2
Combined Variations	2	2	—	5	9	9	9	2	2
Stress Level Variations	—	—	—	2	2	2	2	2	2
Total Number of Spectra Variations					102	102	69	40	22
Total Number of Baseline Spectra					5	5	5	5	8

GP76-0714-22

## 6.2 Data Presentation

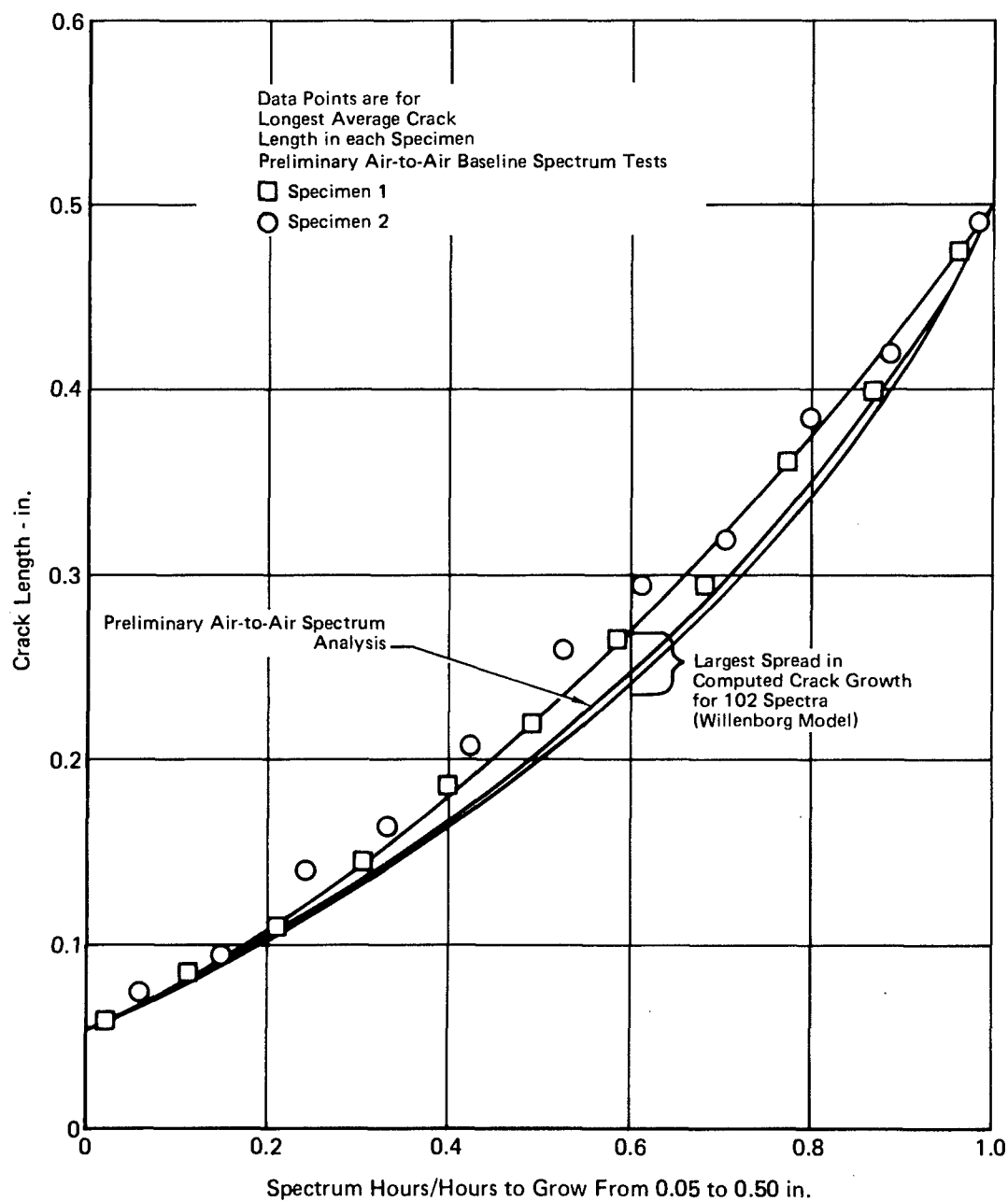
Over 300 crack growth analyses and 30 tests were performed. It was not convenient to compare results of these analyses and tests by direct comparison of crack growth curves. Therefore, a method was needed for numerically characterizing these results. The selected procedure was to compare the number of hours required to grow the crack from 0.05 to 0.50 inches ( $\Delta N$ ). The length 0.05 was selected to avoid the rapid variation of elastic stress intensity with crack length for small cracks (shown in Figure 28). This rapid change in stress intensity could accentuate the effect of errors in crack measurement and the effects of any crack front curvature and skewness, thus invalidating comparisons of crack growth for the test spectra. The length 0.50 was selected to provide a sufficient range of crack growth for manifestation of load interaction effects.

Figure 29 shows the overall band of normalized crack growth shapes for all 102 spectra variations and the baseline spectra. For comparison, the test data for the Preliminary Air-to-Air Baseline spectrum is also shown with the prediction of the Willenborg Model. The difference in shape between the Air-to-Air test data and the Willenborg prediction did not justify a recalibration of the model. The range of predicted crack growth shapes is about the same as the test scatter for two specimens tested to the same load spectrum. This agrees with previous MCAIR experience, Reference 38, and Air Force data, Reference 39, that the crack growth curve shape is insensitive to spectrum variations as long as the basic crack geometry remains the same.



GP75-0162-15

**FIGURE 28. ELASTIC STRESS INTENSITY CHANGES RAPIDLY AT SHORT CRACK LENGTH**

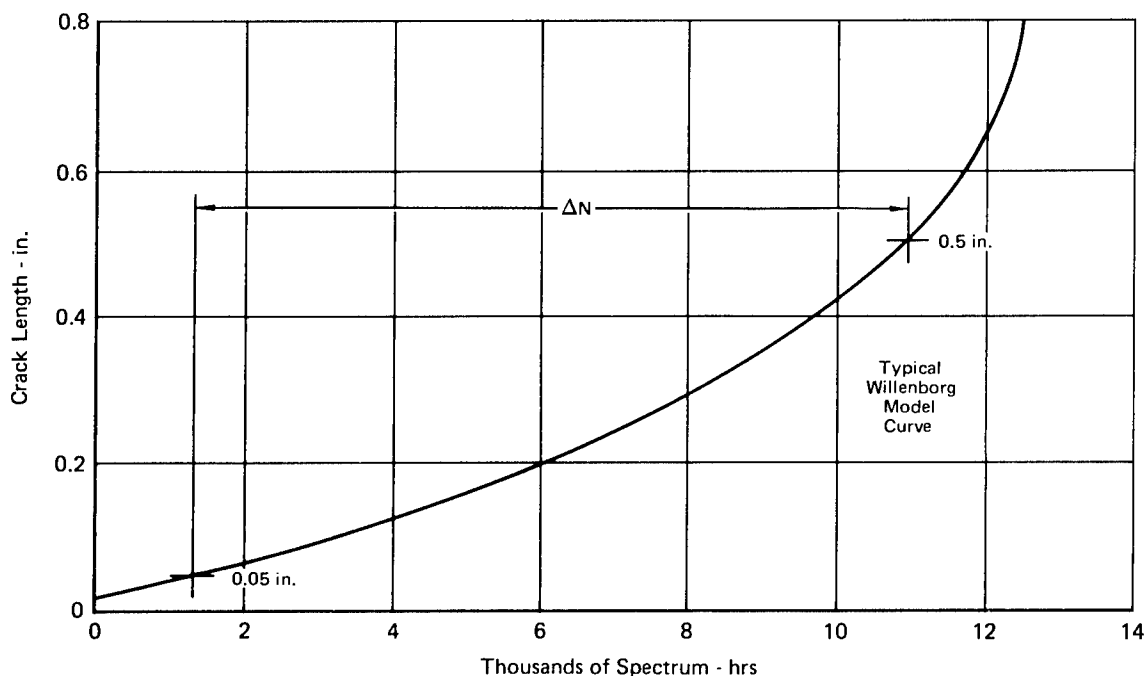


GP76-0714-36

**FIGURE 29. CRACK GROWTH ANALYSIS CURVES FOR 102 SPECTRA  
VARIATIONS HAVE VERY SIMILAR SHAPES**



Since the crack growth curves all have approximately the same shape, the crack growth results can be compared simply by considering the crack growth life, i.e., time ( $\Delta N$ ) to grow from 0.05 to 0.50 inches. This parameter is used to summarize all crack growth predictions and test data presented in the following sections and is shown schematically in Figure 30. To determine  $\Delta N$  from the test data, the surface measurements of crack length at each hole in a specimen were averaged, then interpolated to determine the spectrum hours at which average crack lengths of 0.05 and 0.50 inch occurred. The difference in spectrum hours at these two crack lengths gave  $\Delta N$  for the crack at each hole. These  $\Delta N$ 's were then averaged to obtain the test life ( $\Delta N$ ) of the specimen.



GP76-0714-23

**FIGURE 30. TIME TO GROW CRACK FROM 0.05 TO 0.5 INCHES IS SUFFICIENT TO CHARACTERIZE THE SPECTRUM VARIATIONS**

### 6.3 Baseline Spectra, Crack Growth Analyses, and Test Results

The four baseline spectra described in the following paragraphs are based on the planned operational usage for the F-15 aircraft. Each of the baseline spectra represents 1000 hours of anticipated usage.

o Air-to-Air - The Air-to-Air (A-A) Baseline spectrum represents 1000 hours of air-to-air combat flying. The spectrum consists of 768 air-to-air missions.

The Air-to-Air Baseline spectrum was generated two ways. The Preliminary Air-to-Air Baseline spectrum was generated with a preliminary version of the stress history simulation technique. Later the spectrum was generated using the final version of the computer program used to generate all of the other baseline spectra. These spectra will be referred to as the Preliminary Air-to-Air Baseline and the Air-to-Air Baseline spectra. The difference between these spectra is that a different filtering technique was used in generating the Preliminary Air-to-Air spectrum. This resulted in the addition of about 2000 peaks with small ranges into the Air-to-Air Baseline spectrum.

o Air-to-Ground - The Air-to-Ground (A-G) Baseline spectrum represents 1000 hours of air-to-ground combat flying. The spectrum consists of 1092 air-to-ground missions.

o Instrumentation and Navigation - The Instrumentation and Navigation Baseline spectrum represents 1000 hours of instrumentation and navigation flying. The spectrum consists of 480 instrumentation and navigation missions.

o Composite - The Composite Baseline spectrum represents 1000 hours of A-A, A-G, and I&N flying. The spectrum consists of:

475 hours of A-A = 365 A-A missions

325 hours of A-G = 355 A-G missions

200 hours of I&N = 96 I&N missions

---

1000 hours

The sequence of missions for the Composite Baseline spectrum is:

182 A-A missions

178 A-G missions

48 I&N missions

183 A-A missions

177 A-G missions

48 I&N missions

Table 6 shows the crack growth predictions of the Linear, Willenborg, and Contact Stress Models and the test results for the baseline spectra. The tests of the Preliminary Air-to-Air Baseline spectrum were performed prior to any analysis. The Willenborg, and Contact Stress Models were all calibrated with test results from the Preliminary Air-to-Air spectrum by modifying the plastic zone size assumption. The Linear Model cannot be calibrated. The calibrated

TABLE 6. SUMMARY OF ANALYSES AND TEST RESULTS FOR BASELINE SPECTRA

Baseline Spectra	Linear $\Delta N$	Willenborg $\Delta N$	Contact Stress $\Delta N$	Contact Stress Model II $\Delta N$	Test $\Delta N$ ②	Test Average $\Delta N$
Preliminary Air-to-Air ①	2,221	5,528	5,555	5,469	5,430 5,554	5,492
Air-To-Air	2,238	5,480	6,171	5,098	4,552	4,552
Air-To-Ground	3,110	7,770	6,799	5,253	3,265 3,418	3,341
Instrumentation and Navigation	32,400	109,150	95,898	71,134	53,975	53,975
Composite	3,150	7,440	6,874	6,020	5,965 5,913	5,939

Notes:

GP76-1008-13

- ① All growth models calibrated using the crack growth data for this spectrum  
 ②  $\Delta N$  - Spectrum hours required to growth crack from 0.05 in. to 0.5 in.

models were then used to compute crack growth for the remaining baseline spectra and spectra variations.

Comparisons of test results with predictions and analyses reveal several interesting points. The most noteworthy is that none of the models were able to account for the comparatively short test life with the A-G spectrum as compared to the A-A spectrum. Duplication of tests indicates that those results are valid. Similarly, all of the models overestimated the life with the I&N Baseline spectrum. Both the I&N and A-G spectra have maximum peak loads of only 80 percent of TLL, versus 101 percent for the Composite of 114.5 percent for the A-A spectra. Therefore, the analytical error may be a stress level dependent effect caused by ignoring residual stress effects or, in the case of the Contact Stress Model-II, by incompletely accounting for these effects.

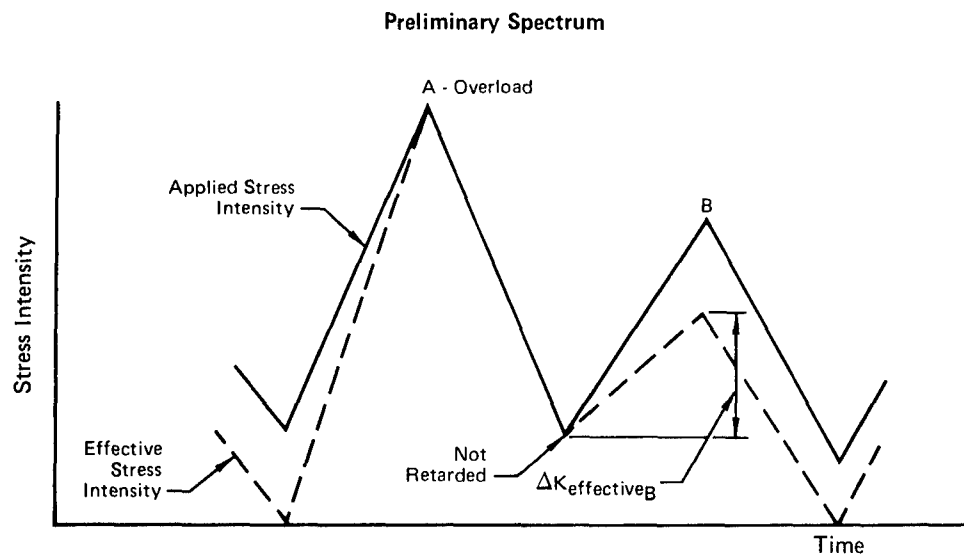
The decreased life of the A-A spectrum with respect to the Preliminary A-A spectrum was not predicted by the Linear, Willenborg, or the Contact Stress Models. As discussed previously, the difference between the preliminary and final A-A spectra is that approximately 2000 peaks with small ranges were added to the preliminary spectrum. This addition reduced the load range for many of the original peaks, causing the Contact Stress Model to predict a life longer than that of the preliminary spectrum. The Willenborg Model also predicted a life increase when the small additional peak preceded the original peak.

However, as depicted in Figure 31, a small additional peak following the original peak produced an increase in growth of the following cycle. In the Willenborg Model the effective stress at each valley depends upon the retardation of the preceding peak. In the original spectrum, the value of the first valley following the high peak was not reduced. However, the valley of a small subsequent peak was reduced. Thus, when the small peak was added, the following peak was reduced, which in turn reduced the next valley and increases the next range beyond the original values. In the Willenborg Model this seemed to negate the reduced crack growth rate effect of precedent small peaks. However, it does not adequately handle all effects of the small peaks. It might be inferred from the test results that the effect of a small added peak is to cause additional crack growth without affecting the growth due to the maximum ranges of the spectrum. This implies that a cycle counting procedure such as that used in spectrum fatigue damage analysis would provide a more accurate analysis. The Contact Stress Model-II was used with rain-flow cycle counting of the test spectra, Reference 40, to provide much better correlation with the trend of the test results.

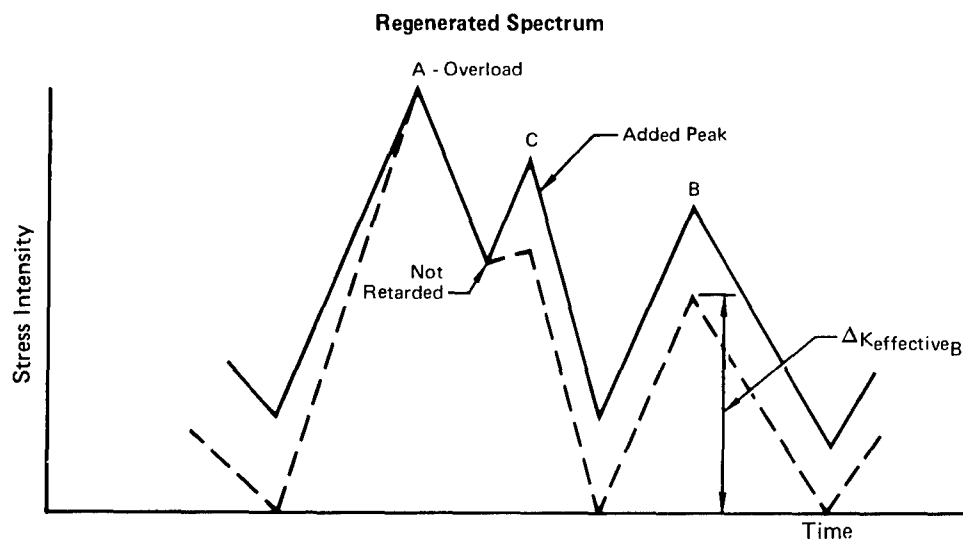
Those spectra to which duplicate tests were run had test lives that were within 5 percent of agreement. Thus, it is concluded that these test results are repeatable.

#### 6.4 Spectra Variations, Crack Growth Analyses, and Test Results

From the four baseline spectra produced with the spectrum generation routine, 102 spectrum variations were created. These variations are outlined in Table 5, along with the number of analyses performed and the spectra selected for test. Twenty-two spectra variations were selected for test, along with eight tests of the baseline spectra; a total of 30 spectrum tests. Generally, the numbers of each type of variation reflect the significance of the variations to fatigue and fracture analyses and the range of crack growth expected from the variation. Linear accumulation (no retardation) and Willenborg Model analyses were performed on each spectrum generated in this program. Willenborg predictions were used to select test spectra. Contact Stress Model predictions were used to support the Willenborg predictions and to determine the relative strengths and weaknesses of yield zone and closure models. The Contact Stress Model-II was developed during the time period of this study. Since analyses using the Contact Stress Model-II include the effects of unanticipated crack growth from a hole on the side opposite the intended flaw, these analyses are correlative in nature. The variations, crack growth analyses, and test results are presented in the following subsections.



In the Willenborg Model the Reduction of any Valley is the Same as that of the Preceding Peak.



$\Delta K_{\text{effective}_B}$  is Greater for the Regenerated Spectrum than for the Preliminary Spectrum

GP76-0714-25

**FIGURE 31. WILLENBORG ANALYSIS OF SUBSEQUENT SMALL PEAK**

6.4.1 Reordering of Loads Within a Mission - For selected baseline spectra, the peak loads within a mission were reordered in Lo-Hi and Hi-Lo sequences. The valley preceding each peak remained with that peak during the reordering process, so that the loading ranges were not affected by these variations. These variations are outlined in Table 7.

Also included in Table 7 are analysis results for reordering loads within a mission. Results for all models show small effects due to these variations. Because the effects were predicted to be so small, and similar results were expected to occur for mission sequence variations, no tests were performed with these variations. Analyses using the Contact Stress Model-II were performed only on variations of the Composite Baseline spectrum, considered to be representative of the results for the other spectra.

**TABLE 7. REORDERING OF LOADS WITHIN A MISSION**  
6 Variations (2 A-A, 2 A-G, 2 Composite)

- 2 Different Sequences (Lo Hi, Hi Lo)
- Reordering Based on Positive Peak of Each Cycle
- Cycle Consists of a Peak and the Valley That Precedes it

		Variation Number		
		Baseline Spectra		
		A-A	A-G	Comp
Load Sequence	Lo Hi	1	2	3
	Hi Lo	4	5	6

**Analysis and Test Results**

Variation Number	Linear $\Delta N$	Willenborg $\Delta N$	Contact Stress $\Delta N$	Contact Stress Model - II $\Delta N$	Test $\Delta N$
1	2299	6036	6417	—	—
2	3210	8038	6994	—	—
3	3249	7953	7148	6339	—
4	2095	5849	5367	—	—
5	2882	8004	6228	—	—
6	2934	7800	6082	6334	—

GP76-0714-43

6.4.2 Sequence of Missions - Variations in mission sequencing were based on the maximum peak load in each mission. For selected baseline spectra, the missions were reordered in Hi-Lo and Lo-Hi sequences. These variations and the corresponding crack growth analysis and test life results are presented in

Table 8. Generally, the analyses all predicted a decrease in life under Hi-Lo sequences with respect to Lo-Hi sequences. Analyses using the Contact Stress Model-II were performed only for variations of the Composite Baseline to verify that these analyses will predict the same trends. Since sequence of mission variations at each baseline spectrum seemed to cause similar changes in crack growth behavior, only the Hi-Lo sequenced Composite Baseline spectrum was tested to characterize these variations.

**TABLE 8. SEQUENCE OF MISSIONS**  
6 Variations (2 A-A, 2 A-G, 2 Composite)

- 2 Different Sequences (Lo Hi, Hi Lo)
- Reordering of Missions Based on Maximum Peak in Each Mission

		Variation Number		
		Baseline Spectra		
		A-A	A-G	Comp
Mission Sequence	Lo Hi	1	2	3
	Hi Lo	4	5	6

**Analysis and Test Results**

Variation Number	Linear $\Delta N$	Willenborg $\Delta N$	Contact Stress $\Delta N$	Contact Stress Model - II $\Delta N$	Test $\Delta N$
1	2219	4102	5860	—	—
2	2893	5472	5633	—	—
3	3118	6039	7022	4790	—
4	2242	3239	4318	—	—
5	3125	4986	5153	—	—
6	3170	4650	5453	3693	4258

GP76-0714-44

6.4.3 Mission Mix - Three different types of mission mix variations were analyzed. The first type involved variations in percentage of flight time spent in the different mission types. These variations are outlined in Table 9. The percentage of Air-to-Air missions per 1000 flight hours increases with increasing variation number.

Based on the exceedance severity of the Air-to-Air missions, crack growth life was expected to decrease as the percentage of Air-to-Air missions increased. Therefore, it was expected that the Air-to-Air Baseline spectrum would be the most severe mix. For contrast, the least severe mix, based on Linear and Willenborg Model analysis, was selected for test. The trends of the Willenborg predictions were the same as for the Linear analyses, and the Contact Stress Models

**TABLE 9. VARIATION IN PERCENTAGE OF FLIGHT TIME  
SPENT IN DIFFERENT MISSIONS**

Number of Missions, → Hours →	Mission Type											
	Air-To-Air					Air-To-Ground					I & N	
	77	230	384	538	691	109	328	546	764	983	48	96
	100	300	500	700	900	100	300	500	700	900	100	200
1*										✓	✓	
2	✓									✓		
3	✓								✓			✓
4		✓							✓			
5		✓						✓				✓
6			✓					✓				
7			✓				✓					✓
8				✓			✓					
9				✓		✓						✓
10					✓	✓					✓	
11					✓							

\* Variation number

● Mission Sequence Same as Composite Baseline Below

1/2 of All A-A Missions  
1/2 of All A-G Missions  
1/2 of All I-N Missions  
1/2 of All A-A Missions  
1/2 of All A-G Missions  
1/2 of All I-N Missions

1000 Hours of Usage

#### Analysis and Test Results

Variation Number	Linear $\Delta N$	Willenborg $\Delta N$	Contact Stress $\Delta N$	Contact Stress Model II $\Delta N$	Test $\Delta N$
1	3440	8510	—	—	—
2	3010	7310	—	—	—
3	3660	9060	8124	6772	7528
4	2820	7110	—	—	—
5	3390	8520	—	—	—
6	2650	6150	—	—	—
7	3120	7280	—	—	—
8	2480	5830	—	—	—
9	2850	6600	—	—	—
10	2300	6040	—	—	—
11	2450	6240	—	—	—

GP78-1008-14



were expected to show the same trends; therefore, the Contact Stress Models were used only for variation 3, which was selected for test.

The second type of mission mix variation involved various assumptions of mission sequences, as outlined in Table 10. Linear and Willenborg predictions of these variations showed so little effect on crack growth life, that neither Contact Stress Model was used to analyze these variations nor were any tests performed on these variations.

The third type of mission mix variation involved mission severity. These variations included increasing the magnitude of peak loads in specified missions by 10 percent, either in the first 1000 hours only or repeated every 1000 hours. Table 11 summarizes these variations and the corresponding test and analysis results; there was little change in crack growth life as the severity of a group of missions was increased. The Contact Stress Models were used only to characterize the maximum range of predicted results. Variation 21 resulted in the shortest predicted life and variation 28 resulted in the shortest predicted life for spectra made directly from the Composite Baseline. These mission mixes were tested to characterize the range of results of severity variations.

TABLE 10. VARIATION IN MISSION SEQUENCE

Variation Number	12	13	14	15
Performed on Mix Variation Number	7	9	3	5
Sequence of Missions	All A-A All A-G All I-N	1/2 of All A-G All A-A 1/2 of All A-G All I-N	1/2 of All A-A All A-G 1/2 of All A-A All I-N	1/2 of All I-N All A-A All A-G 1/2 of All I-N

Analysis and Test Results

Variation Number	Linear $\Delta N$	Willenborg $\Delta N$	Contact Stress $\Delta N$	Contact Stress Model - II $\Delta N$	Test $\Delta N$
12	3130	7130	—	—	—
13	2860	6500	—	—	—
14	3650	8769	—	—	—
15	3450	8170	—	—	—

GP76-0714-27

**TABLE 11. VARIATION IN MISSION SEVERITY**

- Peak Loads for Designated Missions are Increased by 10%

Performed on Mix Variation Number	5	5	9	1	Composite Baseline Spectrum		
Type and Number of Missions Affected	A-A Missions (1 - 100)	A-G Missions (1 - 100)	A-A Missions (1 - 400)	A-G Missions (1 - 400)	A-A Missions (1 - 100)	A-A Missions (266 - 365)	A-A Missions (1 - 365)
Increased Severity for 1st 1000 Hours Only	16*	18	20	22	24	26	27
Increased Severity Repeated Every 1000 Hours	17	19	21	23	25		28

\*Variation number

**Analysis and Test Results**

Variation Number	Linear $\Delta N$	Willenborg $\Delta N$	Contact Stress $\Delta N$	Contact Stress Model - II $\Delta N$	Test $\Delta N$
16	3390	8560	—	—	—
17	3150	8130	—	—	—
18	3390	8550	—	—	—
19	3280	8100	—	—	—
20	2740	6580	—	—	—
21	2260	5200	5137	4305	3864
22	3410	8520	—	—	—
23	3010	7450	—	—	—
24	3160	7440	—	—	—
25	2940	6950	—	—	—
26	3080	7440	—	—	—
27	3030	7430	—	—	—
28	2490	6020	7133	5363	5531

GP76-0714-48

6.4.4 Individual Flight Length - The average flight length for the A-A missions is 1.30 hours, for the A-G missions .92 hours, and for the I&N missions 2.07 hours. The baseline flight-by-flight spectra were formed by including a ground load between each flight. For all four baseline spectra, the individual flight lengths were halved and doubled according to the outline of Table 12. As indicated by the Linear and Willenborg models, the effects of these variations are very small. The Contact Stress Models were used to analyze variations of the Composite Baseline spectrum and little change in life was predicted. A single test was performed using the Composite Baseline spectrum with flight length halved.

6.4.5 High and Low Load Truncation - The truncation variations are outlined in Table 13.

Selection of the lowest loads and highest loads to include in a fatigue spectrum has historically been a difficult process. Elimination of frequently occurring low load levels is generally required based on the economic considerations of test time. However, their elimination at too high a load level may dilute the meaning of the test in terms of demonstrating structural integrity for service usage. In variations 1 & 2, low load levels were added to the A-A and Composite Baseline spectra to match the respective design spectra. The additional cycles consisted of a valley of 12.5% DLS (Design Limit Stress) and a peak of either 30% DLS or 40% DLS. The additional cycles were equally spaced throughout the A-A missions of both spectra. There were 10,000 cycles of 12.5% DLS to 30% DLS and 2,000 cycles of 12.5% DLS to 40% DLS added to the A-A Baseline. In variations 3, 4, 5, and 6, low load level cycles were eliminated by truncating the Composite Baseline at 35, 45, 55, and 65% DLS. The valley of each of the truncated cycles was always the most positive valley on either side of the peak being eliminated.

Linear, Willenborg, and Contact Stress Models were used to analyze these variations. Very little effect was noted until the 55 and 65% DLS levels were deleted in variations 5 and 6. These spectra variations were subsequently selected for test and analyzed with the Contact Stress Model-II.

The potential for saving test time by truncating numerous low load level cycles and adding a few higher load level cycles was evaluated. Based on Willenborg analyses to give equal crack growth, 610 cycles of 12.5% DLS to 65% DLS were added to the Composite Baseline to compensate for truncation of 12,738 cycles of 55% DLS and below. The 12.5% DLS to 65% DLS cycles were distributed throughout all mission types in variation 7. Linear, Willenborg, and

**TABLE 12. INDIVIDUAL FLIGHT LENGTH**  
8 Variations (2 A-A, 2 A-G, 2 I-N, 2 Composite)

- Halve the Flight Length for all Baseline Spectra
- Double the Flight Length for all Baseline Spectra

	Variation Number			
	Baseline Spectra			
	A-A	A-G	I-N	Comp.
Flight Length Halved	1	2	3	4
Flight Length Doubled	5	6	7	8

**Analysis and Test Results**

Variation Number	Linear $\Delta N$	Willenborg $\Delta N$	Contact Stress $\Delta N$	Contact Stress Model - II $\Delta N$	Test $\Delta N$
1	2,170	5,470	—	—	—
2	2,990	7,750	—	—	—
3	28,010	107,990	—	—	—
4	3,020	7,390	6,780	5,939	6,492
5	2,270	5,500	—	—	—
6	3,180	7,700	—	—	—
7	35,190	109,630	—	—	—
8	3,210	7,460	—	6,141	—

GP76-0714-45

TABLE 13. TRUNCATION VARIATIONS

Type of Variation	Variation Number	
	Baseline Spectra	
	A-A	Composite
Addition of Low Load Levels to Match Design Spectra	1	2
Truncation of 35%, 45%, 55%, and 65% Load Levels and Below		3 4 5 6
Equal Crack Growth Analysis		7
Clipping of the Composite Baseline Spectrum at 85% and 95%		8 9
Truncation of Highest Load in A-A Baseline and Composite Baseline	11	10
Increase Frequency of Application of the Highest Load in the Composite Baseline Spectrum by Two, Three, and Five Times		12 13 14
Addition of Higher Loads to the Composite Baseline Spectrum		
1. Add 1 Cycle of 12.5% to 115% at 2,000, 6,000, 10,000 (etc) Hours and 1 Cycle of 12.5% to 125% at 8,000, 24,000 40,000 (etc) Hours		15
2. Add 1 Cycle of 12.5% to 115% Every 1,000 Hours		16
3. Add 1 Cycle of 12.5% to 125% Every 1,000 Hours		17
4. Add 1 Cycle of 12.5% to 135% Every 1,000 Hours		18
5. Add 2 Cycles of 12.5% to 115% Every 1,000 Hours		19
6. Add 2 Cycles of 12.5% to 125% Every 1,000 Hours		20

Analysis and Test Results

Variation Number	Linear $\Delta N$	Willenborg $\Delta N$	Contact Stress $\Delta N$	Contact Stress Model - II $\Delta N$	Test $\Delta N$
1	2,037	5,241	6,228	—	—
2	2,945	7,042	6,858	—	—
3	3,220	7,450	6,692	—	—
4	3,560	7,600	6,534	—	—
5	4,600	8,710	7,348	6,836	7,088
6	7,420	13,190	11,392	11,104	12,708
7	4,048	7,436	6,502	—	—
8	3,160	6,340	6,673	4,490	4,312
9	3,150	7,100	7,205	—	—
10	3,147	7,207	7,211	—	—
11	2,239	5,065	5,690	—	—
12	3,150	7,460	8,265	—	—
13	3,140	7,770	8,115	—	—
14	3,135	9,433	9,156	6,837	6,838
15	3,140	8,140	—	—	—
16	3,140	8,480	11,716	—	—
17	3,140	13,790	12,507	—	—
18	3,130	57,430	27,852	27,063	38,381
19	3,140	9,810	13,674	—	—
20	3,130	31,110	16,499	—	—

GP78-0714-46

Contact Stress Models were used to analyze this spectrum and results are shown in Table 13. The Willenborg analysis life of 7,436 hours for this spectrum is nearly the same as the 7,440 hours obtained from Willenborg analysis of the Composite Baseline spectrum. No tests were selected for this variation.

The question of truncating at the high load end is also an intricate one, but for different reasons than truncating low loads. Extremely high loads that occur very infrequently can have offsetting effects. They can be damaging in that they can cause significant crack growth themselves or can cause complete rupture of a component. However, high loads can also produce beneficial effects. High positive loads can produce a large plastic zone at the crack tip and retard subsequent propagation. In variations 8 and 9 all peak loads in the Composite Baseline were clipped at 85% DLS and 95% DLS, respectively. In variations 10 and 11 the highest load was truncated in the Composite and A-A Baseline spectra, respectively.

Crack growth life predictions for these spectra were obtained using the Linear, Willenborg, and Contact Stress Models and results are shown in Table 13. Truncation variation 8 showed the greatest variation from the baseline life and so was selected for experimental verification.

In variations 12, 13 and 14, the frequency of application of the highest load in the Composite Baseline spectrum was increased by two, three, and five times per 1000 hours. The additional cycles were equally spaced throughout the Composite Baseline spectrum. Based on the crack growth life predictions of the Linear, Willenborg, and Contact Stress models, truncation variation 14 was selected for test to verify the range of life extension caused by these variations.

Finally, in variations 15, 16, 17, 18, 19, and 20, outlined in Table 13, the effect of adding higher load levels to the Composite Baseline was evaluated. Based on the Linear, Willenborg, and Contact Stress Model analyses, truncation variation 18 was selected for test to verify the impact of adding a high load to the Composite Baseline spectrum. Contact Stress Model-II was used for analysis of this spectrum. Current Contact Stress Models were created for use with repeating blocks of loads. The blocks within variation 15 do not repeat, therefore; the Contact Stress Models were not used for analysis of this variation. The other models indicated this variation had small effect.

**6.4.6 Compression Loads** - The four baseline spectra include compression loads applied as a ground cycle between each flight. The ground load applied for each A-A and I&N mission is minus 5% DLS. The ground load applied for each A-G mission is minus 10% DLS. In addition, the A-A and A-G missions include

compression loads caused by negative g maneuvering. The compression loads variations are outlined in Table 14. In compression load variations, 1, 2, 3, and 4, each baseline was clipped at 0% DLS. The effect of increasing the magnitude of compression loads was determined by making the ground load for all missions in the Composite Baseline -10% DLS, -20% DLS, and -30% DLS, in variations 5, 6, and 7, respectively. Finally, in variations 8, 9, and 10, the magnitude of all negative maneuver loads in the Composite Baseline was increased by 10%, 25% and 50%, respectively.

Crack growth predictions were performed with the Linear, Willenborg, and Contact Stress Models to determine if any of these models could properly account for variations in compression loads. As discussed in Section 4.2, the Willenborg Model cannot account for compression load effects. Since the Contact Stress Model predicted so little effect of these variations, the variations were selected for test based on experience with similar variations and the expected impact of such variations on formulation of spectra. Compression loads variations 4, 7, and 10 were selected to evaluate the most significant effects of each type of compression loads variation described above.

6.4.7 Exceedance Curve Variations - Associated with the A-A Baseline spectrum are values for  $N_p$ ,  $\sigma$ , R, and m described in Equations (3), and (19) and (20).

$N_p$  = 20000 (total number of positive peaks)

$\sigma$  = 9.5 (RMS of Gaussian data)

R = 1.128 (transformation coefficient)

m = 33% DLS (mean value of transformed data).

Exceedance curve variations 1, 2, 3, 4, 5, and 6 represent six variations of the A-A Baseline spectrum shown in Table 15. In these variations, R and m have been held constant while  $N_p$  and  $\sigma$  have been assigned the values outlined in Table 15. A variation of  $\sigma$  is accomplished by changing the area under the PSD curve:  
 $\sqrt{\text{area}}$  = RMS of the unadjusted data.  $N_p$  was changed using more or less of the Gaussian random time history data.

Linear, Willenborg, and Contact Stress Models were used to predict crack growth for each of these spectra variations. These analyses showed that exceedance curve variations have an effect on crack growth life, but the results of the analyses were inconclusive. Spectra variations 2, 5, and 6 were selected for test.

**TABLE 14.COMPRESSION LOADS VARIATIONS**

10 Variations  
(1 A-A, 1 A-G, 1 I-N, 7 Composite)

- For Each Baseline Spectra, Clip All Negative Loads Including Ground Loads at 0% DLS.
- For the Composite Baseline Spectrum
  1. Increase Ground Loads for A-A and I-N From -5% to -10% DLS.
  2. Increase Ground Loads for All Missions to -20% and -30% DLS.
  3. Increase the Magnitude of All Negative Maneuver Loads by 10%, 25%, and 50%

Variation Number			
Baseline Spectra			
A-A	A-G	I-N	Comp.
1	2	3	4
			5
			6 7
			8 9 10

**Analysis and Test Results**

Variation Number	Linear $\Delta N$	Willenborg $\Delta N$	Contact Stress $\Delta N$	Contact Stress Model - II $\Delta N$	Test $\Delta N$
1	2,280	5,480	6,557	—	—
2	3,200	7,770	7,381	—	—
3	34,080	109,150	103,812	—	—
4	3,230	7,440	7,592	7,349	6,357
5	3,120	7,440	6,874	—	—
6	3,040	7,440	6,916	5,661	—
7	2,940	7,440	6,756	5,133	4,714
8	3,140	7,440	6,874	5,942	—
9	3,080	7,440	6,874	5,843	—
10	3,127	7,442	6,874	5,631	5,828

GP78-0714-47



**TABLE 15. EXCEEDANCE CURVE VARIATIONS**

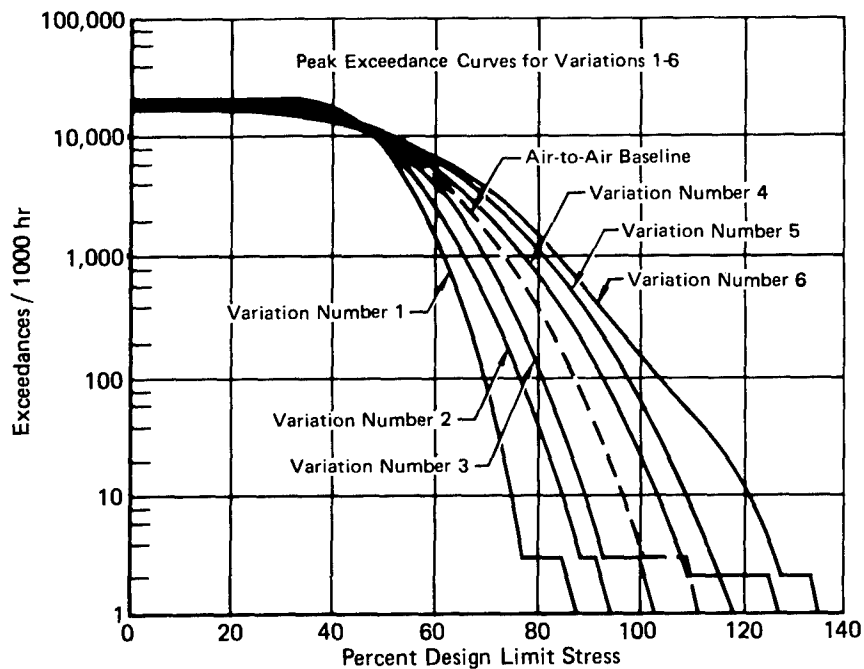
6 Variations (6 A-A)

- 6 Different Values of RMS and  $N_p$  are Used to Generate 6 Variations in the Shape of the A-A Baseline Spectrum Exceedance Curve

	1	2	3	4	5	6
$\sigma$	6.5	7.5	8.5	10.5	11.5	12.5
$N_p$	22,700	20,200	19,100	18,300	19,000	16,800

**Analysis and Test Results**

Variation Number	Linear $\Delta N$	Willenborg $\Delta N$	Contact Stress $\Delta N$	Contact Stress Model - II $\Delta N$	Test $\Delta N$
1	3470	5665	9214	4668	—
2	3166	6013	8257	4797	5254
3	2777	6135	7663	5401	—
4	2042	5163	4748	4853	—
5	1662	4534	3794	4356	4001
6	1547	4834	4114	4344	3253



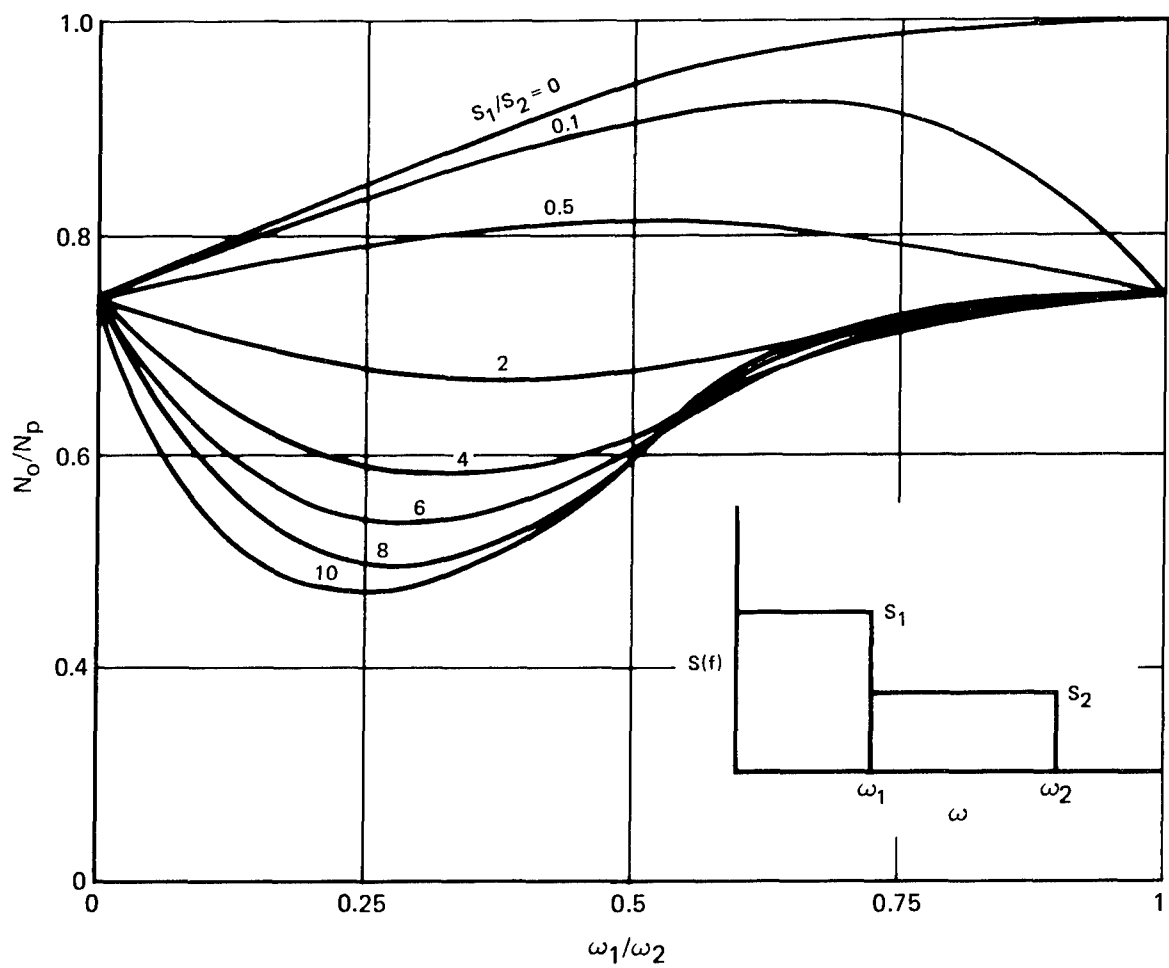
GP78-0714-42

6.4.8 Coupling of Peaks and Valleys - The ratio of  $N_o$ , the number of mean level crossings, to  $N_p$ , the number of peaks, is sometimes termed the irregularity factor. It is the parameter which indicates how peaks and valleys are coupled. With the irregularity factor  $N_o/N_p$  equal to one, there is a mean level crossing for every peak. With  $N_o/N_p$  very small, there are many more peaks than mean level crossings. This represents a wide band process wherein small amplitude cycles are superimposed on large amplitude cycles. The magnitude of the irregularity factor is determined by integration of the PSD versus frequency curve. However, the shape of the PSD versus frequency curve can be varied somewhat and still give the same  $N_o/N_p$  value. Figure 32 shows the variation of  $N_o/N_p$  with different combinations of two rectangles forming the PSD versus frequency curve. Note that  $N_o/N_p = .51$  for  $\omega_1/\omega_2 = .35$  and  $S_1/S_2 = 8$ , and  $N_o/N_p = .59$  for  $\omega_1/\omega_2 = .24$  and  $S_1/S_2 = 4$ . The  $N_o/N_p$  values of .51 and .59 are representative of the irregularity factors for the A-A and A-G PSD vs. frequency curves given in Figures 33 and 34, respectively. The rectangular shaped curves are compared to the A-A and A-G PSD curves in Figures 33 and 34, respectively.

Coupling of peaks and valleys variations are outlined in Table 16. In coupling variations 1 and 2, the A-A and A-G baseline spectra were regenerated with the rectangular PSD curves to determine if the precise shape of the PSD curve is significant. In coupling variations 3, 4, 5, and 6 the effects of significant variations in the irregularity factor were determined. The A-A and A-G baseline spectra were regenerated with  $N_o/N_p = .75$  and  $N_o/N_p = 1$ . This was done to determine the importance of significant variations in the coupling of peaks and valleys. Finally, in variation 7, all positive peaks in the Composite Baseline spectrum were coupled with a 1g minimum stress (12.5% DLS), with the exception of those positive peaks already coupled with a valley less than 1g.

Linear, Willenborg, and Contact Stress Model analyses were performed for all of the above variations. Based on these analyses, coupling variation 5 was selected for test to characterize the range of life variation due to changes in irregularity factor, and coupling variation 7 was selected for test to assess the impact of maintaining a 1g maximum limit on valley stresses.

6.4.9 Combined Variations - The primary purpose of the spectrum variations outlined in the preceding paragraphs was to isolate the effects of each variation on crack growth. However, the effect of combined variations may not be immediately obvious with only the knowledge of the individual effect, and it is combined variations that may occur most often in service. The combined variations that



GP75 0162-50

FIGURE 32. VARIATION IN IRREGULARITY FACTOR WITH SHAPE OF POWER SPECTRAL DENSITY CURVE

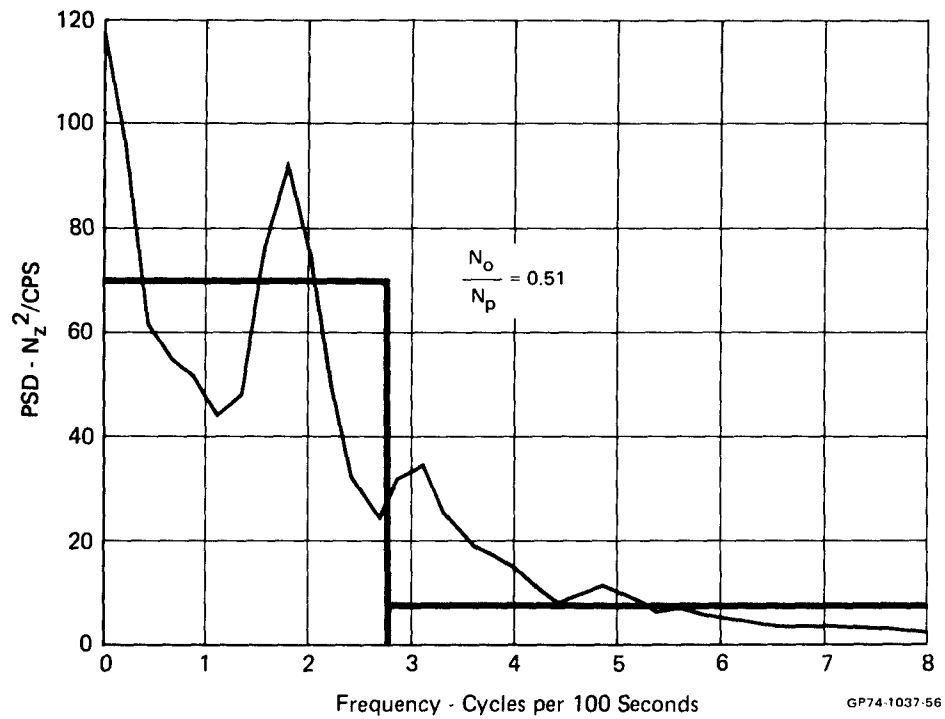


FIGURE 33. COMPARISON OF AIR-TO-AIR POWER SPECTRAL DENSITY CURVE TO RECTANGULAR SHAPE

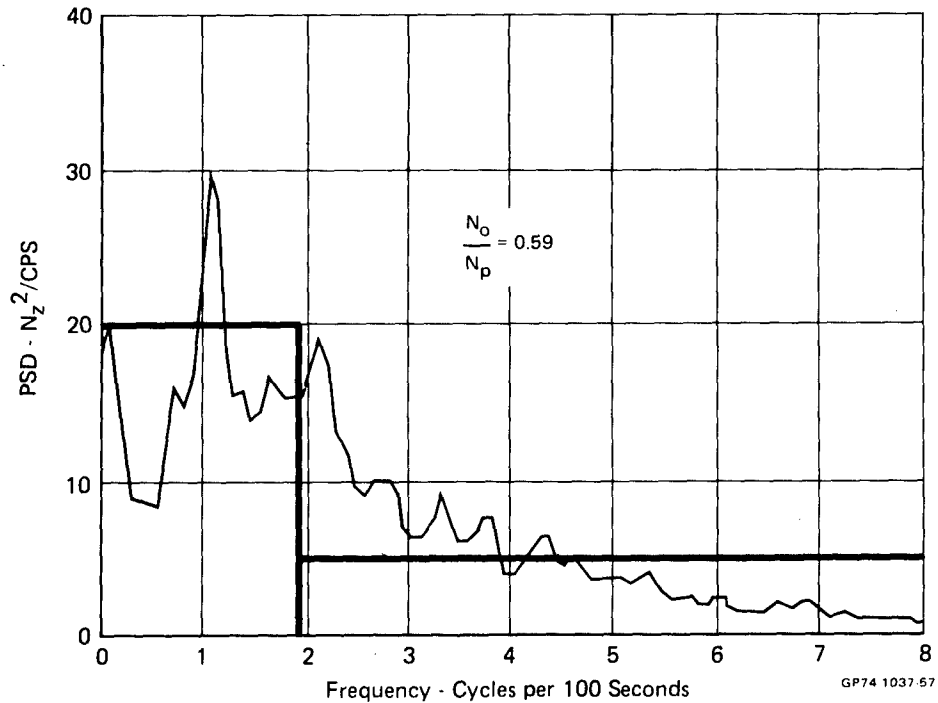


FIGURE 34. COMPARISON OF AIR-TO-GROUND POWER SPECTRAL DENSITY CURVE TO RECTANGULAR SHAPE

**TABLE 16. COUPLING OF PEAKS AND VALLEYS**

7 Variations (3 A-A, 3 A-G, 1 Composite)

- A-A and A-G Baseline Spectra are Regenerated with Rectangular PSD Curves ( $N_0/N_p$  Does Not Change)
- A-A and A-G Baseline Spectra are Regenerated with  $N_0/N_p = 0.75$  and  $N_0/N_p = 1$
- Couple all Positive Peaks in the Composite Baseline Spectrum with a 1 g Minimum Stress, Except Those that are Already Coupled with a Valley Less than 1 g (1 g = 12.5%)

Variation Number		
Baseline Spectra		
A-A	A-G	Comp
1	2	
3 5	4 6	
		7

**Analysis and Test Results**

Variation Number	Linear $\Delta N$	Willenborg $\Delta N$	Contact Stress $\Delta N$	Contact Stress Model - II $\Delta N$	Test $\Delta N$
1	2190	5316	5874	—	—
2	3283	8221	7997	—	—
3	1823	4667	4773	4512	—
4	2875	7511	6225	—	—
5	1467	3977	3244	3097	3978
6	2385	7225	4750	—	—
7	2601	6583	5376	5465	5996

GP78-0714-41

were considered are outlined in Table 17. Combined variations 3 and 4 were selected for test. These variations involve using less and more severe Air-to-Air missions, respectively, in the Composite Baseline Spectrum.

**6.4.10 Test Limit Load Variations** - Test results for specimens tested to previous spectra variations indicated that prediction error of the models was related to the highest stress level attained in a spectrum. To assess this effect, analyses and tests were performed using the Composite Baseline spectrum at two test limit stress levels, 19.8 ksi and 40.2 ksi, as outlined in Table 18. The lesser stress level was selected to maintain elastic stresses at the edge of the hole. The higher limit stress level was selected such that the highest peak stress was equal to the highest peak stress in the tested spectra variations. Tests were performed at each limit stress level.

**TABLE 17. COMBINED VARIATIONS**  
**9 Variations of the Composite Baseline Spectrum**

- 1 Mission Mix Variation 21 + Truncation Variation 6
- 2 Mission Mix Variation 21 + Compression Loads Variation 7
- 3 Composite Baseline + Exceedance Curve Variation 6
- 4 Composite Baseline + Exceedance Curve Variation 1
- 5 Truncation Variation 6 + Compression Loads Variation 7
- 6 Composite Baseline + Coupling Variation 5 + Coupling Variation 6
- 7 Composite Baseline + Coupling Variation 1 + Coupling Variation 2
- 8 Compression Loads Variation 10 + Coupling Variation 5 + Coupling Variation 6
- 9 Reordering of Loads Within a Mission Variation 6 + Coupling Variation 1 + Coupling Variation 2

**Analysis and Test Results**

Variation Number	Linear $\Delta N$	Willenborg $\Delta N$	Contact Stress $\Delta N$	Contact Stress Model - II $\Delta N$	Test $\Delta N$
1	3,569	6,628	5,572	—	—
2	2,130	5,208	4,937	—	—
3	2,486	8,689	7,207	5,380	5,161
4	4,156	7,827	9,798	5,917	5,598
5	5,627	13,189	11,100	—	—
6	2,186	6,886	4,143	—	—
7	3,099	8,045	9,033	—	—
8	2,169	6,886	4,143	—	—
9	2,861	8,586	6,478	—	—

GP76-0714-40

**TABLE 18. TEST LIMIT STRESS LEVEL VARIATIONS**

**2 Variations of Composite Baseline Spectrum**

- 1 Composite Baseline at 19.8 ksi Test Limit Stress
- 2 Composite Baseline at 40.2 ksi Test Limit Stress  
All Other Tests Run at 30.0 ksi Test Limit Stress

**Analysis and Test Results**

Variation Number	Linear $\Delta N$	Willenborg $\Delta N$	Contact Stress $\Delta N$	Contact Stress Model II $\Delta N$	Test $\Delta N$
1	10,309	26,437	29,414	19,046	16,632
2	1,293	2,653	2,682	2,526	2,456

GP76-1008-15

## 7. SUMMARY AND RECOMMENDATIONS

### 7.1 Impact of Spectra Variations

To establish recommendations and guidelines for development of realistic loads spectra, the impact of spectra variations on crack growth life and the accuracy of available crack growth models in assessing this impact must be known. The variations were categorized according to their ranges of crack growth life. A summary of this assessment is given in Table 19; variations shown to have the greatest impact are those involving modifications of the maximum peak loads. These variations include mission mix, high and low load truncation, exceedance curve variations, and test limit load variations. Variations shown to have significant impact include those which modify all but the highest peak loads throughout the spectrum, such as sequence of missions, compression loads, and peak and valley coupling. Spectra variations shown to produce the least effect are those which modify lesser loads in each mission. These consist of reordering of loads within a mission and flight length variations.

Spectra variations generated in this program represent the stress levels and exceedance content of loads applied to a lower wing skin of a fighter aircraft, therefore the assessment of these variations is restricted to such applications. Similar variations of spectra generated for different locations or aircraft types might result in a different assessment of variation severity.

**TABLE 19. EFFECT OF SPECTRA VARIATIONS ON CRACK GROWTH**

Spectrum Variation Type	Range of Crack Growth Life		
	Less Than 10% Variation	Less Than 50% Variation	Greater Than 50% Variation
Reordering of Loads Within a Mission	✓		
Sequence of Missions		✓	
Mission Mix			✓
Individual Flight Length	✓		
High and Low Load Truncation			✓
Compression Loads		✓	
Exceedance Curve Variations			✓
Coupling of Peaks and Valleys		✓	
Test Limit Stress Level			✓

GP78-0714-38



Ability of available models to predict spectrum crack growth is indicated in Table 20. This table shows that the Willenborg and Contact Stress Models have nearly equal predictive ability. Contact Stress Model-II has significantly improved analytical capability including accurate analysis of important variations of exceedance curves and test limit stress.

Reordering of Loads Within a Mission - Figure 35 indicates the effect of reordering loads within a mission on crack growth life. These variations were created from the Composite Baseline spectrum which is a random loads spectrum. No tests were performed for these variations; therefore all data shown are analytical. The figures in this section are plots of the ratio of the crack growth life from 0.05 to 0.50 inch to the corresponding baseline spectrum life. Thus values greater than unity indicate increased life, and those less than unity decreased life. The abscissa of each figure is a parameter descriptive of the variation and its magnitude.

**TABLE 20. EFFECT OF SPECTRA VARIATIONS ON CRACK GROWTH LIFE PREDICTION ACCURACY**

Spectrum Variation Type	Maximum Error Within 25% of Life		
	Willenborg	Contact Stress	Contact Stress Model - II
Recording of Loads Within a Mission	No Tests Performed		
Sequence of Missions	✓	✓	✓
Mission Mix	✓	✓	✓
Individual Flight Length	✓	✓	✓
High and Low Load Truncation	✓		
Compression Loads		✓	✓
Exceedance Curve Variations			✓
Coupling of Peaks and Valleys			
Test Limit Stress Level			✓

GP76-0714-37

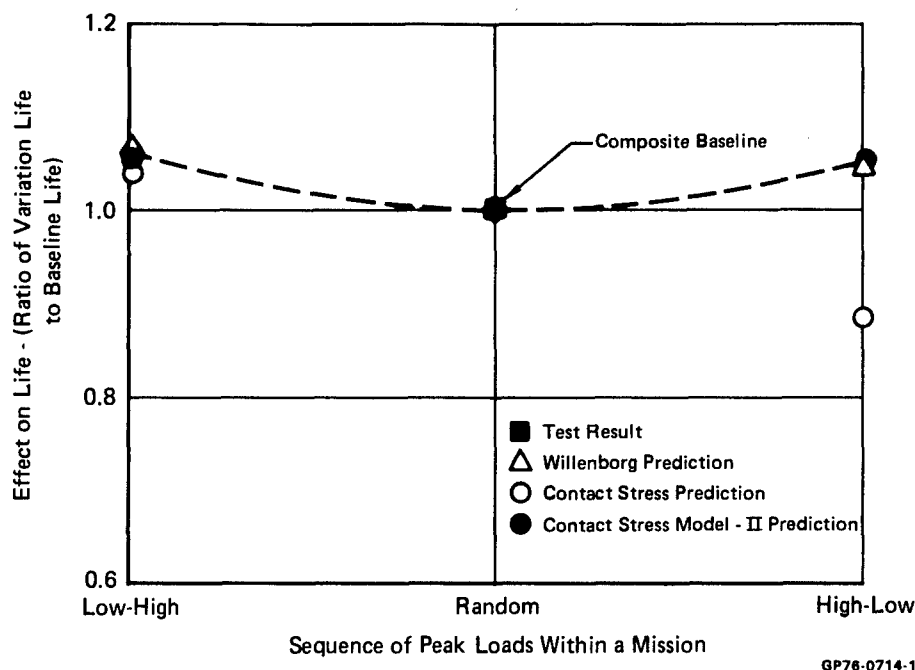


**FIGURE 35. REORDERING LOADS WITHIN A MISSION**  
Effect of Reordering Loads Within a Mission on Crack Growth Life

Sequence of Missions - The effect of this variation is shown in Figure 36, where the missions were sequenced Lo-Hi or Hi-Lo based on the highest load in each mission. Here the Contact Stress Model-II and Willenborg Model predict reductions in crack growth life with either Lo-Hi or Hi-Lo sequencing, in contrast to the increased lives predicted for reordering of loads within a mission.

Mission Mix - Two types of mission mix effects were tested. The first involved varying the ratio of Air-to-Air missions to total missions in the 1000 hour Composite Baseline spectrum. The analysis and test data presented in Figure 37 indicate that the effect of this variation is to reduce life as the number of Air-to-Air missions increases.

The second mission mix studied involved increasing the severity of a portion of the Air-to-Air missions. This effect is shown in Figure 38, which indicates the same trend as noted in the previous figure, although the increased severity produces a more dramatic reduction in life. Variation 28 is the Composite Baseline spectrum with all 365 Air-to-Air mission peak loads increased by 10%. Variation 21 has 700 Air-to-Air missions, and the peak loads for the first 400 of these were increased by 10%. All models predict the trends of the test data.

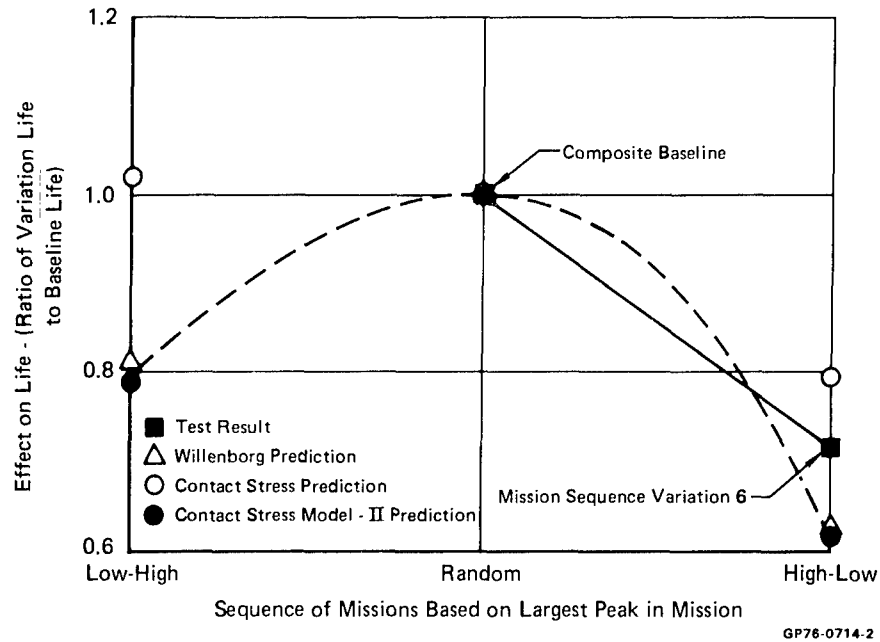


**FIGURE 36. SEQUENCE OF MISSIONS**  
Effect of Mission Sequence on Crack Growth Life

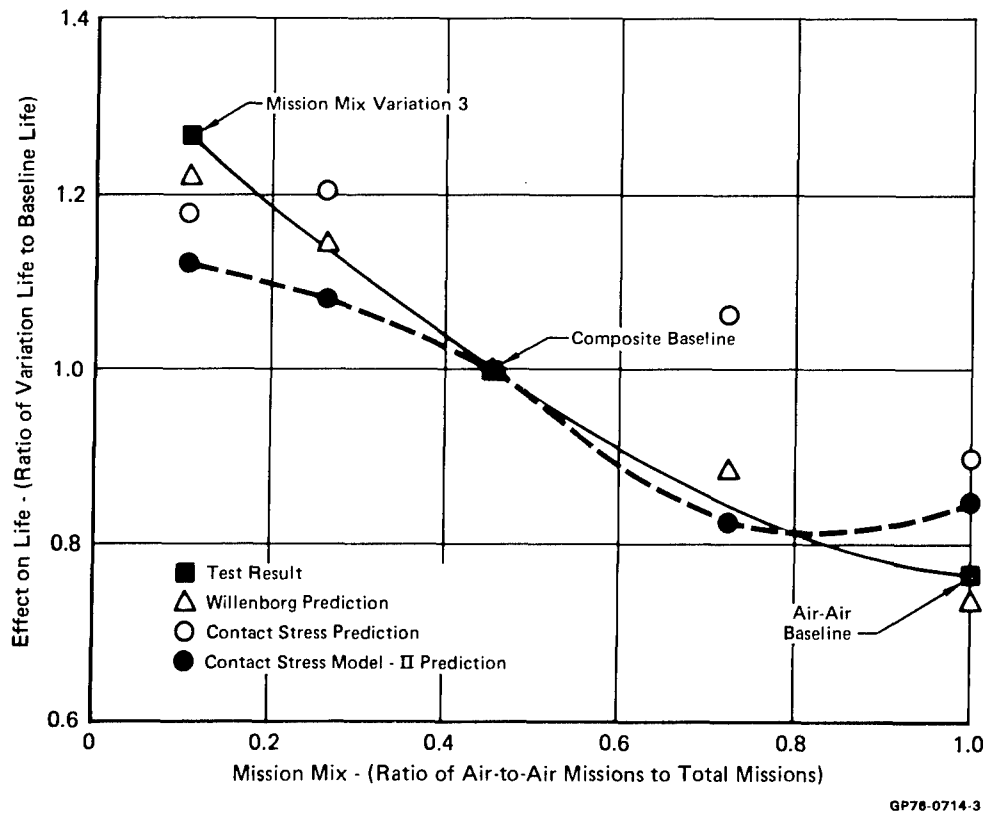
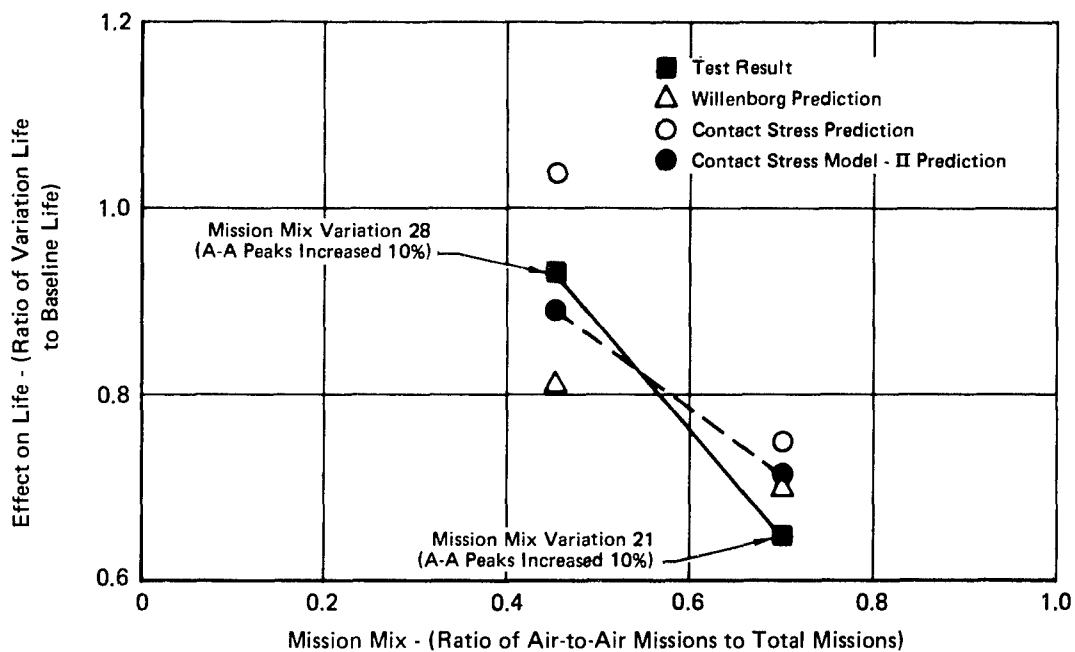


**FIGURE 37. MISSION MIX**  
Effect of Mission Mix on Crack Growth Life

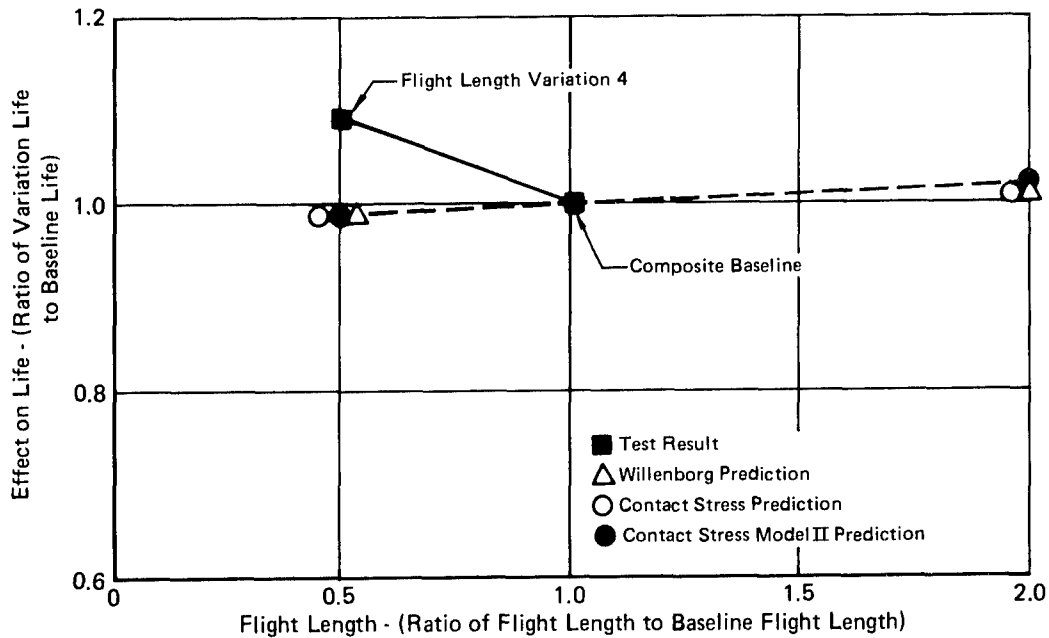


GP78-0714-4

**FIGURE 38. MISSION MIX**  
Effect of Increased Severity on Crack Growth Life

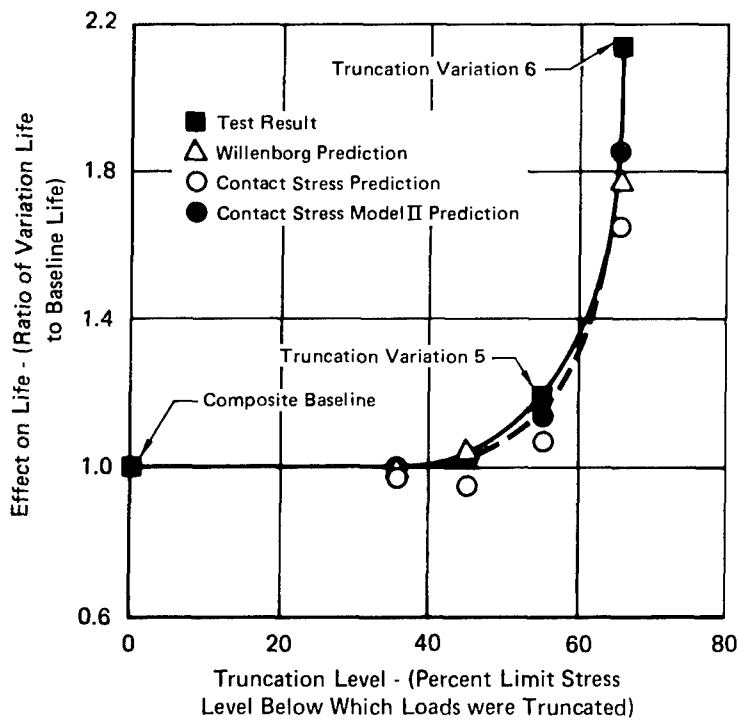
Individual Flight Length - The trend of the test data under flight length variations was not predicted by any of the models as indicated in Figure 39. As expected, all of the models predicted very small influence of flight length: slightly reduced life for half of the baseline flight length and slightly increased life for double the flight length. Test of variation 4, however, indicates that halving the flight length increased life by 10% over the Composite Baseline life. No explanation other than test scatter has been found for this unexpected result.

High and Low Load Truncation - Three separate types of high and low truncation were tested. These variations had the greatest impact on crack growth life of all the variations. The first variation is that of truncation of cycles having small peaks from the Baseline Composite spectrum. As shown in Figure 40 life of the Composite Baseline is sensitive to the truncation level imposed. When cycles with peaks below 45 percent DLS were removed from the spectrum very little effect on life was predicted. However, once cycles with peaks greater than 50 percent DLS were removed, crack growth life was predicted to increase markedly, reaching a factor of two over the baseline for variation 6 in which cycles with peaks less than 65% DLS were removed from the spectrum.



GP76-0714-5

**FIGURE 39. INDIVIDUAL FLIGHT LENGTH**  
Effect of Flight Length on Crack Growth Life



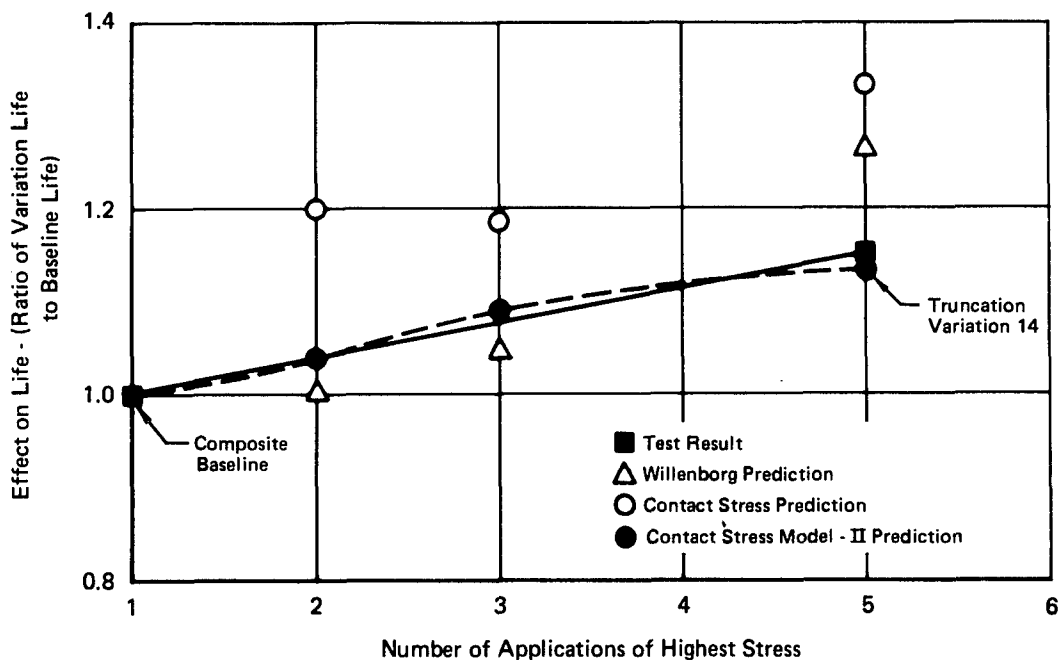
GP76-1008-16

**FIGURE 40. HIGH AND LOW LOAD TRUNCATION**  
Effect of Low Load Truncation on Crack Growth Life

Figure 41 shows the effect of the second truncation variation evaluated in test: repeated application of the highest stress in the spectrum. The highest stress in the Composite Baseline spectrum was 101.0% DLS. The results presented in Figure 41 indicate crack growth life is increased with number of applications of the highest stress.

The third truncation variation studied involved modifications of the highest loads in the spectrum. Shown in Figure 42 are the effects of such modifications on the Composite Baseline spectrum. Several variations involved adding a single overload cycle to the 1000 flight hour block. These variations had the most significant impact on crack growth life of all variations tested. A single cycle with a peak stress level of 135% DLS applied once every 1000 hours increased the crack growth life by more than a factor of six. In contrast, clipping the highest load in the spectrum to some lower level decreased the crack growth life, e.g., when loads were clipped to 85% DLS the life was 75% of the baseline value.

All of the crack growth models predicted the trends of high and low load truncation results.



GP76-0714-7

**FIGURE 41. HIGH AND LOW LOAD TRUNCATION**  
Effect of Repeating High Load Application on Crack Growth Life

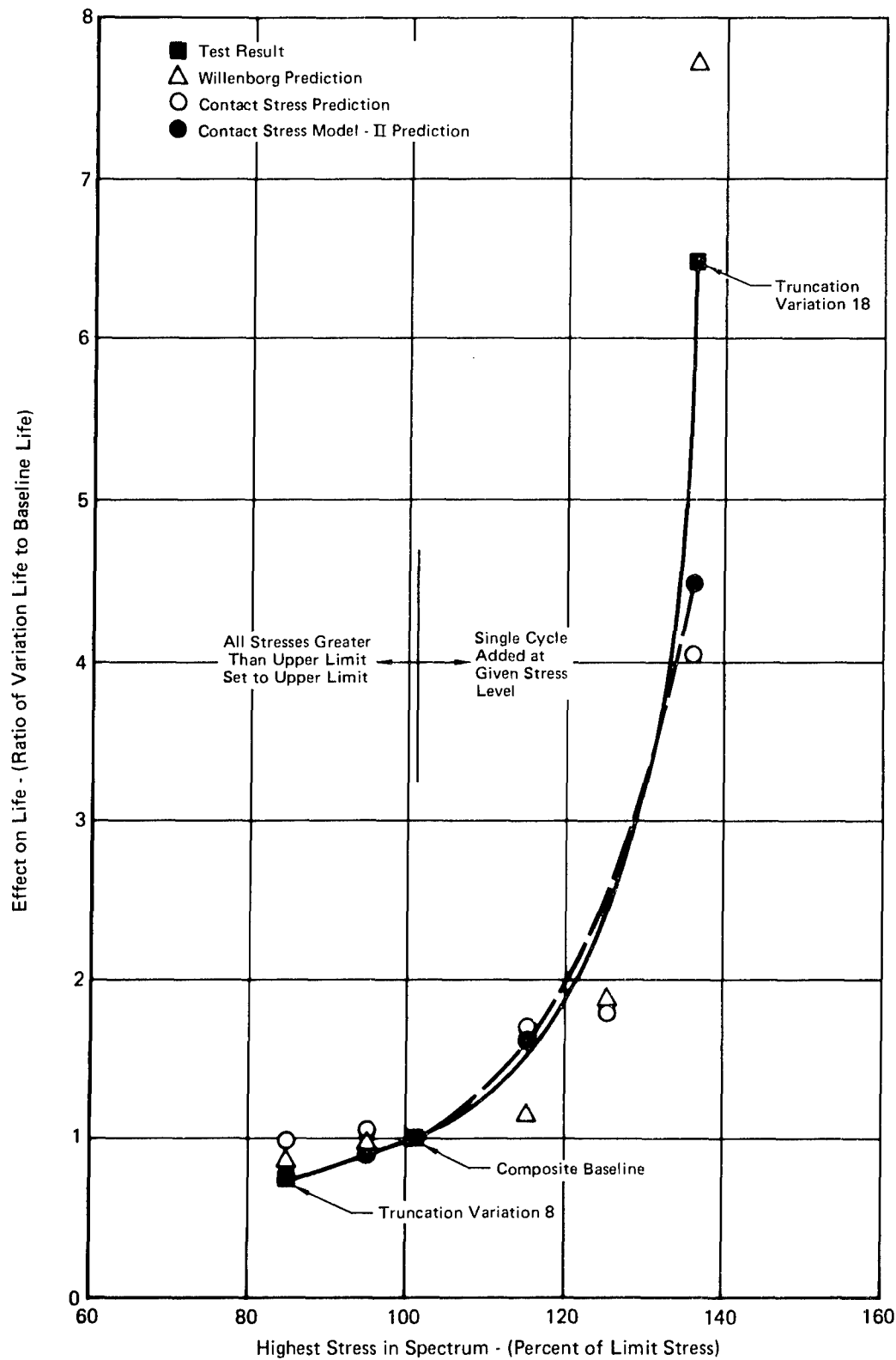


**FIGURE 42. HIGH AND LOW LOAD TRUNCATION**  
Effect of Modifying Highest Load Level in Spectrum on Crack Growth Life

Compression Loads - Compression loads were found to have moderate effects on crack growth life, as indicated in Figure 43. This figure indicates the effect of ground load variations on life as compared to the Composite Baseline spectrum life. The Composite Baseline spectrum includes ground loads of -5% DLS and -10% DLS. Increasing these loads to -30% DLS reduced life by 20 percent, while setting all ground loads to zero increased life by less than 10 percent. The Willenborg Model cannot account for compression load variations. The Contact Stress Model accurately predicted the life increase for reduced ground loads but did not account for effects of increased ground loads. The Contact Stress Model-II correlates much better with the trends of the test data, but overestimates the increase in life associated with clipping all negative loads to zero.

Another type of compression loads variation involved increasing the negative maneuver loads within the Composite Baseline spectrum. Results shown in Figure 44 and indicate this variation has no effect on life. This is probably due to the small number of negative maneuver loads within this spectrum and the small magnitude of these loads. The Willenborg Model and Contact Stress Model predict less effect than that resulting from test, while Contact Stress Model-II predicts a slightly larger effect than that measured from test.

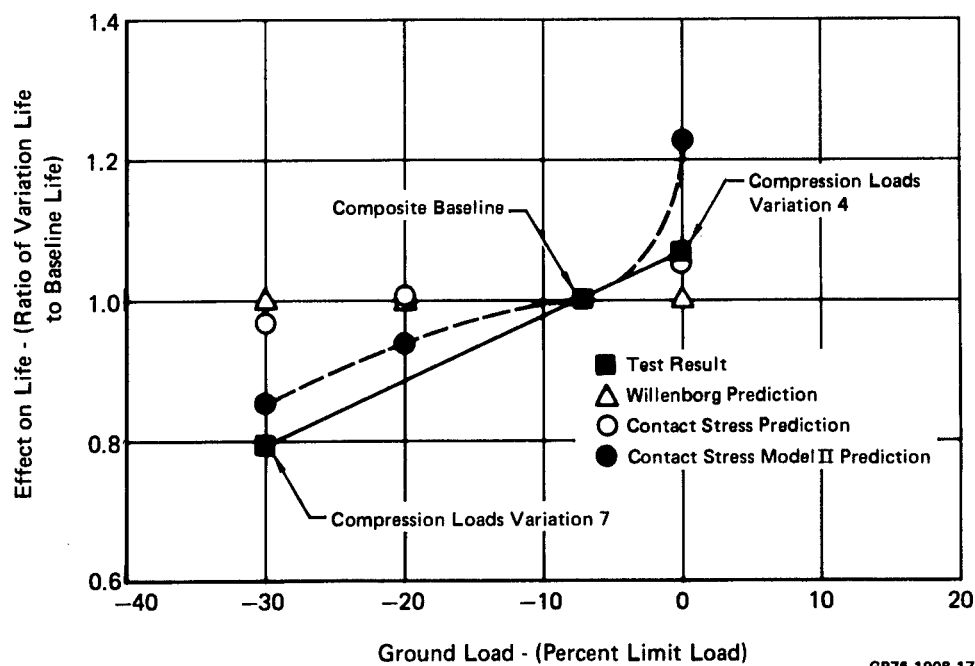
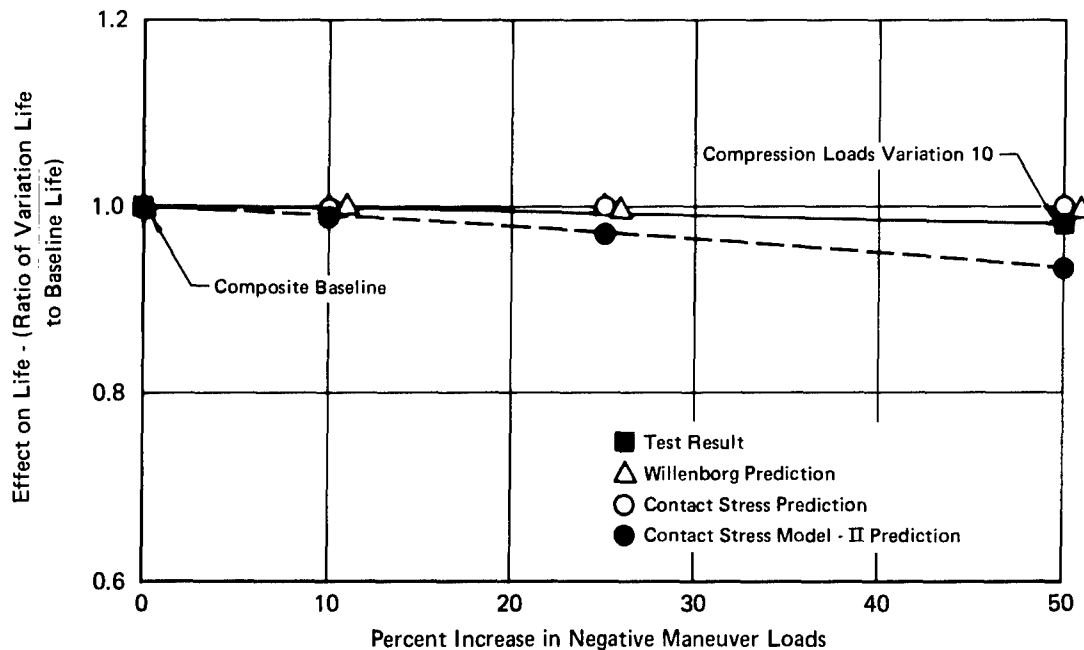


**FIGURE 43. COMPRESSION LOADS**  
Effect of Ground Load Variation on Crack Growth Life



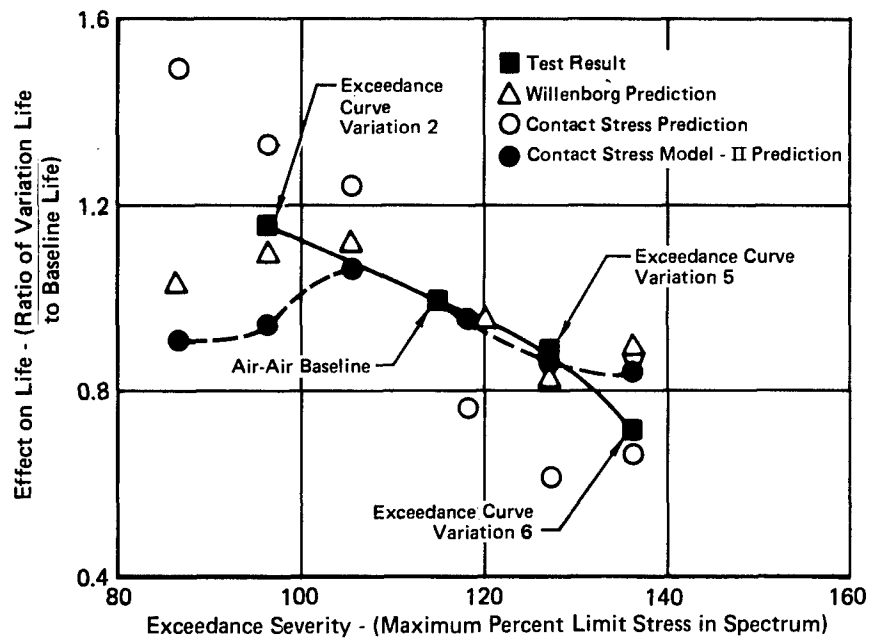


GP76-0714-10

**FIGURE 44. COMPRESSION LOADS**  
Effect of Increasing Maneuver Loads on Crack Growth Life

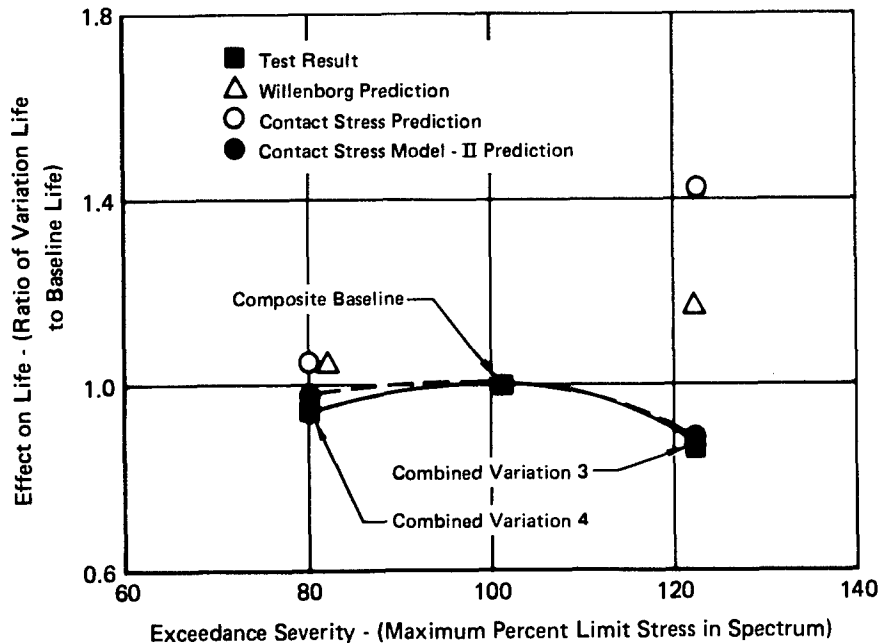
Exceedance Curve Variations - Exceedance curve variations are among the most common variations encountered during aircraft design and analysis. Figure 45 depicts the effect of these variations on crack growth life of the Air-to-Air Baseline spectrum; spectrum severity is characterized by the maximum stress level in the spectrum. Variations included three exceedance curves of lesser apparent severity and three curves of increasing apparent severity. The results indicate that crack growth life decreases monotonically with increasing apparent exceedance curve severity. The agreement between analysis and test is erratic for all the crack growth models.

Two of the combined variations dealing with exceedance curve variations of the Composite Baseline spectrum were tested. The Air-to-Air missions used in these variations were generated under the most mild and most severe of the previous exceedance curve variations. No other missions were affected. The variations summarized in Figure 46 produced different effects than the Air-to-Air exceedance variations summarized in Figure 45; the test data in Figure 46 indicate both mild and severe variations produced slight reductions in crack growth life. There is considerable difference in the predictions of the crack growth models for these variations.



GP76-0714-11

**FIGURE 45. EXCEEDANCE CURVE VARIATIONS**  
Effect of Exceedance Curve Variations of Air-Air Baseline Spectrum on Crack Growth Life

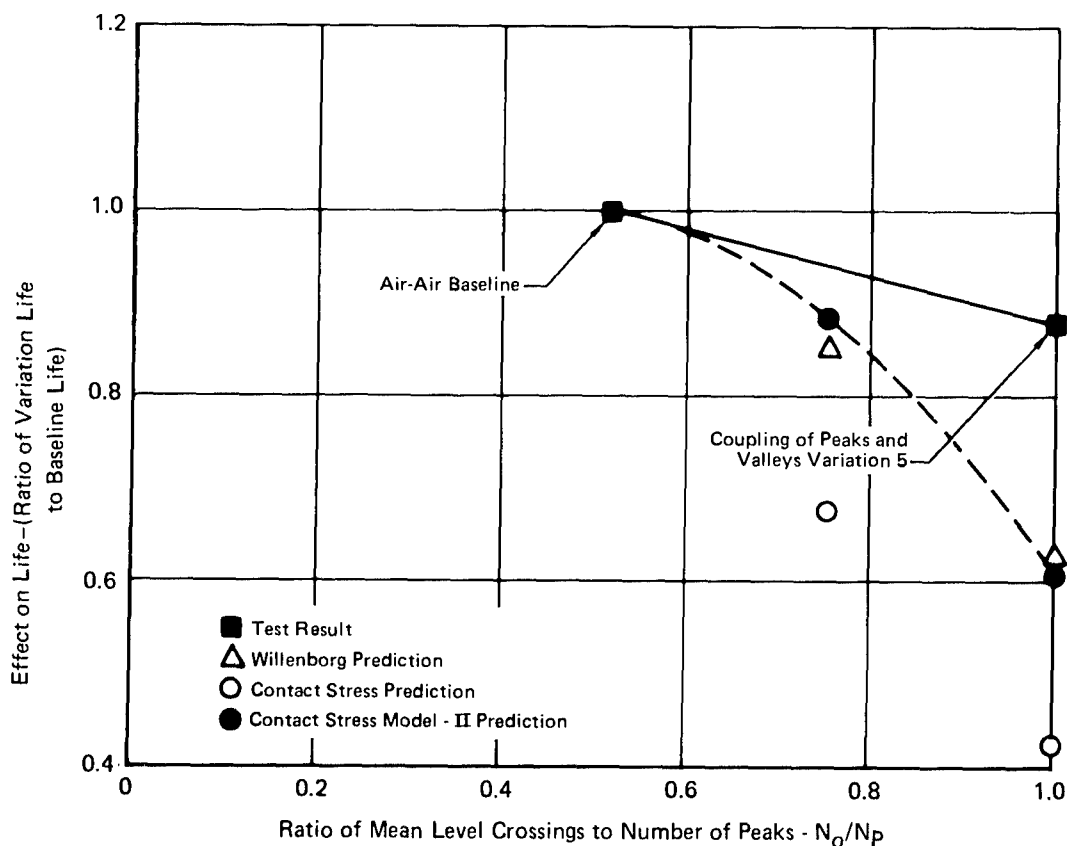


GP76-0714-12

**FIGURE 46. EXCEEDANCE CURVE VARIATIONS**  
Effect of Exceedance Curve Variations of Composite Baseline Spectrum on Crack Growth Life

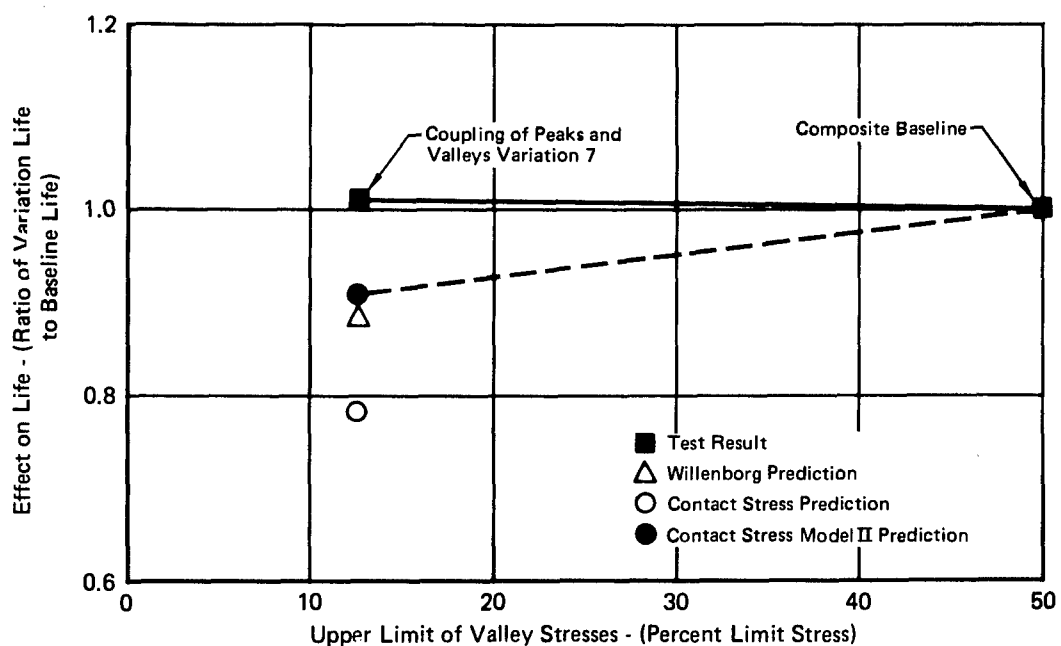
Coupling of Peaks and Valleys - Coupling of peaks and valleys was determined by the PSD shape used to generate the baseline spectra. Therefore, the impact of PSD shape variations on crack growth is of interest. Two variations of the Air-to-Air Baseline spectrum were created. Figure 47 presents the effects of these variations versus the  $N_o/N_p$  ratio described in Section 6.4. As  $N_o/N_p$  approaches unity, the load ranges are increased since peaks are forced to have valleys less than the mean stress. As expected, the test data shows a reduction in life when  $N_o/N_p = 1$ , but the reduction is not nearly as large as that predicted by the models. From these results it appears that further investigation into the effects of PSD shape on predicted crack growth life is warranted.

Variations in the coupling of peaks and valleys included limiting all valleys to a maximum of 1g (12.5% DLS). A single variation of this type was generated from the Composite Baseline spectrum and tested; the test result is presented in Figure 48 and indicates this variation has no effect on life.



GP78-0714-13

**FIGURE 47. COUPLING OF PEAKS AND VALLEYS**  
Effect of PSD Shape Variation on Crack Growth Life

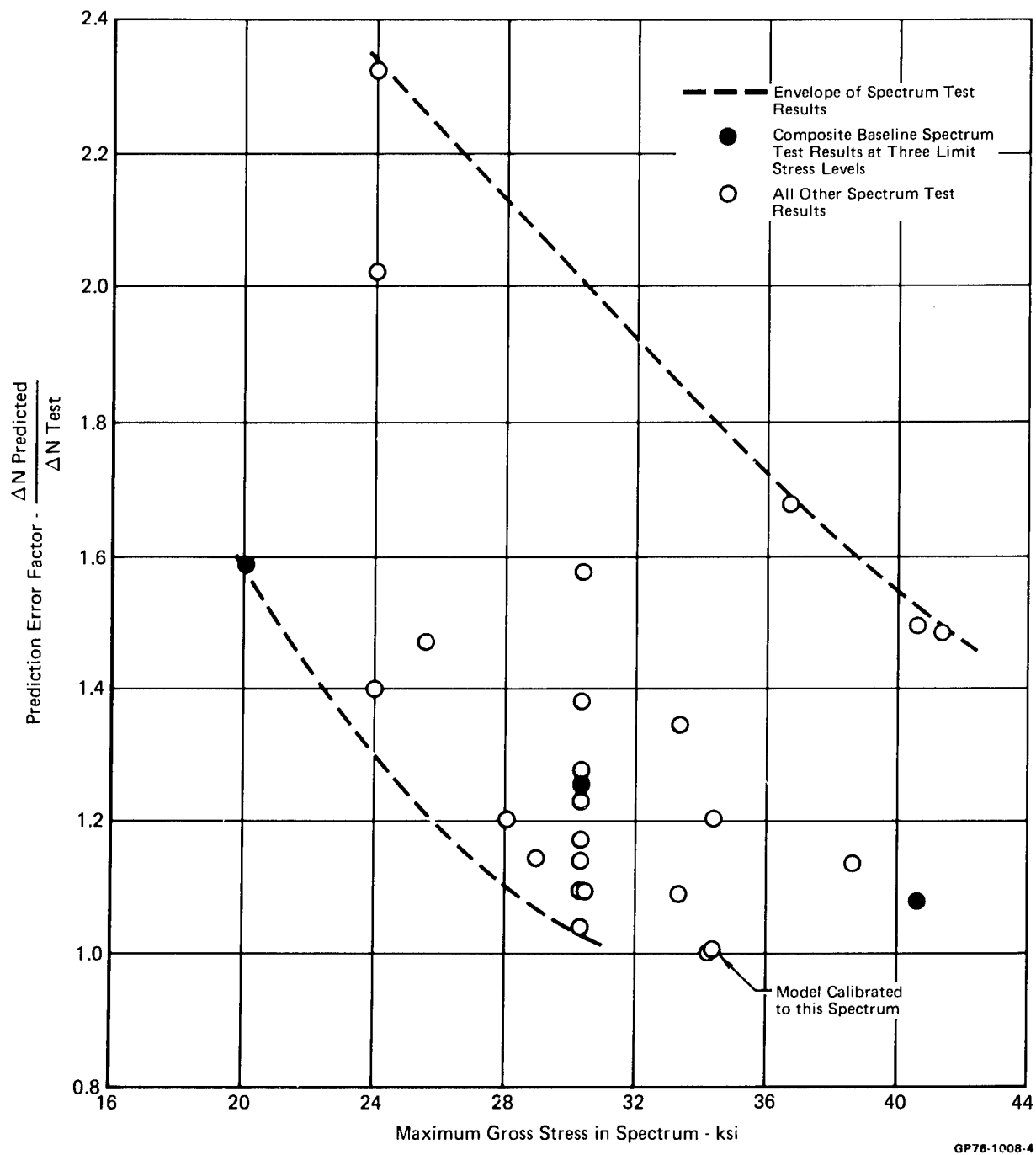


GP78-1008-18

**FIGURE 48. COUPLING OF PEAKS AND VALLEYS**  
Effect of Imposing 1 g Maximum Value on Valleys on Crack Growth Life

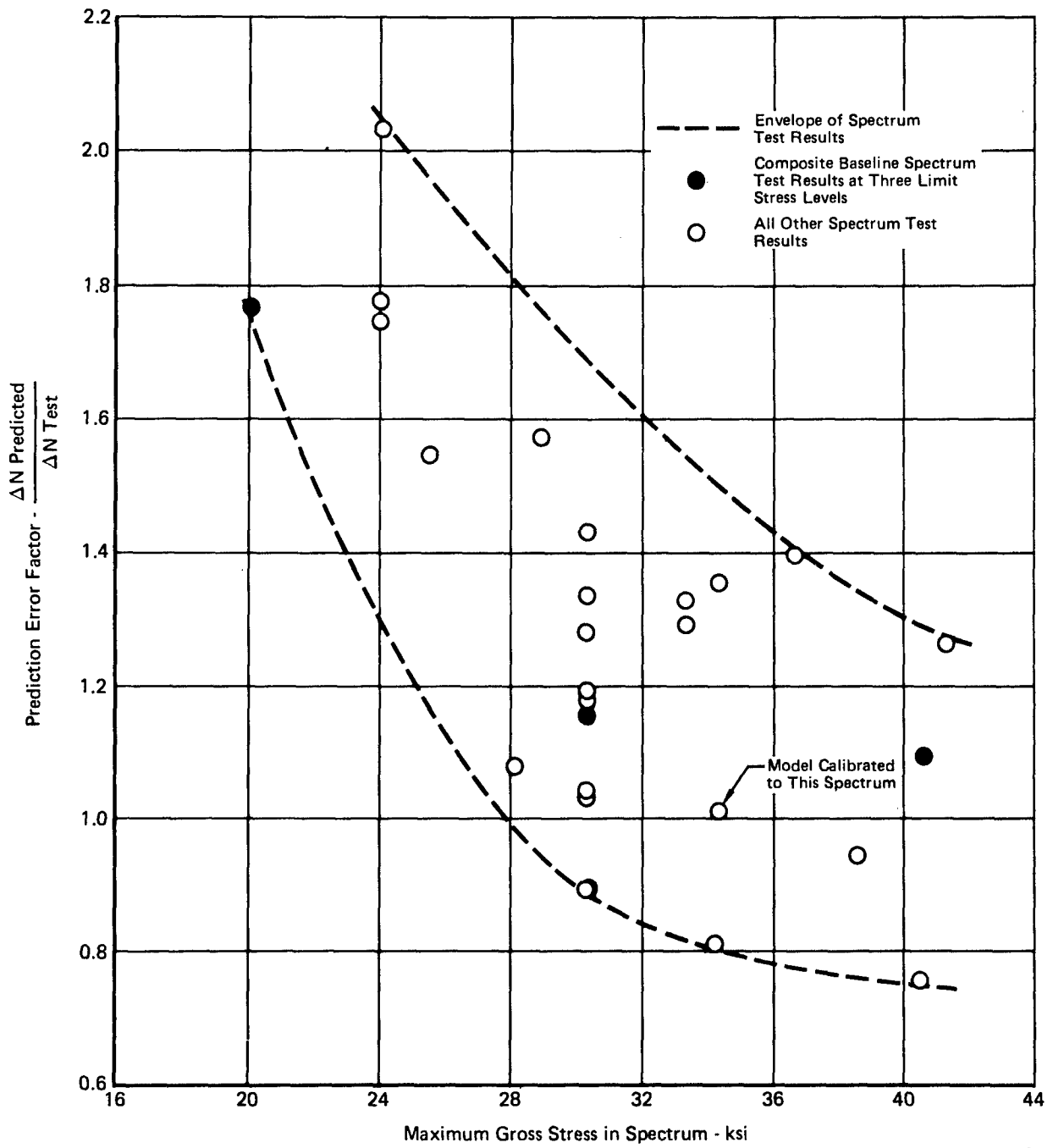
Test Limit Stress - The effects of test limit stress became apparent during the performance of the test program when it was found that the prediction errors of the Willenborg Model and Contact Stress Model could be correlated with the maximum stress level in each spectrum as shown in Figures 49 and 50. In order to assess these effects, two specimens were tested to the Composite Baseline spectrum, one at 19.8 ksi and one at 40.2 ksi DLS. Results of these tests and analyses are shown in Figure 51. As shown in Figures 51 and 52 the Contact Stress Model-II correlates best with this data since it accounts for the effects of residual stresses near the hole caused by high loads. Willenborg Model and Contact Stress Model do not correlate as well.

Summary - In conclusion, spectra variations involving mission mix, high and low load truncation, exceedance curves, and stress level appear to have the greatest impact on crack growth life. These factors probably encompass the main ingredients of spectrum development and could be expected to have the greatest impact on fatigue and fracture analyses. The most accurate of the crack growth models is the Contact Stress Model-II. The Willenborg Model appeared to be slightly more accurate than the Contact Stress Model in accounting for spectrum variations; however, the Contact Stress Model predicted the baseline spectra results more accurately than the Willenborg Model.



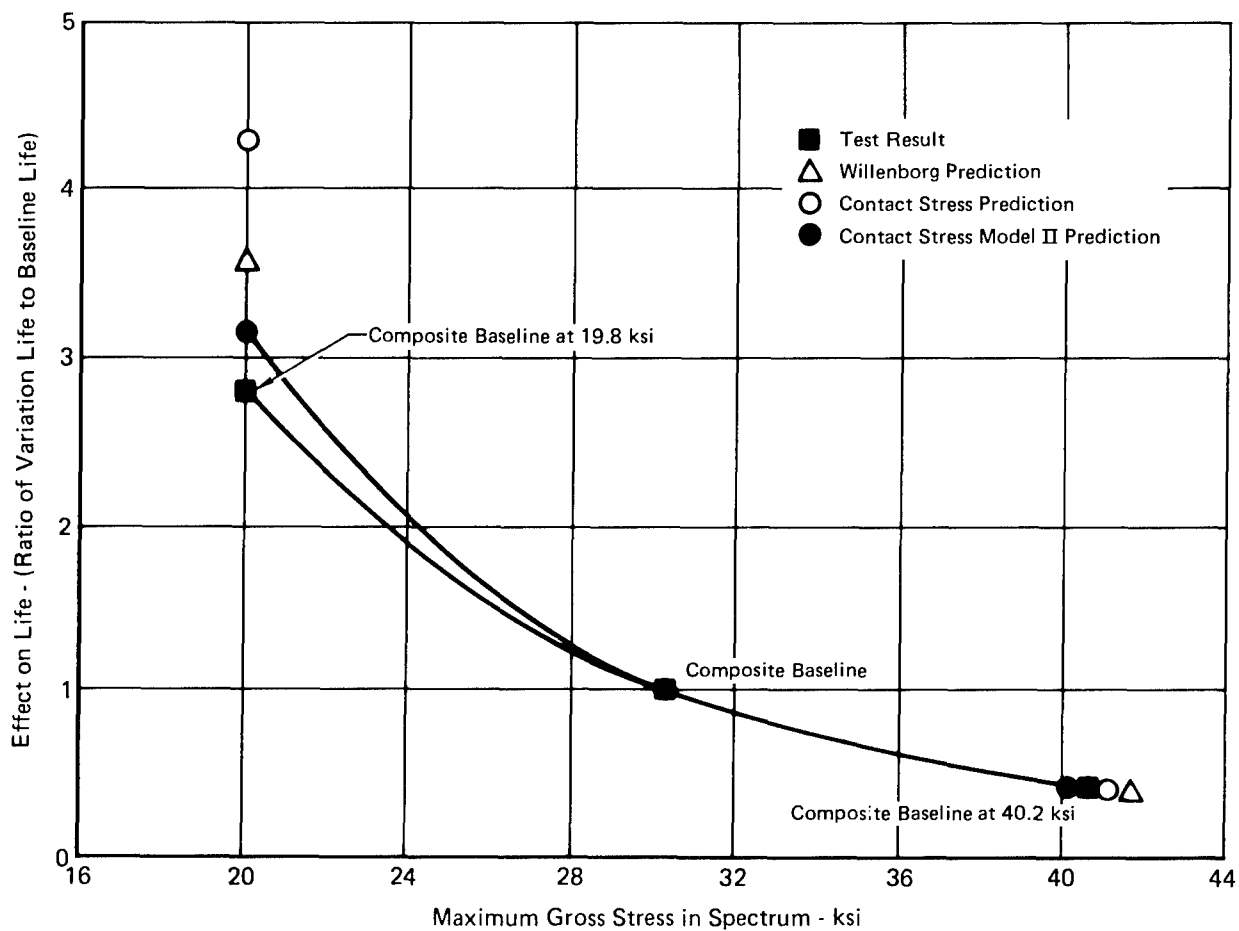
GP76-1008-4

**FIGURE 49. EFFECT OF STRESS LEVEL ON CRACK GROWTH PREDICTION WITH WILLENBORG MODEL**



GP76-1008-5

FIGURE 50. EFFECT OF STRESS LEVEL ON CRACK GROWTH PREDICTION WITH CONTACT STRESS MODEL



GP76-1008-6

**FIGURE 51. TEST LIMIT STRESS**  
Effect of Test Limit Stress on Crack Growth Life

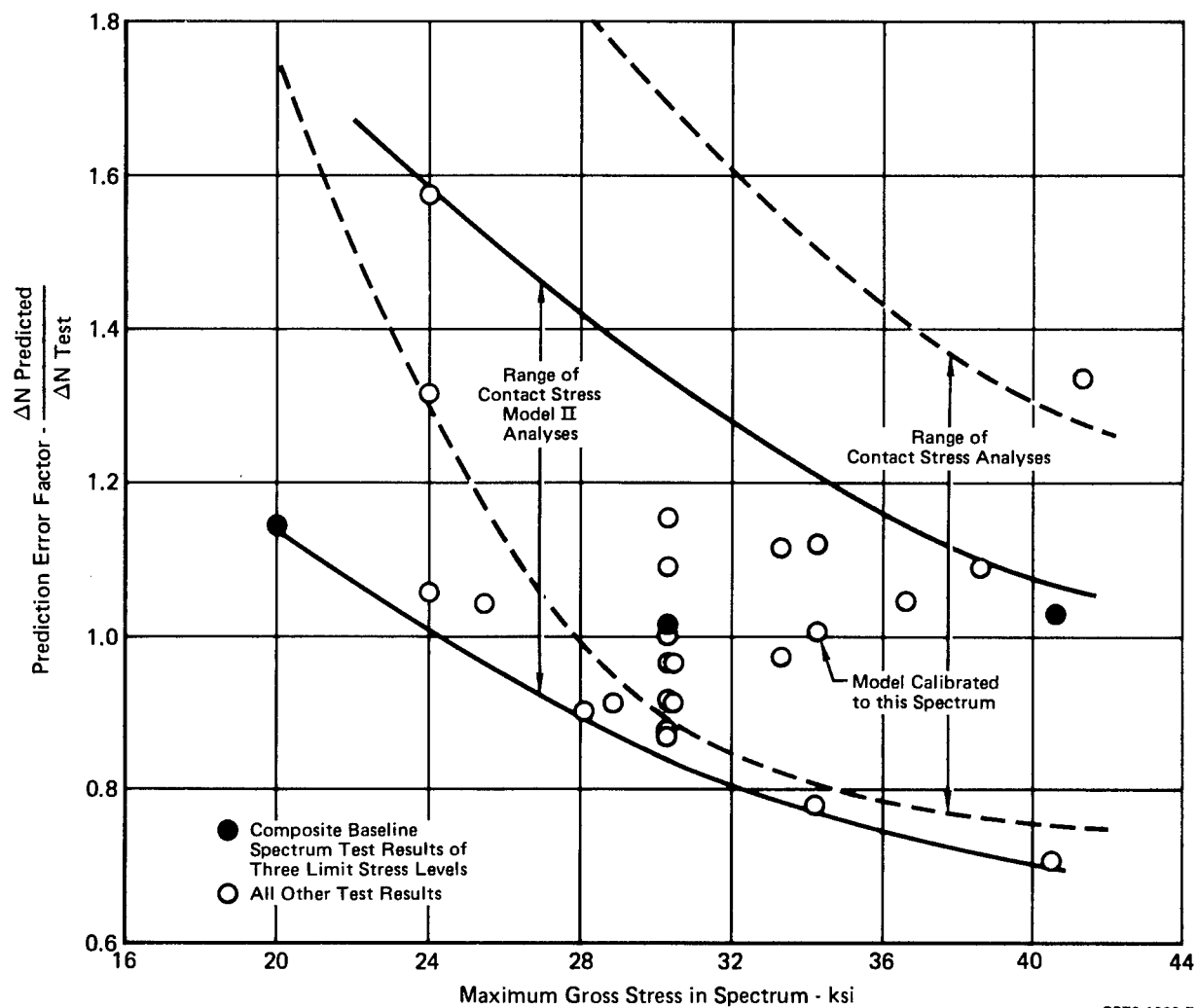


FIGURE 52. EFFECT OF STRESS LEVEL ON CRACK GROWTH PREDICTION WITH CONTACT STRESS MODEL II



## 7.2 Estimate of Range of Crack Growth that can Occur in a Fleet

During development of USAF damage tolerance requirements and fracture control procedures, numerous research programs were conducted to assess the impact of various factors on crack growth life. These factors included variations in material and fabrication processes, flight load and environment histories, structural geometries and attachments, initial flaw size assumptions, and failure modes. In a recent Air Force study, Reference 41, the relative effect of these factors on crack growth life was determined. Crack growth lives were computed for extreme variations in initial flaw size, service usage, crack growth rates, and fracture parameters. Spectrum variations and material crack growth rate variations were found to have the greatest impact on life. The interactions of these variations in fleet aircraft will produce a wider range of crack growth lives than any single variation. Fleet usage scatter is examined in this study.

One of the first extensive fleet usage monitoring programs was conducted on the F-4 aircraft. This program has provided a considerable knowledge of the fleet history of a multi-mission fighter/bomber aircraft. In a study to determine the effect of fleet usage variation on structural life (Reference 42) F-4 usage data was summarized to show the scatter in load factor exceedances as a function of the average fleet aircraft flight hours. Figures 53 and 54 present 4g and 6g usage scatter data, respectively, for Air Force aircraft. On each figure an estimate of the total scatter factor at the end of 1000 and 2000 flight hours is indicated. In both cases the scatter at the end of 2000 flight hours is considerably less than at 1000 flight hours. This trend reflects the fact that, as an aircraft accumulates flight time, it becomes more likely that the aircraft will be subjected to a variety of usages and its loading will have averaged to that of the rest of the fleet. As this averaging process continues with increasing flight time, the scatter will continue to decrease, so the scatter present at 2000 hours is an upper bound to that expected later in the fleet history.

To determine the impact of this usage scatter on crack growth, load spectra representing the upper and lower bounds of usage at 1000 and 2000 hours were developed. The Composite Baseline spectrum was selected to represent the average fleet usage. The upper and lower limits of the scatter data were determined at 4g's and 6g's which correspond to 50% DLS and 75% DLS on the Composite Baseline spectrum. Exceedance curves representing the upper and lower bounds at both 1000 and 2000 flight are shown in Figures 55 and 56,

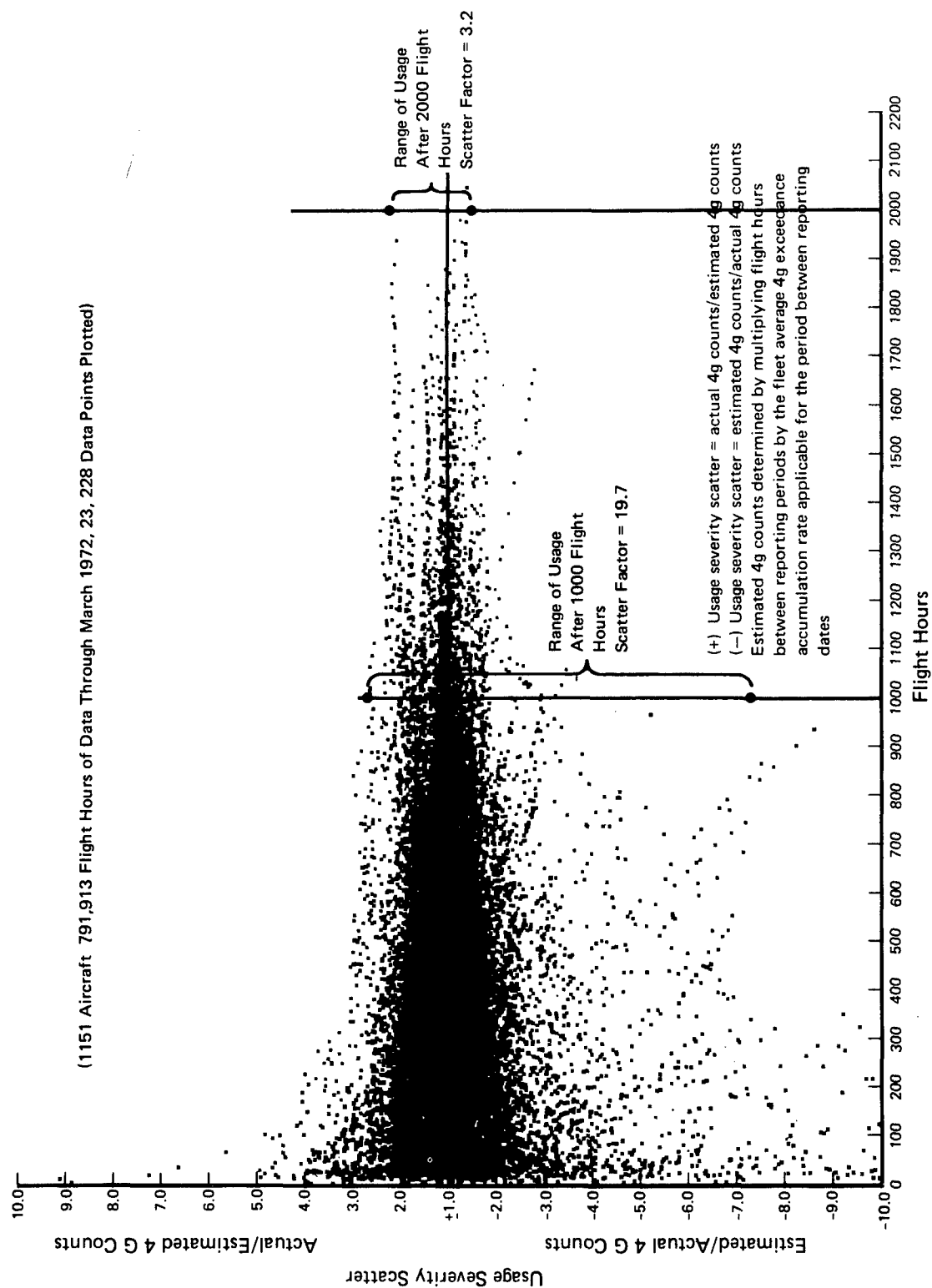
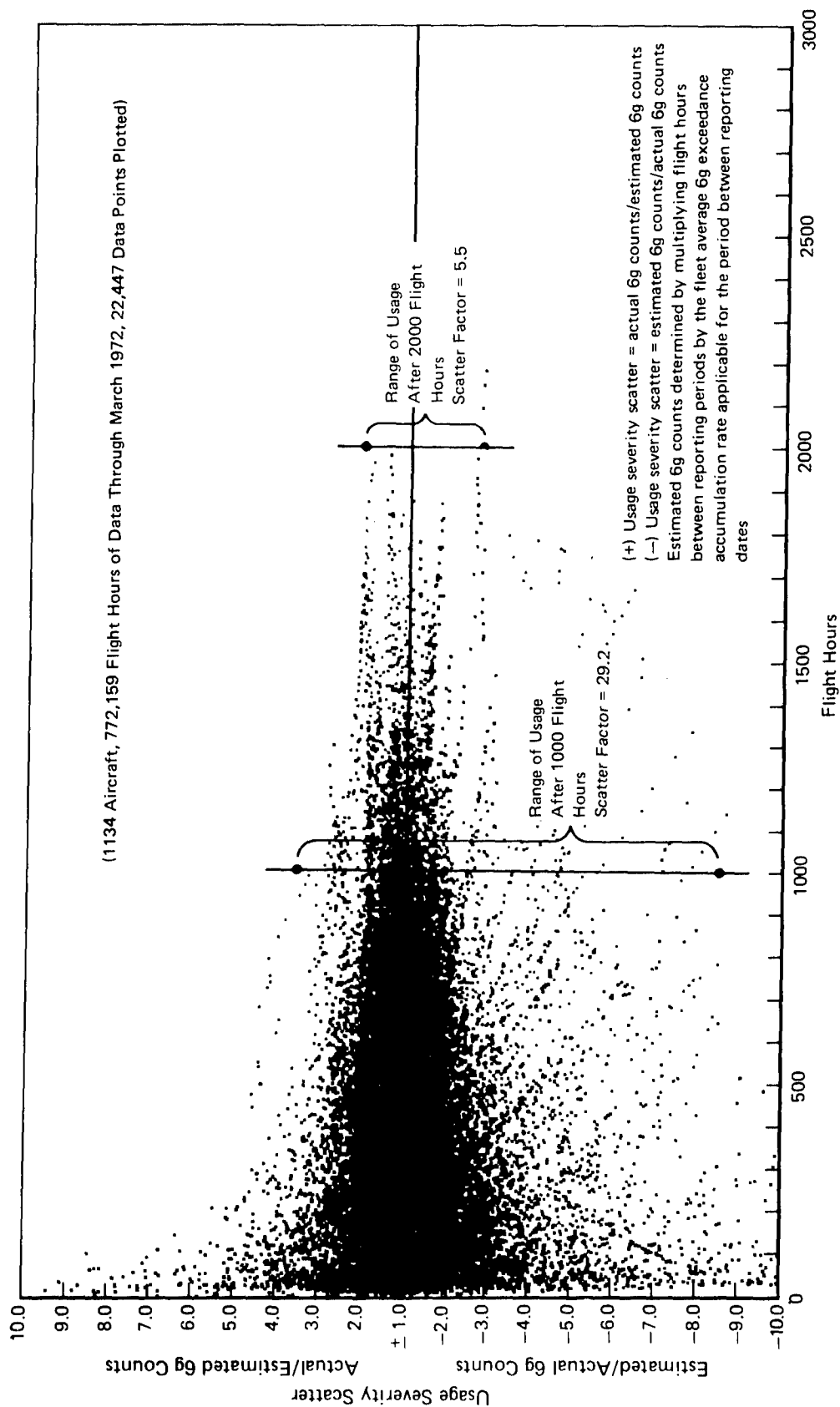


FIGURE 53. 4G USAGE SEVERITY SCATTER vs FLIGHT HOURS FOR AIR FORCE F-4 AIRCRAFT REPORTING COUNTING ACCELEROMETER DATA



GP76-0714-76

FIGURE 54. 6 G USAGE SEVERITY SCATTER vs FLIGHT HOURS FOR AIR FORCE F-4 AIRCRAFT  
REPORTING COUNTING ACCELEROMETER DATA

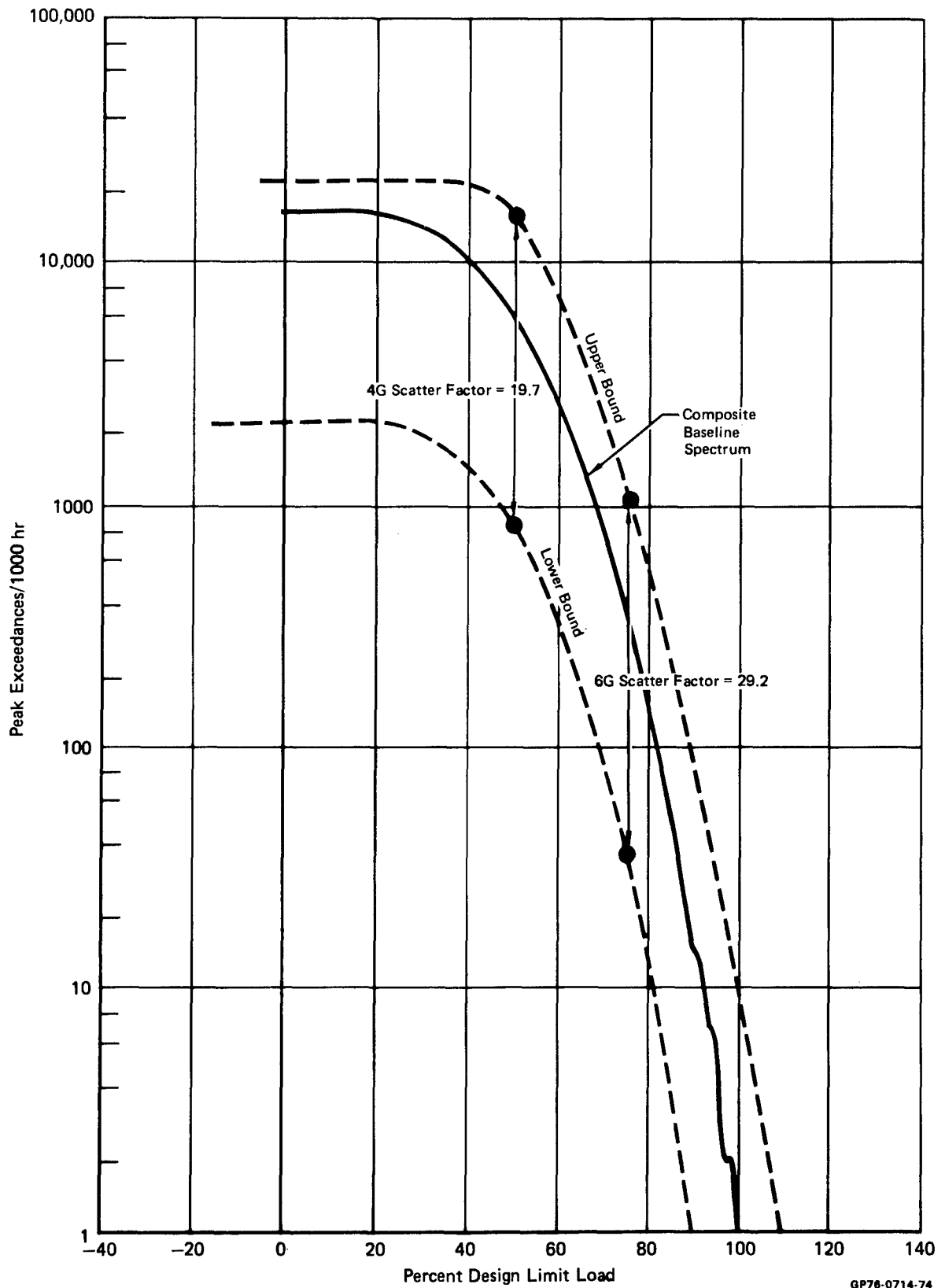


FIGURE 55. FLEET USAGE SCATTER AT 1000 FLIGHT HOURS

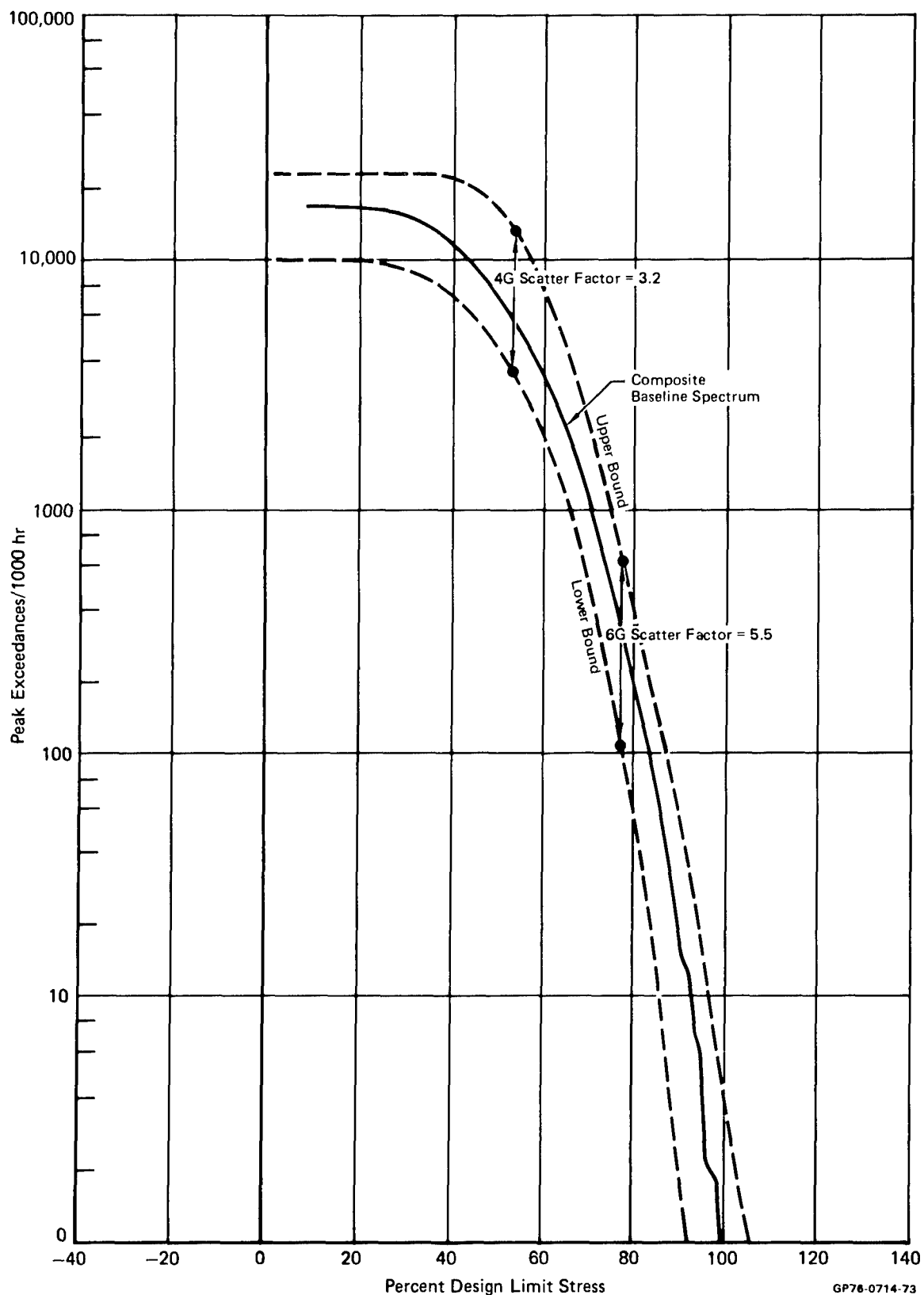


FIGURE 56. FLEET USAGE SCATTER AT 2000 FLIGHT HOURS

respectively. To develop the upper and lower bound cycle-by-cycle stress spectra, the sequence of peaks of the Composite Baseline spectrum was retained, and the values adjusted in order to match the upper or lower bound exceedance curves. For example, in Figure 55, the lower bound load corresponding to 90% DLS in the baseline spectrum is that load which is exceeded approximately 15 times per 1000 hours. On the lower bound curve this value is roughly 80% DLS. This type of load transformation was used for each peak load in the bounding spectra. Thus, the bounding spectra had the same load sequence as the baseline spectrum but had modified load values.

Crack growth predictions for the four usage bounds were computed with both the Willenborg Model and the Contact Stress Model-II. The initial flaw was assumed to be a 0.05 inch thru crack emanating from a 0.25 inch diameter hole. Results of these analyses are shown in Figures 57 and 58. These figures indicate that the crack growth predictions of the two models are nearly identical.

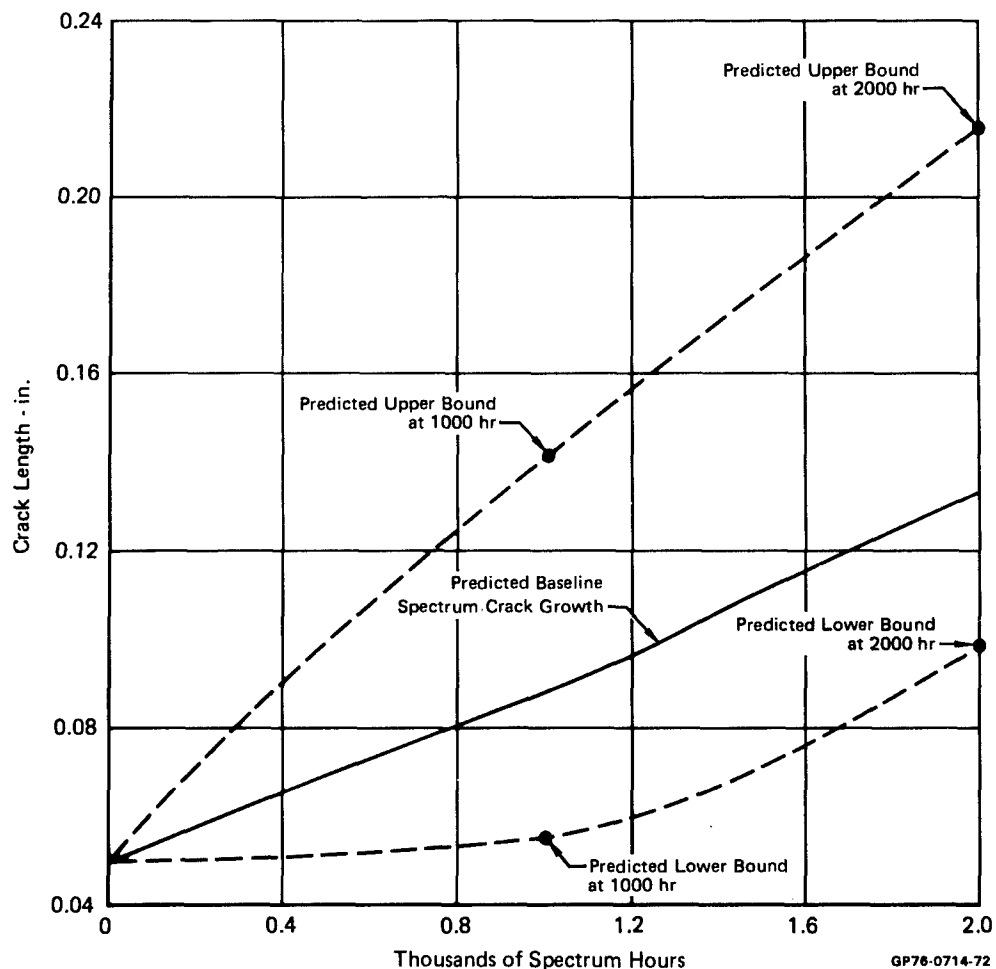
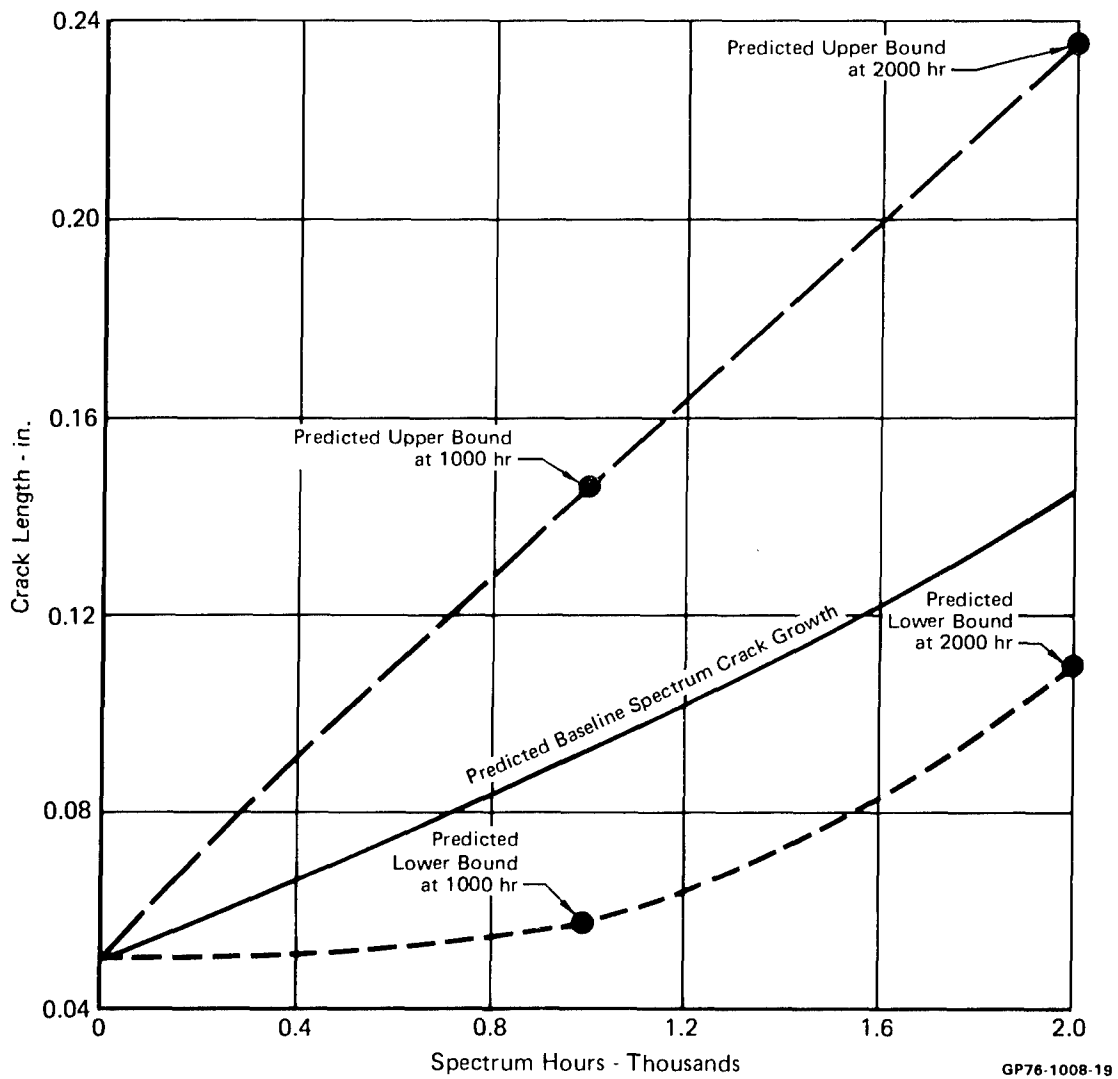


FIGURE 57. RANGE OF CRACK GROWTH PREDICTED BY WILLENBORG MODEL DUE TO FLEET USAGE SCATTER



**FIGURE 58. RANGE OF CRACK GROWTH PREDICTED BY CONTACT STRESS MODEL  
DUE TO FLEET USAGE SCATTER**

However, Table 21 shows that the Contact Stress Model-II predicts slightly faster crack growth and less scatter than the Willenborg Model. There is a small increase in the range of crack growth from 1000 to 2000 hours and a great decrease in scatter factor during the same time span. Figure 59 depicts the trend of crack growth scatter factor as fleet usage time increases. Since usage scatter factor is known to decrease with fleet usage, a corresponding decrease in crack growth scatter factor is expected as fleet usage increased.

The range of crack growth estimated in this study was predicted without consideration of material and geometric property variation or variations of load sequence and design limit stress. As such it represents the crack growth variations expected from fleet usage variation alone. Since material property variations and environmental attack can be expected to interact with individual aircraft usage to produce a wider range of crack growth rate than any single effect, the range of crack growth obtained in this study is expected to be less than the actual range of crack growth in a fleet.

**TABLE 21. SUMMARY OF CRACK GROWTH PREDICTIONS OF FLEET USAGE EFFECTS**

Usage Parameter	Crack Growth from 0.05 in.			
	Willenborg Model		Contact Stress Model - II	
	1000 hr	2000 hr	1000 hr	2000 hr
Upper Bound	0.09101	0.16612	0.09589	0.18612
Lower Bound	0.00508	0.04817	0.00728	0.05921
Range (Upper-Lower)	0.08593	0.11795	0.08861	0.12691
Scatter (Upper/Lower)	17.92	3.45	13.17	3.14

GP76-0714-70



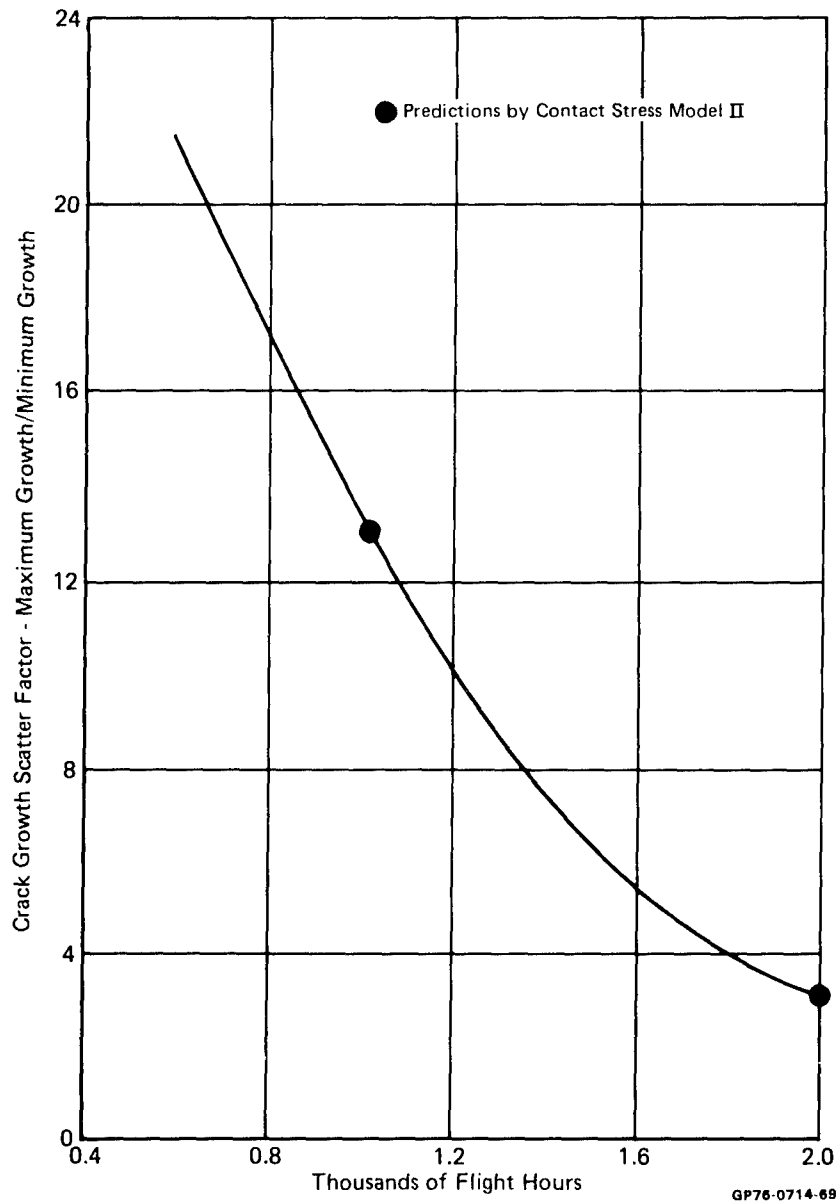


**FIGURE 59. VARIATION OF CRACK GROWTH SCATTER FACTOR WITH FLEET FLIGHT TIME**

### 7.3 Recommendations for Formulating Spectra

Spectra variations generated in this program represent stress levels and exceedance content of loads applied to the lower wing skin of a fighter aircraft; therefore the recommendations for spectra formulation is restricted to such applications. The development of spectra from the baseline stress exceedance curves presented in Figure 7 was the focus of this program. Table 19, page 75, summarizes the type and impact of variations that may be considered in developing spectra. As shown in that table, reordering of loads within a mission and individual flight length have little effect on crack growth. Sequence of missions, compression loads, and coupling of peaks and valleys have significant impact on crack growth. The greatest effect on crack growth is caused by mission mix, high and low load truncation, exceedance curve variations, and test limit stress level. Recommendations for formulating spectra, based on these observations, are outlined in the following paragraphs.

As shown in Table 13, the order of loads within a mission and individual flight length have minimum effect on crack growth rate. Therefore, any rational choice of order of loads within a mission and individual flight length will not lead to unrepresentative test results.

The effects of the sequence of missions, compression loads, and coupling of peaks and valleys is greater than for reordering of loads within a mission and individual flight length; however, the range of crack growth rate that can be expected from these variations is less than 50% of the baseline life, as shown in Table 19. This range is significant, but not so profound as to require extraordinary care in developing test spectra. Figure 36 indicates that a reasonable selection of sequence of missions will result in a representative crack growth life; even when missions were sequenced Hi-Lo and Lo-Hi for a 1000 hour block, the change in life from the baseline life was less than 30%. The effects of compression loads have similar impact; as indicated in Figures 43 and 44, there was less than 30% range in life for the greatest changes in compression loads considered in the test program. Difficulty in completely accounting for compression loads through analysis requires that they be included in test spectra. There was less than 20% change in life from the baseline life for the largest change in peak and valley coupling, as indicated in Figure 47. Sequence of missions might also be considered a type of peak and valley coupling, Figure 36 indicates sequence of mission variations caused less than 30% variation in life from the baseline

life. The PSD technique described in Section 3 is a good approach to obtain realistic peak and valley coupling.

Table 19 shows that the spectrum variations which cause greater than a 50% range in crack growth are mission mix, high and low load truncation, exceedance curve variations, and test limit stress. Of these, the greatest variations in life were caused by high and low load truncation. Figure 40 indicates that nearly an order of magnitude range in life can result from changes in the peak load applied in the spectrum. Truncation of high loads decreased life to about 70% of the baseline life for the most extreme case considered. However, adding single high loads increased the life to nearly 650% of the baseline for the most extreme case. Thus, the high loads in the spectrum exceedance are very important in determining crack growth life and care should be exercised in their selection to insure that they represent expected service usage. The high loads represent the extreme values of the probability distribution of peaks; accurate prediction of extreme values is more difficult than prediction of mean values or moderate probability values and greater care must be used. Figures 45, 46, and 49 show that when the exceedance curve is kept continuous, the effect of increasing the maximum stress is to reduce crack growth life. This in contrast to the effect of introducing single, discrete, high loads which is to increase crack growth life.

The selection, at the time of aircraft design, of the mission mix to be used in formulating spectra is based on mission analysis. Service experience has shown that the fleet use of aircraft can change from the original planned use, during the life of the fleet, as described in Reference 42, and this should be considered in formulating mission mix.

Figure 49 shows that test limit stress can significantly affect crack growth life, as expected. Stress levels in full scale fatigue tests are established by the structural arrangement and external loads, and therefore stress level is not an independent variable. In the design phase of an aircraft system, element tests at several limit stress values are used to aid in the selection of design limit stress and structural sizing, hence test limit stress is an independent variable. Figures 50, 51 and 52 show that one effect of stress level is upon prediction accuracy, which may vary significantly when applied to spectrum tests performed at different limit stress levels. All three models used in this study appear to overestimate life at lower limit stress-levels, or conversely underestimate life at higher limit stress levels. This effect should be considered when developing life estimates.

## 8. REFERENCES

1. Dill, H. D., Young, H. T., "Stress History Simulation, Vol. I - A User's Manual for a Computer Program to Generate Stress History Simulations," AFFDL-TR-76-113, Vol. I, November 1976.
2. Young, H. T., Foster, F. R., and Dill, H. D., "Stress History Simulation, Vol. II - A User's Manual for a Computer Program to Modify Stress History Simulations," AFFDL-TR-76 , Vol. II, November 1976.
3. Cooley, J. W., and Tukey, J. W., "An Algorithm for the Machine Calculation of Complex Fourier Series," Mathematics of Computations, Vol. 19, April 1965, p. 297.
4. IBM Manual C20-8011, "IBM Data Processing Techniques - Random Number Generation and Testing"
5. Wheeler, O. E., "Crack Propagation under Spectrum Loading," FZM-5602, 30 June 1970, General Dynamics, Forth Worth Division.
6. Willenborg, J., Engle, R. M., and Wood, H. A., "A Crack Growth Prediction Model Using an Effective Stress Concept," AFFDL-TM-71-1-FBR, 1971.
7. Vroman, G. A., "Analytical Prediction of Crack Growth Retardation Using a Residual Stress Concept," North American Rockwell, Los Angeles Division, May 1971.
8. Porter, T. R., "Method of Analysis and Prediction of Variable Amplitude Fatigue Crack Growth," Engineering Fracture Mechanics, Vol. 4, 1972.
9. Elber, W., "The Significance of Fatigue Crack Closure," Damage Tolerance in Aircraft Structures, ASTM STP 486, American Society of Testing and Materials, 1971, pp. 230-242.
10. Bell, P. D., et. al., "Crack Growth Analysis for Arbitrary Spectrum Loading," AFFDL-TR-74-129, Volume I, October 1974.
11. Dill, H. D. and Saff, C. R., "Spectrum Crack Growth Prediction Method Based on Crack Surface Displacement and Contact Analyses," Fatigue Crack Growth Under Spectrum Loads, ASTM STP 595, American Society for Testing and Materials, 1976, pp. 306-319.
12. Gallagher, J. P., and Hughes, T. F., "Influence of Yield Strength on Overload Affected Fatigue Crack Behavior in 4340 Steel," AFFDL-TR-74-27, March 1974.
13. Wood, H. A., "A Summary of Crack Growth Prediction Techniques," Chapter 8 of Fatigue Life Prediction for Aircraft Structures and Materials, AGARD LS 62, May 1973.

14. Engle, R. M., and Rudd, J. L., "Analysis of Crack Propagation Under Variable Amplitude Loading Using the Willenborg Retardation Model," AIAA Paper 74-369, Presented at the 15th Structures, Structural Dynamics and Materials Conference, April 17-19, 1974.
15. Dill, H. D., and Saff, C. R., "Analysis of Crack Growth Following Compressive High Loads Based on Crack Surface Displacements and Contact Analysis", MCAIR Report 76-006, April 1976.
16. Gallagher, J. P., "A Generalized Development of Yield Zone Models," AFFDL-TM-74-28-FBR, January 1974.
17. Forman, R. G., Kearney, V. E., and Engle, R. M., "Numerical Analysis of Crack Propagation in Cyclic-Loaded Structures," Journal of Basic Engineering, September 1967.
18. Probst, E. P., and Hillberry, B. M., "Fatigue Crack Delay and Arrest Due to Single Peak Tensile Overloads," AIAA Paper 73-325, AIAA Dynamics Specialists Conference, Williamsburg, Va., March 19-20, 1973.
19. Wei, R. P., and Shih, T. T., "Delay in Fatigue Crack Growth," International Journal of Fracture, Volume 10, No. 1, March 1974, pp. 77-85.
20. Gallagher, J. P. and Stalnaker, H. D., "Methods for Analyzing Fatigue Crack Growth Rate Behavior Associated with Flight-by-Flight Loading," AIAA Paper 74-367, Presented at the 15th Structures, Structural Dynamics, and Materials Conference, April 17-19, 1974.
21. Engle, R. M., "CRACKS II, User's Manual", AFFDL-TM-74-173.
22. von Ew, E. F. J., "Effect of Overload Cycle(s) on Subsequent Fatigue Crack Propagation in 2024-T3 Aluminum Alloy," Ph.D Thesis, 1971, Lehigh University, Bethlehem, Pa.
23. Trebules, V. W., Roberts, R. and Hertzberg, R. W., "The Effects of Multiple Overloads on Fatigue Crack Propagation in 2024-T3 Aluminum Alloy," Progress in Flaw Growth and Fracture Toughness Testing, ASTM STP 536, American Society for Testing and Materials, 1973, pp. 115-146.
24. McMillan, J. C., and Pelloux, R. M. N., "Fatigue Crack Propagation Under Program and Random Loads," Fatigue Crack Propagation, ASTM STP 415, Philadelphia, Pa., 1967, pp. 505-535.
25. Corbly, D. M. and Packman, P. F., "On the Influence of Single and Multiple Peak Overloads on Fatigue Crack Propagation in 7075-T6511 Aluminum," Engineering Fracture Mechanics, Volume 5, 1973, pp. 479-497.

26. Ho, C. L., Buck, O., and Marcus, H. L., "Application of Strip Model to Crack Tip Resistance and Crack Closure Phenomena," Progress in Flaw Growth and Fracture Toughness Testing, ASTM STP 536, American Society for Testing and Materials, 1973, pp. 5-21.
27. Jones, R. E., "Fatigue Crack Growth Retardation After Single-Cycle Peak Overload in Ti-6Al-4V Alloy," Engineering Fracture Mechanics, Volume 5, 1973, pp. 585-604.
28. Elber, W., "Equivalent Constant-Amplitude Concept for Crack Growth Under Spectrum Loading," Fatigue Crack Growth Under Spectrum Loads, ASTM STP 595, American Society for Testing and Materials, 1976, pp. 236-250.
29. Bell, P. D., and Wolfman, A., "Mathematical Modeling of Crack Growth Interaction Effects," Fatigue Crack Growth Under Spectrum Loads, ASTM STP 595, American Society for Testing and Materials, 1976, pp. 157-171.
30. Buck, O., Frandsen, J. D., and Marcus, H. L., "Spike Overload and Humidity Effects on Fatigue Crack Delay in Al 7075-T651," Fatigue Crack Growth Under Spectrum Loads, ASTM STP 595, American Society for Testing and Materials, 1976, pp. 101-112.
31. Alzos, W. X., Skat, A. C., Jr., and Hillberry, B. M., "Effect of Single Overload/Underload Cycles on Fatigue Crack Propagation," Fatigue Crack Growth Under Spectrum Loads, ASTM STP 595, American Society for Testing and Materials, 1976, pp. 41-60.
32. Grandt, A. F., Jr. and Gallagher, J. P., "Proposed Fracture Mechanics Criteria to Select Mechanical Fasteners for Long Service Lives," Fracture Toughness and Slow-Stable Cracking, ASTM STP 559, American Society for Testing and Materials, 1974, pp. 283-297.
33. Rice, J. R., "Mechanics of Crack Tip Deformation and Extension by Fatigue," Fatigue Crack Propagation, ASTM STP 415, American Society for Testing and Materials, 1967, pp. 247-309.
34. Nordmark, G. E. and Kaufman, J. G., "Fatigue Crack Propagation Characteristics of Aluminum Alloys in Thick Sections," Alcoa Research Lab, 1970.
35. Brownhill, D. J., Babilon, C. F., Nordmark, G. E., and Sprowls, D. O., "Mechanical Properties, Including Fracture Toughness and Fatigue, Corrosion Characteristics and Fatigue Propagation Rates of Stress Relieved Aluminum Alloy Hand Forgings," AFML-TR-70-10, Alcoa, 1970.
36. MCAIR MDC A2883, "F-4 Fatigue and Damage Tolerance Assessment Program - Volume II," June 1974.
37. Campbell, J. E., Berry, W. E., and Feddersen, C. E., "Damage Tolerant Design Handbook," Wright-Patterson Air Force Base, 1972.

38. MCAIR MDC A2883, "F-4 Fatigue and Damage Tolerance Assessment Program - Volume I," June 1974.
39. Gallagher, J. P., and Bader, R. M., "A Normalization Scheme for Describing Crack Growth Behavior," Presented at the 4th Army Materials Technology Conference, September 1975.
40. Dowling, N. E., "Fatigue Failure Predictions for Complicated Stress-Strain Histories," Journal of Materials, JMLSA, Volume 7, No. 1, March 1972, pp. 71-87.
41. Wood, H. A., "Application of Fracture Mechanics to Aircraft Structural Safety," Engineering Fracture Mechanics, Volume 7, 1975, pp 557-564.
42. Impellizzeri, L. F., Siegel, A. E., and McGinnis, R. A., "Evaluation of Structural Reliability Analysis Procedures as Applied to a Fighter Aircraft," AFML-TR-73-150, September 1973.

## APPENDIX - EXPERIMENTAL DATA

### Constant Amplitude Crack Growth Data

Constant amplitude crack growth data generated in this study are presented in Tables A-1 thru A-3. These tables contain a record of the total number of load cycles applied to the specimen prior to measuring crack length, the maximum load applied during the accumulated cycles, surface measurements of crack length, and the average measured length. The test procedure used to develop these data is presented in Section 5.3 and the constant amplitude test results are summarized in Section 5.4

### Baseline Spectra Crack Growth Data

Data recorded during and after baseline spectra crack growth tests are presented in Tables A-4 thru A-11. These data include surface measurements of crack length on each side of the specimen at each hole, records of the spectrum hours applied prior to measurement, and the results of fractographic examinations to determine the crack length at the mid-plane (center) of the specimen for one crack in each of the test specimens. The test procedure used to develop these data is presented in Section 5.3 and the test results are summarized in Section 6.3

Crack growth from the side of the hole opposite the intended flaw was measured whenever it was noted to occur during test, however, no fractographic examination of this growth was performed. During the post-test fractographic examinations, prominent striations were identified and correlated with the known sequence of high loads in each test spectrum. The crack length measured at each prominent striation could then be correlated with the cumulative number of spectrum hours. Crack front curvature throughout all of the spectrum tests appears from fracture surface observation to have been convex, however, a few of the fractographic measurements at the specimen mid-plane (center), when compared to the surface measurement taken during testing, are not consistent with this observation. In these cases the surface measurements were taken to be more reliable due to the difficulty in fractographically determining the occurrence of particular loads. In studying the fracture surface of a specimen tested to random load spectra such as these, it is difficult to determine whether a particular striation was caused by a high peak load or a smaller load which was not affected by retardation. This problem makes fractographic study of random load spectra test specimens somewhat difficult. In addition, as crack growth became rapid prior to fracture, high loads appeared to cause significantly more crack



growth at the mid-plane than at the surface during a single load application. This growth is referred to as a static burst in these and subsequent tables. All comparisons with test data reported in Section 6.3 were made to the average of the surface measurements of each specimen.

#### Spectra Variations Crack Growth Data

Data recorded from tests of spectra variations are presented in Tables A-12 thru A-33. These data include surface measurement of crack lengths, records of the spectrum hours applied prior to measurement, and the results of fractographic examinations of the test specimens. The test procedure used to develop these data is presented in Section 5.3 and test results are summarized in Sections 6.4 and 7.1. The post-test fractographic examinations were performed in the same manner as for the baseline spectrum tests. Fractographic measurements occasionally indicated concave crack front curvature not shown by direct observation of the fracture surface. In these cases the surface measurements are assumed to be more reliable. All comparisons with test data are based on the average of the surface measurement data.

**TABLE A-1**  
**CONSTANT AMPLITUDE CRACK GROWTH DATA, R = 0.02**

Cycles	Maximum Load (kip)	Crack Length		
		Side 1 (in.)	Side 2 (in.)	Average (in.)
0	9.2	—	—	(Precrack) 0.200
5,566	↓	0.220	0.200	0.210
15,566		0.230	0.227	0.228
25,566		0.250	0.243	0.247
35,566		0.280	0.275	0.278
45,566		0.290	0.310	0.300
55,566		0.320	0.320	0.320
65,566		0.350	0.370	0.360
75,566		0.400	0.420	0.410
85,566		0.450	0.470	0.460
95,566		0.520	0.550	0.535
105,566		0.620	0.630	0.625
115,566		0.720	0.720	0.720
125,566		0.830	0.850	0.840
130,566		0.900	0.900	0.900
133,066		0.950	0.950	0.950
135,566		1.000	1.000	1.000
137,566		1.040	1.040	1.040
139,566	↓	1.060	1.060	1.060
140,566	9.2	1.100	1.100	1.100
141,066	12.0	1.110	1.110	1.110
143,066	↓	1.200	1.200	1.200
145,066		1.310	1.310	1.310
147,066	↓	1.450	1.450	1.450
147,566	12.0	1.500	1.500	1.500
148,566	15.3	1.720	1.720	1.720
149,463	15.3	2.000	2.000	2.000
149,927	17.0	2.500	2.500	2.500
149,966	19.0	2.900	2.900	2.900

GP76-0803-1

**TABLE A-2**  
**CONSTANT AMPLITUDE CRACK GROWTH DATA, R = 0.5**

Cycles	Maximum Load (kip)	Crack Length		
		Side 1 (in.)	Side 2 (in.)	Average (in.)
0	11.25	—	—	(Precrack) 0.190
8,100		0.22	0.19	0.210
18,100		0.23	0.20	0.215
28,100		0.24	0.20	0.220
38,100		0.25	0.21	0.230
48,100		0.26	0.22	0.240
58,100		0.27	0.22	0.245
68,100		0.28	0.23	0.255
78,100		0.28	0.25	0.265
88,100		0.29	0.26	0.275
98,100		0.30	0.27	0.285
108,100		0.31	0.28	0.295
118,100		0.33	0.29	0.310
128,100		0.35	0.30	0.325
138,100		0.36	0.31	0.335
148,100		0.38	0.32	0.350
158,100		0.39	0.35	0.370
168,100		0.41	0.37	0.390
178,100		0.43	0.40	0.415
188,100		0.45	0.43	0.440
198,100		0.49	0.47	0.480
208,100		0.54	0.50	0.520
213,100		0.56	0.52	0.540
218,100		0.58	0.56	0.570
228,100		0.63	0.60	0.615
238,100		0.68	0.66	0.670
243,100		0.72	0.70	0.710
248,100		0.76	0.74	0.750
253,100		0.80	0.78	0.790
258,100	11.25	0.86	0.83	0.845

GP76-0803-2

**TABLE A-2 (Concluded)**  
**CONSTANT AMPLITUDE CRACK GROWTH DATA, R = 0.5**

Cycles	Maximum Load (kip)	Crack Length		
		Side 1 (in.)	Side 2 (in.)	Average (in.)
263,100	11.25	0.89	0.87	0.880
268,100	↓	0.93	0.93	0.930
273,100		0.98	0.98	0.980
275,100		1.00	1.00	1.000
277,100		1.02	1.02	1.020
279,100		1.05	1.05	1.050
281,100	↓	1.08	1.08	1.080
282,100	11.25	1.10	1.10	1.100
284,100	12.00	1.12	1.12	1.120
286,100	↓	1.15	1.15	1.150
289,100		1.20	1.20	1.200
292,100		1.24	1.24	1.240
295,100		1.30	1.30	1.300
298,100		1.35	1.35	1.350
300,100		1.42	1.42	1.420
303,100	↓	1.48	1.48	1.480
303,551	12.00	1.50	1.50	1.500
304,551	15.30	1.55	1.55	1.550
305,551	↓	1.60	1.60	1.600
306,551		1.70	1.70	1.700
307,551	↓	1.78	1.78	1.780
309,551	15.30	2.00	2.00	2.000
310,100	17.00	2.10	2.10	2.100
311,165	19.00	2.50	2.50	2.500
311,396	19.00	2.80	2.80	2.800

GP76-0803-44

**TABLE A-3**  
**CONSTANT AMPLITUDE CRACK GROWTH DATA,  $R = -0.3$**

Cycles	Maximum Load (kip)	Crack Length		
		Side 1 (in.)	Side 2 (in.)	Average (in.)
0	9.2	—	—	(Precrack) 0.208
10,000	↓	0.243	0.197	0.220
20,000		0.273	0.228	0.250
30,000		0.313	0.262	0.290
40,000		0.370	0.310	0.340
50,000		0.450	0.380	0.415
60,000		0.510	0.450	0.480
70,000		0.600	0.520	0.560
80,000		0.700	0.640	0.670
84,738		0.780	0.700	0.740
86,738		0.800	0.740	0.770
89,738		0.850	0.780	0.815
92,238		0.880	0.820	0.850
94,738		0.920	0.860	0.890
97,238		0.960	0.900	0.930
99,738		1.010	0.960	0.985
101,738		1.040	1.000	1.020
102,738		1.050	1.020	1.035
103,738	↓	1.090	1.030	1.060
104,738	9.2	1.100	1.060	1.080
106,738	12.0	1.200	1.190	1.195
107,738	↓	1.270	1.260	1.265
108,738		1.340	1.340	1.340
109,238		1.380	1.380	1.380
109,738		1.420	1.420	1.420
109,938		1.440	1.440	1.440
110,238	↓	1.460	1.460	1.460
110,567	12.0	1.500	1.500	1.500
111,567	15.3	1.820	1.820	1.820
111,738	↓	1.900	1.900	1.900
111,838	15.3	2.000	2.000	2.000
112,088	17.0	2.200	2.200	2.200
112,288	17.0	2.500	2.500	2.500
112,307	19.0	2.900	2.900	2.900

GP76-0803-3

**TABLE A-4**  
**PRELIMINARY AIR-TO-AIR BASELINE SPECTRUM CRACK GROWTH DATA**  
**Specimen 1**

Spectrum (hr)	Crack Length at Hole 1			Crack Length at Hole 2		
	Side A (in.)	Side B (in.)	Center (in.)	Side A (in.)	Side B (in.)	Center (in.)
0	—	—	—	—	—	0.0278
500	0.042	0.045	—	0.045	0.030	—
880	—	—	—	—	—	0.0464
1000	0.065	0.064	—	0.066	0.050	—
1500	0.082	0.096	—	0.091	0.073	—
1880	—	—	—	—	—	0.0872
2000	0.122	0.136	—	0.118	0.103	—
2500	0.147	0.161	—	0.159	0.131	—
2880	—	—	—	—	—	0.1685
3000	0.178	0.208	—	0.198	0.175	—
3050	—	0.210	—	—	—	—
3100	—	0.210	—	—	—	—
3150	—	0.210	—	—	—	—
3200	—	0.211	—	—	—	—
3250	—	0.215	—	—	—	—
3300	—	0.219	—	—	—	—
3350	—	0.220	—	—	—	—
3400	—	0.222	—	—	—	—
3450	—	0.227	—	—	—	—
3500	0.222	0.228	—	0.229	0.208	—
3550	—	0.231	—	—	—	—
3600	—	0.236	—	—	—	—
3650	—	0.239	—	—	—	—
3700	—	0.248	—	—	—	—
3750	—	0.255	—	—	—	—
3800	—	0.263	—	—	—	—
3850	—	0.266	—	—	—	—
3880	—	—	—	—	—	0.3077
3900	—	0.272	—	—	—	—
3950	—	0.277	—	—	—	—
4000	0.262	0.280	—	0.268	0.262	—
4500	0.289	0.316	—	0.306	0.291	—
4880	—	—	—	—	—	0.4044
5000	0.360	0.380	—	0.370	0.350	—
5500	0.420	0.420	—	0.410	0.390	—
5880	—	—	—	—	—	0.5150
6000	0.500	0.480	—	0.490	0.460	—
6500	0.550	0.520	—	0.540	0.530	—
6880	—	—	—	—	—	0.6682-0.6800 (1)
7000	0.640	0.640	—	0.660	0.650	—
7500	0.720/0.230 (2)	0.740/0.220	—	0.800/0.290	0.740/0.280	—
7725	—	—	—	—	—	0.8837-0.9424
7745	—	—	—	—	—	0.9479-0.9849
7870	0.890/0.500	0.810/0.450	—	1.010/0.520	1.020/0.500	1.0259

(1) Number on right side of "/" indicates crack growth from side of hole opposite intended flaw

GP78-0803-4

(2) Crack lengths separated by a "/" indicate a static burst between these values

**TABLE A-5**  
**PRELIMINARY AIR-TO-AIR BASELINE SPECTRUM CRACK GROWTH DATA**  
Specimen 2

Spectrum (hr)	Crack Length at Hole 1			Crack Length at Hole 2		
	Side A (in.)	Side B (in.)	Center (in.)	Side A (in.)	Side B (in.)	Center (in.)
0	—	—	—	—	—	0.0160
500	0.038	0.045	—	0.020	0	—
880	—	—	—	—	—	0.0327
1000	0.067	0.079	—	0.039	0	—
1500	0.088	0.100	—	0.056	0	—
1880	—	—	—	—	—	0.0974
2000	0.125	0.138	—	0.081	0.051	—
2500	0.161	0.165	—	0.104	0.075	—
2880	—	—	—	—	—	0.1671
3000	0.199	0.208	—	0.139	0.113	—
3050	—	0.213	—	—	—	—
3100	—	0.216	—	—	—	—
3150	—	0.218	—	—	—	—
3200	—	0.220	—	—	—	—
3250	—	0.220	—	—	—	—
3300	—	0.223	—	—	—	—
3350	—	0.229	—	—	—	—
3400	—	0.234	—	—	—	—
3450	—	0.236	—	—	—	—
3500	0.235	0.241	—	0.168	0.149	—
3550	—	0.242	—	—	—	—
3600	—	0.246	—	—	—	—
3650	—	0.255	—	—	—	—
3700	—	0.264	—	—	—	—
3750	—	0.269	—	—	—	—
3800	—	0.275	—	—	—	—
3850	—	0.281	—	—	—	—
3880	—	—	—	—	—	0.2482
3900	—	0.287	—	—	—	—
3950	—	0.293	—	—	—	—
4000	0.291	0.299	—	0.211	0.195	—
4500	0.315	0.325	—	0.237	0.225	—
4880	—	—	—	—	—	0.3414
5000	0.390	0.380	—	0.290	0.290	—
5500	0.420	0.420	—	0.320	0.310	—
5880	—	—	—	—	—	0.5189
6000	0.490/0.016	0.490/0.180 (1)	—	0.380	0.370	—
6500	0.520/0.067	0.530/0.051	—	0.400	0.400	—
6880	—	—	—	—	—	0.6608
7000	0.650/0.170	0.640/0.110	—	0.470/0.200	0.460	—
7500	0.740/0.262	0.730/0.267	—	0.510/0.059	0.510/0.052	—
7880	—	—	—	—	—	0.9406-1.034 (2)
8000	1.100/0.590	0.100/0.590	—	0.600/0.132	0.600/0.117	1.1093

(1) Number on right side of "/" indicates crack growth from side of hole opposite intended flaw

(2) Crack lengths separated by a "-" indicate a static burst between these values

GP76-0803-5

**TABLE A-6**  
**AIR-TO-AIR BASELINE SPECTRUM CRACK GROWTH DATA**

Spectrum (hr)	Crack Length at Hole 1			Crack Length at Hole 2		
	Side A (in.)	Side B (in.)	Center (in.)	Side A (in.)	Side B (in.)	Center (in.)
0	0.015	0.018	—	0.016	0.022	0.0238
500	0.040	0.040	—	0.040	0.055	—
885	—	—	—	—	—	0.0491
1000	0.070	0.070	—	0.060	0.100	—
1500	0.110	0.120	—	0.095	0.120	—
1885	—	—	—	—	—	0.0872
2000	0.150	0.150	—	0.130	0.150	—
2500	0.180	0.180	—	0.170	0.180	—
2885	—	—	—	—	—	0.1691
3000	0.200	0.220	—	0.220	0.200	—
3500	0.280	0.220	—	0.240	0.200	—
3885	—	—	—	—	—	0.3242
4000	0.320	0.300	—	0.310/0.045	0.300/0.055 (1)	—
4500	0.350	0.350	—	0.350/0.075	0.350/0.085	—
4885	—	—	—	—	—	0.4703
5000	0.450/0.070	0.450/0.050	—	0.460/0.190	0.470/0.200	—
5500	0.550/0.130	0.550/0.130	—	0.570/0.300	0.570/0.300	—
5885	—	—	—	—	—	0.7584-0.8230 (2)
6000	0.670/0.250	0.680/0.250	—	0.880/0.560	0.870/0.550	—
6215	0.700/0.280	0.750/0.300	—	1.030/0.700	1.000/0.700	1.0236

(1) Number on right side of "/" indicates crack growth from side of hole opposite intended flaw

GP78-0803-6

(2) Crack lengths separated by a "-" indicate a static burst between these values



**TABLE A-7**  
**AIR-TO-GROUND BASELINE SPECTRUM CRACK GROWTH DATA**  
Specimen 1

Spectrum (hr)	Crack Length at Hole 1			Crack Length at Hole 2		
	Side A (in.)	Side B (in.)	Center (in.)	Side A (in.)	Side B (in.)	Center (in.)
0	0.007	0.003	0.0318	0.013	0.050	—
500	0.025	0.012	—	0.035	0.065	—
704	—	—	0.0883	—	—	—
1000	0.050	0.045	—	0.045	0.110	—
1500	0.120	0.100	—	0.120	0.150	—
1704	—	—	0.1800	—	—	—
2000	0.130	0.150	—	0.150	0.200	—
2050	—	—	—	—	0.210	—
2100	—	—	—	—	0.220	—
2150	—	—	—	—	0.230	—
2200	—	—	—	—	0.240	—
2250	—	—	—	—	0.250	—
2300	—	—	—	—	0.255	—
2350	—	—	—	—	0.260	—
2400	—	—	—	—	0.270	—
2450	—	—	—	—	0.275	—
2500	0.210	0.200	—	0.200	0.285	—
2550	—	—	—	—	0.300	—
2600	—	—	—	—	0.300	—
2650	—	—	—	—	0.305	—
2700	—	—	—	—	0.310	—
2704	—	—	0.2978	—	—	—
2750	—	—	—	—	0.315	—
2800	—	—	—	—	0.315	—
2850	—	—	—	—	0.320	—
2900	—	—	—	—	0.320	—
2950	—	—	—	—	0.330	—
3000	0.280	0.280	—	0.320	0.350	—
3500	0.350/0.160 (1)	0.380/0.140	—	0.400	0.450	—
3704	—	—	0.4050	—	—	—
4000	0.480/0.180	0.450/0.160	—	0.500	0.550	—
4500	0.550/0.200	0.580/0.170	—	0.600	0.650	—
4704	—	—	0.6472	—	—	—
5000	0.660/0.270	0.670/0.220	—	0.680	0.730	—
5500	0.800/0.420	0.820/0.450	—	0.840	0.750/0.120	—
5750	1.040/0.560	1.050/0.590	1.0520	0.880/0.150	0.900/0.460	—

(1) Number on right side of "/" indicates crack growth from side of hole opposite intended flaw

GP76-0803-7

**TABLE A-8**  
**AIR-TO-GROUND BASELINE SPECTRUM CRACK GROWTH DATA**  
Specimen 2

Spectrum (hr)	Crack Length at Hole 1			Crack Length at Hole 2		
	Side A (in.)	Side B (in.)	Center (in.)	Side A (in.)	Side B (in.)	Center (in.)
0	0.024	0.005	0.0350	0.006	0.012	—
500	0.040	0.005	—	0.006	0.012	—
704	—	—	0.0605	—	—	—
1000	0.050	0.005	—	0.006	0.040	—
1500	0.065	0.005	—	0.006	0.070	—
1704	—	—	0.0960	—	—	—
2000	0.140	0.005	—	0.006	0.140	—
2500	0.190	0.005	—	0.006	0.200	—
2550	—	—	—	—	0.200	—
2600	—	—	—	—	0.200	—
2650	—	—	—	—	0.200	—
2700	—	—	—	—	0.210	—
2704	—	—	0.1591	—	—	—
2750	—	—	—	—	0.210	—
2800	—	—	—	—	0.210	—
2850	—	—	—	—	0.220	—
2900	—	—	—	—	0.220	—
2950	—	—	—	—	0.230	—
3000	0.210	0.005	—	0.180	0.230	—
3050	—	—	—	—	0.230	—
3100	—	—	—	—	0.240	—
3150	—	—	—	—	0.240	—
3200	—	—	—	—	0.240	—
3250	—	—	—	—	0.240	—
3300	—	—	—	—	0.240	—
3350	—	—	—	—	0.250	—
3400	—	—	—	—	0.260	—
3450	—	—	—	—	0.270	—
3500	0.280	0.220	—	0.260	0.280	—
3704	—	—	0.2308	—	—	—
4000	0.400	0.300	—	0.340	0.360	—
4500	0.450	0.420	—	0.420	0.370	—
4704	—	—	0.4125	—	—	—
5000	0.500/0.017 (1)	0.500/0.020	—	0.480/0.006	0.450	—
5500	0.570/0.055	0.550/0.050	—	0.550/0.010	0.550	—
5704	—	—	0.6903	—	—	—
6000	0.670/0.130	0.680/0.130	—	0.670/0.013	0.670/0.030	—
6500	0.820/0.280	0.820/0.250	—	0.750/0.020	0.730/0.070	—
6704	—	—	0.9760	—	—	—
6800	1.040/0.530	1.060/0.480	—	0.850/0.040	0.840/0.130	—

(1) Number on right side of "/" indicates crack growth from side of hole opposite intended flaw

GP76-0803-8

**TABLE A-9**  
**INSTRUMENTATION AND NAVIGATION BASELINE**  
**SPECTRUM CRACK GROWTH DATA**

Spectrum (hr)	Crack Length at Hole 1			Crack Length at Hole 2		
	Side A (in.)	Side B (in.)	Center (in.)	Side A (in.)	Side B (in.)	Center (in.)
0	0.012	0.020	0.0280	0.012	0.025	—
500	0.012	0.020	—	0.012	0.025	—
1,000	0.020	0.020	—	0.012	0.027	—
1,500	0.022	0.030	—	0.020	0.031	—
2,000	0.022	0.030	—	0.020	0.032	—
2,500	0.022	0.031	—	0.022	0.037	—
3,000	0.022	0.031	—	0.022	0.037	—
3,500	0.022	0.031	—	0.022	0.037	—
4,000	0.030	0.036	—	0.026	0.040	—
4,500	0.030	0.036	—	0.026	0.040	—
4,842	—	—	0.5350	—	—	—
5,000	0.033	0.037	—	0.027	0.045	—
5,500	0.033	0.037	—	0.027	0.045	—
6,000	0.033	0.037	—	0.027	0.045	—
6,500	0.033	0.037	—	0.027	0.045	—
6,842	—	—	0.7220	—	—	—
7,000	0.033	0.037	—	0.027	0.045	—
7,500	0.040	0.050	—	0.040	0.060	—
8,000	0.040	0.050	—	0.040	0.060	—
8,500	0.040	0.050	—	0.040	0.060	—
9,000	0.040	0.050	—	0.040	0.060	—
9,500	0.040	0.050	—	0.040	0.060	—
10,000	0.040	0.050	—	0.040	0.060	—
10,500	0.045	0.050	—	0.045	0.060	—
11,000	0.045	0.050	—	0.050	0.060	—
11,500	0.050	0.055	—	0.055	0.065	—
11,842	—	—	0.1015	—	—	—
12,000	0.050	0.055	—	0.055	0.065	—
12,500	0.050	0.060	—	0.055	0.070	—
13,000	0.050	0.060	—	0.055	0.070	—
13,500	0.060	0.065	—	0.060	0.075	—
14,000	0.070	0.065	—	0.065	0.075	—
14,500	0.070	0.065	—	0.075	0.085	—
14,842	—	—	0.1550	—	—	—
15,000	0.070	0.075	—	0.065	0.085	—
15,500	0.070	0.075	—	0.065	0.085	—
16,000	0.070	0.075	—	0.065	0.085	—
16,500	0.075	0.080	—	0.070	0.090	—
17,000	0.075	0.080	—	0.070	0.090	—
17,500	0.075	0.080	—	0.070	0.090	—
18,000	0.080	0.085	—	0.070	0.095	—
18,500	0.080	0.085	—	0.070	0.095	—
18,842	—	—	0.2055	—	—	—
19,000	0.085	0.090	—	0.085	0.100	—
19,500	0.085	0.090	—	0.085	0.100	—
20,000	0.090	0.095	—	0.090	0.110	—

GP76-0803-9

**TABLE A-9 (Continued)**  
**INSTRUMENTATION AND NAVIGATION BASELINE**  
**SPECTRUM CRACK GROWTH DATA**

Spectrum (hr)	Crack Length at Hole 1			Crack Length at Hole 2		
	Side A (in.)	Side B (in.)	Center (in.)	Side A (in.)	Side B (in.)	Center (in.)
20,500	0.090	0.095	—	0.090	0.110	—
20,842	—	—	0.2290	—	—	—
21,000	0.090	0.100	—	0.090	0.120	—
21,500	0.090	0.100	—	0.095	0.120	—
22,000	0.090	0.100	—	0.095	0.125	—
22,500	0.100	0.100	—	0.100	0.130	—
23,000	0.110	0.110	—	0.120	0.140	—
23,500	0.110	0.110	—	0.120	0.140	—
23,842	—	—	0.2530	—	—	—
24,000	0.110	0.110	—	0.120	0.140	—
24,500	0.110	0.120	—	0.120	0.140	—
25,000	0.110	0.120	—	0.120	0.140	—
25,500	0.120	0.120	—	0.120	0.140	—
26,000	0.120	0.120	—	0.120	0.140	—
26,500	0.120	0.120	—	0.120	0.140	—
26,842	—	—	0.2773	—	—	—
27,000	0.120	0.120	—	0.120	0.150	—
27,500	0.120	0.120	—	0.120	0.150	—
28,000	0.120	0.120	—	0.120	0.150	—
28,500	0.120	0.120	—	0.120	0.150	—
29,000	0.120	0.120	—	0.120	0.150	—
29,500	0.120	0.120	—	0.120	0.150	—
29,842	—	—	0.3031	—	—	—
30,000	0.120	0.120	—	0.120	0.150	—
30,500	0.120	0.120	—	0.120	0.150	—
31,000	0.120	0.130	—	0.120	0.160	—
31,500	0.130	0.140	—	0.130	0.160	—
32,000	0.140	0.140	—	0.140	0.160	—
32,500	0.140	0.160	—	0.180	0.200	—
33,000	0.170	0.160	—	0.180	0.210	—
33,050	—	—	—	—	0.210	—
33,100	—	—	—	—	0.210	—
33,150	—	—	—	—	0.210	—
33,200	—	—	—	—	0.210	—
33,250	—	—	—	—	0.210	—
33,300	—	—	—	—	0.210	—
33,350	—	—	—	—	0.210	—
33,400	—	—	—	—	0.210	—
33,450	—	—	—	—	0.210	—
33,500	0.180	0.190	—	0.190	0.210	—
33,550	—	—	—	—	0.210	—
33,600	—	—	—	—	0.210	—
33,650	—	—	—	—	0.210	—
33,700	—	—	—	—	0.210	—
33,750	—	—	—	—	0.215	—

GP76-0803-10

**TABLE A-9 (Continued)**  
**INSTRUMENTATION AND NAVIGATION BASELINE**  
**SPECTRUM CRACK GROWTH DATA**

Spectrum (hr)	Crack Length at Hole 1			Crack Length at Hole 2		
	Side A (in.)	Side B (in.)	Center (in.)	Side A (in.)	Side B (in.)	Center (in.)
33,800	—	—	—	—	0.215	—
33,850	—	—	—	—	0.215	—
33,900	—	—	—	—	0.215	—
33,950	—	—	—	—	0.215	—
34,000	0.180	0.190	—	0.200	0.215	—
34,500	0.180	0.190	—	0.200	0.215	—
34,842	—	—	0.3400	—	—	—
35,000	0.180	0.190	—	0.200	0.220	—
35,500	0.200	0.021	—	0.200	0.220	—
36,000	0.200	0.220	—	0.200	0.230	—
36,500	0.210	0.230	—	0.210	0.240	—
37,000	0.210	0.230	—	0.210	0.240	—
37,500	0.210	0.240	—	0.220	0.240	—
37,842	—	—	0.3600	—	—	—
38,000	0.220	0.240	—	0.240	0.250	—
38,500	0.230	0.240	—	0.250	0.260	—
39,000	0.230	0.250	—	0.250	0.260	—
39,500	0.230	0.250	—	0.250	0.260	—
40,000	0.230	0.250	—	0.260	0.260	—
40,500	0.230	0.250	—	0.260	0.260	—
41,000	0.230	0.250	—	0.260	0.260	—
41,500	0.240	0.260	—	0.260	0.270	—
42,000	0.240	0.260	—	0.260	0.270	—
42,500	—	—	—	—	—	—
43,000	—	—	—	—	—	—
43,500	0.260	0.270	—	0.260	0.300	—
43,842	—	—	0.4275	—	—	—
44,000	0.260	0.270	—	0.260	0.300	—
44,500	0.300	0.290	—	0.300	0.300	—
45,000	0.300	0.300	—	0.310	0.320	—
45,500	0.300	0.310	—	0.310	0.340	—
46,000	0.300	0.310	—	0.310	0.340	—
46,500	0.300	0.320	—	0.310	0.350	—
47,000	0.300	0.320	—	0.320	0.350	—
47,500	0.300	0.320	—	0.320	0.350	—
48,000	0.300	0.320	—	0.320	0.350	—
48,500	0.300	0.320	—	0.320	0.350	—
48,842	—	—	0.4500	—	—	—
49,000	0.320	0.320	—	0.350	0.360	—
49,500	0.320	0.340	—	0.350	0.370	—
50,000	0.350	0.350	—	0.360	0.370	—
50,500	0.350	0.350	—	0.360	0.370	—
51,000	0.350	0.350	—	0.360	0.370	—
51,500	0.350	0.350	—	0.370	0.370	—
52,000	0.380	0.380	—	0.400	0.380	—

GP76-0803-11

**TABLE A-9 (Continued)**  
**INSTRUMENTATION AND NAVIGATION BASELINE**  
**SPECTRUM CRACK GROWTH DATA**

Spectrum (hr)	Crack Length at Hole 1			Crack Length at Hole 2		
	Side A (in.)	Side B (in.)	Center (in.)	Side A (in.)	Side B (in.)	Center (in.)
52,500	0.380	0.380	—	0.400	0.400	—
53,000	0.380	0.380	—	0.400	0.400	—
53,500	0.400	0.400	—	0.420	0.420	—
54,000	0.400	0.400	—	0.420	0.420	—
54,500	0.400	0.400	—	0.420	0.420	—
55,000	0.400	0.400	—	0.420	0.420	—
55,500	0.400	0.400	—	0.430	0.430	—
55,842	—	—	0.4987	—	—	—
56,000	0.400	0.400	—	0.430	0.430	—
56,500	0.400	0.400	—	0.430	0.430	—
57,000	0.410	0.410	—	0.440	0.440	—
57,500	0.410	0.410	—	0.440	0.440	—
58,000	0.410	0.420	—	0.440	0.450	—
58,500	0.410	0.420	—	0.440	0.450	—
58,842	—	—	0.5230	—	—	—
59,000	0.410	0.420	—	0.440	0.450	—
59,500	0.420	0.430	—	0.440	0.460	—
60,000	0.420	0.430	—	0.440	0.460	—
60,500	0.430	0.440	—	0.460	0.470	—
61,000	0.440	0.450	—	0.460	0.480	—
61,500	0.440	0.460	—	0.470	0.480	—
62,000	0.450	0.470	—	0.480	0.490	—
62,500	0.460	0.480	—	0.480	0.500	—
63,000	0.460	0.480	—	0.480	0.500	—
63,500	0.480	0.500	—	0.520	0.510	—
63,842	—	—	0.5640	—	—	—
64,000	0.480	0.500	—	0.520	0.510	—
64,500	0.500	0.500	—	0.510	0.520	—
65,000	0.500	0.500	—	0.510	0.520	—
65,500	0.510	0.510	—	0.520	0.530	—
66,000	0.510	0.510	—	0.520	0.530	—
66,500	0.520	0.530	—	0.540	0.550	—
67,000	0.520	0.530	—	0.540	0.550	—
67,500	0.520	0.530	—	0.540	0.550	—
68,000	0.520	0.550	—	0.560	0.560	—
68,500	0.520	0.550	—	0.560	0.560	—
69,000	0.530	0.560	—	0.570	0.570	—
69,500	0.530	0.560	—	0.570	0.570	—
69,842	—	—	0.6320	—	—	—
70,000	0.540	0.560	—	0.580	0.580	—
70,500	0.550	0.570	—	0.590	0.590	—
71,000	0.560	0.580	—	0.590	0.600	—
71,500	0.580	0.590	—	0.610	0.600	—
72,000	0.600	0.600	—	0.620	0.620	—
72,500	0.610	0.620	—	0.620	0.640	—

GP76-0803-12

**TABLE A-9 (Concluded)**  
**INSTRUMENTATION AND NAVIGATION BASELINE**  
**SPECTRUM CRACK GROWTH DATA**

Spectrum (hr)	Crack Length at Hole 1			Crack Length at Hole 2		
	Side A (in.)	Side B (in.)	Center (in.)	Side A (in.)	Side B (in.)	Center (in.)
73,000	0.610	0.630	—	0.630	0.650	—
73,500	0.620	0.640	—	0.640	0.660	—
74,000	0.620	0.640	—	0.640	0.660	—
74,500	0.630	0.650	—	0.650	0.660	—
75,000	0.640	0.650	—	0.660	0.670	—
75,500	0.640	0.650	—	0.660	0.670	—
76,000	0.650	0.650	—	0.670	0.670	—
76,500	0.660	0.660	—	0.680	0.680	—
76,842	—	—	0.7172	—	—	—
77,000	0.660	0.660	—	0.680	0.680	—
77,500	0.670	0.680	—	0.700	0.690	—
78,000	0.680	0.690	—	0.710	0.700	—
78,500	0.680	0.690	—	0.710	0.700	—
79,000	0.690	0.690	—	0.730	0.710	—
79,500	0.700/0.060 (1)	0.70	—	0.740/0.100	0.720/0.080	—
79,842	—	—	0.7669	—	—	—
80,000	0.720/0.090	0.720	—	0.750/0.120	0.740/0.100	—
80,500	0.740/0.140	0.740/0.050	—	0.750/0.120	0.760/0.120	—
80,842	—	—	0.7855	—	—	—
81,000	0.750/0.140	0.760/0.050	—	0.770/0.140	0.760/0.120	—
81,500	0.760/0.140	0.760/0.060	—	0.780/0.140	0.760/0.120	—
82,000	0.770/0.140	0.770/0.080	—	0.780/0.150	0.770/0.140	—
82,500	0.780/0.140	0.780/0.100	—	0.780/0.170	0.780/0.160	—
82,842	—	—	0.8227	—	—	—
83,000	0.800/0.160	0.790/0.120	—	0.790/0.180	0.790/0.170	—
83,500	0.800/0.160	0.800/0.150	—	0.800/0.180	0.800/0.180	—
84,000	0.800/0.160	0.800/0.150	—	0.800/0.180	0.800/0.180	—
84,500	0.820/0.200	0.800/0.160	—	0.800/0.200	0.810/0.210	—
84,842	—	—	0.8678	—	—	—
85,000	0.830/0.210	0.820/0.180	—	0.820/0.220	0.830/0.220	—
85,500	0.840/0.220	0.840/0.200	—	0.840/0.240	0.850/0.240	—
86,000	0.840/0.220	0.840/0.200	—	0.840/0.240	0.850/0.240	—
86,500	0.860/0.240	0.860/0.220	—	0.840/0.240	0.880/0.260	—
86,842	—	—	0.9136	—	—	—
87,000	0.900/0.250	0.900/0.240	—	0.900/0.250	0.900/0.280	—
87,500	0.900/0.250	0.900/0.260	—	0.900/0.300	0.910/0.300	—
88,000	0.900/0.300	0.910/0.260	—	0.900/0.300	0.910/0.300	—
88,500	0.920/0.300	0.940/0.300	—	0.920/0.300	0.920/0.300	—
88,842	—	—	0.9758	—	—	—
89,000	0.950/0.300	0.950/0.310	—	0.940/0.300	0.950/0.340	—
89,500	0.970/0.330	0.980/0.350	—	0.950/0.330	0.970/0.350	—
90,000	0.970/0.350	1.000/0.350	—	0.950/0.350	0.970/0.350	—
90,500	1.020/0.370	1.020/0.370	1.0519	1.000/0.370	1.000/0.380	—

(1) Number on right side of "/" indicates crack growth from side of hole opposite intended flaw

GP76-0803-43

**TABLE A-10**  
**COMPOSITE BASELINE SPECTRUM CRACK GROWTH DATA**  
Specimen 1

Spectrum (hr)	Crack Length at Hole 1			Crack Length at Hole 2		
	Side A (in.)	Side B (in.)	Center (in.)	Side A (in.)	Side B (in.)	Center (in.)
0	0.009	0.025	—	0.035	0.018	0.0342
500	0.025	0.042	—	0.045	0.033	—
714	—	—	—	—	—	0.0872
1000	0.055	0.065	—	0.100	0.055	—
1500	0.070	0.100	—	0.110	0.070	—
1714	—	—	—	—	—	0.1507
2000	0.100	0.130	—	0.140	0.130	—
2500	0.150	0.160	—	0.160	0.140	—
2714	—	—	—	—	—	0.2149
3000	0.170	0.170	—	0.190	0.180	—
3500	0.200	0.190	—	0.230	0.210	—
3550	—	—	—	0.230	—	—
3600	—	—	—	0.240	—	—
3650	—	—	—	0.250	—	—
3700	—	—	—	0.250	—	—
3714	—	—	—	—	—	0.2810
3750	—	—	—	0.260	—	—
3800	—	—	—	0.260	—	—
3850	—	—	—	0.260	—	—
3900	—	—	—	0.260	—	—
3950	—	—	—	0.260	—	—
4000	0.230	0.230	—	0.260	0.250	—
4050	—	—	—	0.260	—	—
4100	—	—	—	0.265	—	—
4150	—	—	—	0.270	—	—
4200	—	—	—	0.280	—	—
4250	—	—	—	0.290	—	—
4300	—	—	—	0.300	—	—
4350	—	—	—	0.300	—	—
4400	—	—	—	0.300	—	—
4450	—	—	—	0.300	—	—
4500	0.270	0.280	—	0.300	0.300	—
4714	—	—	—	—	—	0.3717
5000	0.320	0.315	—	0.350	0.350	—
5500	0.360	0.360	—	0.380	0.380	—
5714	—	—	—	—	—	0.4530
6000	0.410	0.400	—	0.440	0.450	—
6500	0.460	0.440	—	0.500	0.480	—
6714	—	—	—	—	—	0.5655
7000	0.520/0.060 (1)	0.540/0.080	—	0.560/0.100	0.560/0.120	—
7500	0.600/0.180	0.600/0.180	—	0.650/0.200	0.660/0.220	—
7714	—	—	—	—	—	0.7486
8000	0.680/0.240	0.660/0.240	—	0.760/0.340	0.760/0.320	—
8500	0.780/0.340	0.780/0.360	—	0.950/0.520	0.920/0.460	—
8585	0.820/0.340	0.820/0.380	—	1.060/0.620	1.080/0.580	1.0281

(1) Number on right side of "/" indicates crack growth from side of hole opposite intended flaw

GP78-0803-13



**TABLE A-11**  
**COMPOSITE BASELINE SPECTRUM CRACK GROWTH DATA**  
Specimen 2

Spectrum (hr)	Crack Length at Hole 1			Crack Length at Hole 2		
	Side A (in.)	Side B (in.)	Center (in.)	Side A (in.)	Side B (in.)	Center (in.)
0	0.007	0.027	—	0.015	0.015	0.0304
500	0.015	0.030	—	0.025	0.035	—
714	—	—	—	—	—	0.0714
1000	0.030	0.040	—	0.040	0.060	—
1500	0.080	0.100	—	0.080	0.080	—
1714	—	—	—	—	—	0.1191
2000	0.100	0.100	—	0.100	0.080	—
2500	0.120	0.120	—	0.120	0.110	—
2714	—	—	—	—	—	0.1756
3000	0.150	0.160	—	0.150	0.150	—
3500	0.180	0.180	—	0.180	0.180	—
3714	—	—	—	—	—	0.2433
4000	0.210	0.210	—	0.210	0.210	—
4050	—	—	—	—	0.210	—
4100	—	—	—	—	0.210	—
4150	—	—	—	—	0.220	—
4200	—	—	—	—	0.230	—
4250	—	—	—	—	0.230	—
4300	—	—	—	—	0.235	—
4350	—	—	—	—	0.240	—
4400	—	—	—	—	0.240	—
4450	—	—	—	—	0.240	—
4500	0.240	0.240	—	0.240	0.240	—
4550	—	—	—	—	0.250	—
4600	—	—	—	—	0.260	—
4650	—	—	—	—	0.265	—
4700	—	—	—	—	0.275	—
4714	—	—	—	—	—	0.3495
4750	—	—	—	—	0.290	—
4800	—	—	—	—	0.295	—
4850	—	—	—	—	0.300	—
4900	—	—	—	—	0.300	—
4950	—	—	—	—	0.305	—
5000	0.270	0.280	—	0.300	0.310	—
5500	0.340	0.340	—	0.380/0.046 (1)	0.380/0.017	—
5714	—	—	—	—	—	0.4829
6000	0.370	0.370	—	0.440/0.090	0.440/0.050	—
6500	0.400	0.400	—	0.510/0.160	0.500/0.140	—
6714	—	—	—	—	—	0.6348
7000	0.460	0.470	—	0.610/0.250	0.600/0.250	—
7500	0.500	0.500	—	0.700/0.350	0.700/0.350	—
7714	—	—	—	—	—	0.8879
7890	0.600/0.100	0.600/0.120	—	1.000/0.570	1.000/0.580	—
7945	—	—	—	—	—	1.0160

(1) Number on right side of "/" indicates crack growth from side of hole opposite intended flaw

GP76-0803-14

**TABLE A-12**  
**SEQUENCE OF MISSIONS VARIATION 6 CRACK GROWTH DATA**

Spectrum (hr)	Crack Length at Hole 1			Crack Length at Hole 2		
	Side A (in.)	Side B (in.)	Center (in.)	Side A (in.)	Side B (in.)	Center (in.)
0	0.033	0.042	0.0700	0.003	0.022	0.0309
500	0.080	0.090	—	0.007	0.045	—
1000	0.140	0.120	0.1469	0.020	0.070	0.0821
1500	0.180	0.160	—	0.100	0.100	—
2000	0.220	0.200	0.2410	0.140	0.160	0.1553
2050	0.225	—	—	—	—	—
2100	0.230	—	—	—	—	—
2150	0.235	—	—	—	—	—
2200	0.240	—	—	—	—	—
2250	0.245	—	—	—	—	—
2300	0.250	—	—	—	—	—
2350	0.255	—	—	—	—	—
2400	0.260	—	—	—	—	—
2450	0.265	—	—	—	—	—
2500	0.270	0.260	—	0.180	0.190	—
2550	0.275	—	—	—	—	—
2600	0.280	—	—	—	—	—
2650	0.285	—	—	—	—	—
2700	0.290	—	—	—	—	—
2750	0.295	—	—	—	—	—
2800	0.300	—	—	—	—	—
2850	0.305	—	—	—	—	—
2900	0.310	—	—	—	—	—
2950	0.315	—	—	—	—	—
3000	0.320	0.320	0.3386	0.210	0.210	0.2453
3500	0.380	0.380	—	0.260	0.260	—
4000	0.420	0.420	0.4421	0.340	0.340	0.3517
4500	0.500	0.480	—	0.420	0.400	—
5000	0.600	0.580/0.050 (1)	0.5765	0.460	0.480	0.4893
5500	0.660	0.710/0.070	—	0.570	0.580	—
6000	0.720/0.050	0.730/0.055	0.7395	0.650/0.010	0.680	0.6846
6500	0.930/0.260	0.940/0.030	—	0.880/0.150	0.900/0.200	—
6620	1.030/0.350	1.030/0.400	1.0357	0.960/0.220	1.000/0.300	1.0135

(1) Number on right side of "/" indicates crack growth from side of hole opposite intended flaw

GP76-0803-15

TABLE A-13  
MISSION MIX VARIATION 3 CRACK GROWTH DATA

Spectrum (hr)	Crack Length at Hole 1			Crack Length at Hole 2		
	Side A (in.)	Side B (in.)	Center (in.)	Side A (in.)	Side B (in.)	Center (in.)
0	0.011	0.003	0.0324	0.007	0.022	—
500	0.020	0.007	—	0.015	0.030	—
530	—	—	0.0463	—	—	—
1,000	0.040	0.030	—	0.030	0.055	—
1,500	0.054	0.049	—	0.051	0.067	—
1,530	—	—	0.0857	—	—	—
2,000	0.072	0.068	—	0.066	0.085	—
2,500	0.092	0.091	—	0.095	0.120	—
2,530	—	—	0.1342	—	—	—
3,000	0.120	0.120	—	0.120	0.140	—
3,500	0.140	0.160	—	0.150	0.160	—
3,530	—	—	0.1811	—	—	—
4,000	0.150	0.180	—	0.170	0.190	—
4,500	0.180	0.200	—	0.190	0.220	—
4,530	—	—	0.2324	—	—	—
4,550	—	—	—	—	0.230	—
4,600	—	—	—	—	0.245	—
4,650	—	—	—	—	0.250	—
4,700	—	—	—	—	0.250	—
4,750	—	—	—	—	0.250	—
4,800	—	—	—	—	0.250	—
4,850	—	—	—	—	0.250	—
4,900	—	—	—	—	0.250	—
4,950	—	—	—	—	0.250	—
5,000	0.210	0.220	—	0.230	0.250	—
5,050	—	—	—	—	0.250	—
5,100	—	—	—	—	0.260	—
5,150	—	—	—	—	0.260	—
5,200	—	—	—	—	0.270	—
5,250	—	—	—	—	0.270	—
5,300	—	—	—	—	0.270	—
5,350	—	—	—	—	0.270	—
5,400	—	—	—	—	0.275	—
5,450	—	—	—	—	0.275	—
5,500	0.220	0.240	—	0.250	0.275	—
5,530	—	—	0.2919	—	—	—
6,000	0.260	0.280	—	0.290	0.300	—
6,500	0.300	0.310	—	0.330	0.340	—
6,530	—	—	0.3497	—	—	—
7,000	0.330	0.350	—	0.350	0.370	—
7,500	0.350	0.370	—	0.390	0.400	—
7,530	—	—	0.4122	—	—	—
8,000	0.400	0.410	—	0.430	0.440	—
8,500	0.420	0.450	—	0.470	0.480	—
8,530	—	—	0.4938	—	—	—
9,000	0.500	0.500	—	0.53/0.10 (1)	0.53/0.06	—
9,500	0.550	0.550	—	0.60/0.15	0.60/0.12	—
9,530	—	—	0.5839	—	—	—
10,000	0.60/0.05	0.60/0.06	—	0.68/0.25	0.68/0.18	—
10,500	0.62/0.08	0.64/0.08	—	0.84/0.36	0.84/0.38	—
10,530	—	—	0.6923	—	—	—
10,675	0.70/0.09	0.74/0.08	0.7209	1.00/0.38	1.02/0.40	—

(1) Number on right side of "/" indicates crack growth from side of hole opposite intended flaw

GP78-0803-18

**TABLE A-14**  
**MISSION MIX VARIATION 21 CRACK GROWTH DATA**

Spectrum (hr)	Crack Length at Hole 1			Crack Length at Hole 2		
	Side A (in.)	Side B (in.)	Center (in.)	Side A (in.)	Side B (in.)	Center (in.)
0	0.003	0.008	—	0.015	0.047	0.0514
500	0.005	0.009	—	0.020	0.050	—
686	—	—	—	—	—	0.0668
1000	0.008	0.010	—	0.045	0.080	—
1500	0.010	0.060	—	0.110	0.130	—
1686	—	—	—	—	—	0.0940
2000	0.020	0.080	—	0.150	0.160	—
2500	0.100	0.140	—	0.180	0.190	—
2686	—	—	—	—	—	0.1272
3000	0.150	0.180	—	0.260	0.270	—
3050	—	—	—	—	0.275	—
3100	—	—	—	—	0.280	—
3150	—	—	—	—	0.290	—
3200	—	—	—	—	0.295	—
3250	—	—	—	—	0.300	—
3300	—	—	—	—	0.310	—
3350	—	—	—	—	0.320	—
3400	—	—	—	—	0.325	—
3450	—	—	—	—	0.330	—
3500	0.200	0.220	—	0.320	0.340	—
3550	—	—	—	—	0.350	—
3600	—	—	—	—	0.360	—
3650	—	—	—	—	0.370	—
3686	—	—	—	—	—	0.2061
3700	—	—	—	—	0.370	—
3750	—	—	—	—	0.375	—
3800	—	—	—	—	0.375	—
3850	—	—	—	—	0.375	—
3900	—	—	—	—	0.380	—
3950	—	—	—	—	0.380	—
4000	0.290	0.300	—	0.370	0.380	—
4500	0.350	0.350	—	0.450	0.450	—
5000	0.400	0.400	—	0.500	0.500	—
5500	0.500/0.050 (1)	0.500/0.050	—	0.650/0.160	0.650/0.160	—
5686	—	—	—	—	—	0.8070
6000	0.580/0.140	0.580/0.140	—	0.840/0.320	0.840/0.340	—
6100	0.600/0.180	0.600/0.180	—	1.010/0.400	1.010/0.430	1.0122

(1) Number on right side of "/" indicates crack growth from side of hole opposite intended flaw

GP78-0803-17

**TABLE A-15**  
**MISSION MIX VARIATION 28 CRACK GROWTH DATA**

Spectrum (hr)	Crack Length at Hole 1			Crack Length at Hole 2		
	Side A (in.)	Side B (in.)	Center (in.)	Side A (in.)	Side B (in.)	Center (in.)
0	0.020	0.045	0.0570	0.003	0.043	—
500	0.048	0.069	—	0.025	0.063	—
714	—	—	0.0798	—	—	—
1000	0.078	0.093	—	0.050	0.090	—
1500	0.100	0.130	—	0.080	0.120	—
1714	—	—	0.1179	—	—	—
2000	0.140	0.160	—	0.120	0.160	—
2500	0.160	0.180	—	0.160	0.180	—
2714	—	—	0.1875	—	—	—
3000	0.200	0.210	—	0.190	0.200	—
3050	—	0.220	—	—	—	—
3100	—	0.220	—	—	—	—
3150	—	0.230	—	—	—	—
3200	—	0.230	—	—	—	—
3250	—	0.240	—	—	—	—
3300	—	0.250	—	—	—	—
3350	—	0.260	—	—	—	—
3400	—	0.260	—	—	—	—
3450	—	0.270	—	—	—	—
3500	0.260	0.280	—	0.250	0.260	—
3550	—	0.280	—	—	—	—
3600	—	0.280	—	—	—	—
3650	—	0.280	—	—	—	—
3700	—	0.280	—	—	—	—
3714	—	—	0.2608	—	—	—
3750	—	0.280	—	—	—	—
3800	—	0.280	—	—	—	—
3850	—	0.290	—	—	—	—
3900	—	0.290	—	—	—	—
3950	—	0.290	—	—	—	—
4000	0.280	0.300	—	0.260	0.290	—
4500	0.310	0.350	—	0.320	0.360	—
4714	—	—	0.3400	—	—	—
5000	0.330	0.370	—	0.350	0.380	—
5500	0.420	0.440	—	0.430	0.430	—
5714	—	—	0.5393	—	—	—
6000	0.520	0.520	—	0.500	0.480	—
6500	0.540/0.100 (1)	0.540/0.080	—	0.520	0.540/0.060	—
6714	—	—	0.7240	—	—	—
7000	0.660/0.280	0.640/0.220	—	0.580/0.100	0.620/0.180	—
7500	0.860/0.380	0.840/0.380	—	0.740/0.260	0.760/0.380	—
7570	1.020/0.540	1.000/0.550	0.9986	0.820/0.320	0.820/0.340	—

(1) Number on right side of "/" indicates crack growth from side of hole opposite intended flaw

GP76-0803-18

**TABLE A-16**  
**FLIGHT LENGTH VARIATION 4 CRACK GROWTH DATA**

Spectrum (hr)	Crack Length at Hole 1			Crack Length at Hole 2		
	Side A (in.)	Side B (in.)	Center (in.)	Side A (in.)	Side B (in.)	Center (in.)
0	0.020	0.022	0.0384	0.022	0.022	—
500	0.043	0.041	—	0.044	0.050	—
552	—	—	0.0792	—	—	—
1000	0.063	0.061	—	0.062	0.068	—
1500	0.082	0.083	—	0.077	0.086	—
1552	—	—	0.1330	—	—	—
2000	0.105	0.105	—	0.100	0.110	—
2500	0.130	0.135	—	0.120	0.145	—
2552	—	—	0.1908	—	—	—
3000	0.160	0.165	—	0.155	0.155	—
3500	0.210	0.185	—	0.175	0.190	—
3550	0.210	—	—	—	—	—
3552	—	—	0.2550	—	—	—
3600	0.210	—	—	—	—	—
3650	0.220	—	—	—	—	—
3700	0.225	—	—	—	—	—
3750	0.225	—	—	—	—	—
3800	0.225	—	—	—	—	—
3850	0.235	—	—	—	—	—
3900	0.235	—	—	—	—	—
3950	0.240	—	—	—	—	—
4000	0.240	0.205	—	0.225	0.200	—
4050	0.240	—	—	—	—	—
4100	0.240	—	—	—	—	—
4150	0.240	—	—	—	—	—
4200	0.240	—	—	—	—	—
4250	0.240	—	—	—	—	—
4300	0.240	—	—	—	—	—
4350	0.250	—	—	—	—	—
4400	0.250	—	—	—	—	—
4450	0.250	—	—	—	—	—
4500	0.260	0.260	—	0.260	0.250	—
4552	—	—	0.3185	—	—	—
5000	0.300	0.310	—	0.280	0.290	—
5500	0.380	0.380	—	0.350	0.360	—
5552	—	—	0.3990	—	—	—
6000	0.400	0.410	—	0.390	0.400	—
6500	0.440	0.440	—	0.420	0.420	—
6552	—	—	0.4878	—	—	—
7000	0.500	0.480	—	0.480	0.500	—
7500	0.540/0.060 (1)	0.520	—	0.500	0.550/0.080	—
7552	—	—	0.5935	—	—	—
8000	0.600/0.120	0.580/0.040	—	0.580/0.100	0.060/0.120	—
8500	0.680/0.220	0.660/0.180	—	0.650/0.160	0.700/0.240	—
8552	—	—	0.7457	—	—	—
9000	0.780/0.340	0.760/0.300	—	0.760/0.280	0.800/0.340	—
9500	0.860/0.460	0.860/0.460	—	0.860/0.380	0.880/0.400	—
9625	1.150/0.720	1.120/0.680	1.1362	1.000/0.480	1.020/0.500	—

(1) Number on right side of "/" indicates crack growth from side of hole opposite intended flaw

GP76-0803-19

**TABLE A-17**  
**TRUNCATION VARIATION 5 CRACK GROWTH DATA**

Spectrum (hr)	Crack Length at Hole 1			Crack Length at Hole 2		
	Side A (in.)	Side B (in.)	Center (in.)	Side A (in.)	Side B (in.)	Center (in.)
0	0.015	0.005	0.0250	0.017	0.020	—
500	0.020	0.005	—	0.020	0.030	—
668	—	—	0.0570	—	—	—
1000	0.040	0.020	—	0.050	0.060	—
1500	0.060	0.050	—	0.080	0.090	—
1668	—	—	0.0965	—	—	—
2000	0.080	0.075	—	0.090	0.105	—
2500	0.105	0.100	—	0.110	0.120	—
2668	—	—	0.1395	—	—	—
3000	0.120	0.120	—	0.130	0.140	—
3500	0.140	0.130	—	0.150	0.160	—
3668	—	—	0.1900	—	—	—
4000	0.155	0.150	—	0.170	0.180	—
4500	0.180	0.180	—	0.190	0.200	—
4550	—	—	—	—	0.205	—
4600	—	—	—	—	0.210	—
4650	—	—	—	—	0.215	—
4668	—	—	0.2458	—	—	—
4700	—	—	—	—	0.220	—
4750	—	—	—	—	0.220	—
4800	—	—	—	—	0.225	—
4850	—	—	—	—	0.225	—
4900	—	—	—	—	0.230	—
4950	—	—	—	—	0.230	—
5000	0.210	0.200	—	0.220	0.235	—
5050	—	—	—	—	0.235	—
5100	—	—	—	—	0.240	—
5150	—	—	—	—	0.240	—
5200	—	—	—	—	0.245	—
5250	—	—	—	—	0.245	—
5300	—	—	—	—	0.250	—
5350	—	—	—	—	0.250	—
5400	—	—	—	—	0.255	—
5450	—	—	—	—	0.255	—
5500	0.230	0.235	—	0.250	0.260	—
5668	—	—	0.3056	—	—	—
6000	0.285	0.280/0.080 (1)	—	0.280	0.290	—
6500	0.340/0.040	0.360/0.100	—	0.340	0.340	—
6668	—	—	0.3958	—	—	—
7000	0.390/0.080	0.400/0.140	—	0.370	0.370	—
7500	0.460/0.220	0.440/0.200	—	0.400	0.400	—
7668	—	—	0.5135	—	—	—
8000	0.540/0.300	0.540/0.300	—	0.440	0.450	—
8500	0.630/0.380	0.620/0.400	—	0.460	0.480/0.060	—
8668	—	—	0.7168	—	—	—
9000	0.780/0.540	0.820/0.560	—	0.540/0.100	0.540/0.120	—
9310	1.020/0.740	1.040/0.750	1.0158	0.560/0.120	0.560/0.140	—

(1) Number on right side of "/" indicates crack growth from side of hole opposite intended flaw.

GP76-0803-20

**TABLE A-18**  
**TRUNCATION VARIATION 6 CRACK GROWTH DATA**

Spectrum (hr)	Crack Length at Hole 1			Crack Length at Hole 2		
	Side A (in.)	Side B (in.)	Center (in.)	Side A (in.)	Side B (in.)	Center (in.)
0	0.006	0.004	—	0.026	0.037	0.0473
500	0.010	0.020	—	0.040	0.050	—
678	—	—	—	—	—	0.0725
1,000	0.030	0.050	—	0.060	0.060	—
1,500	0.040	0.060	—	0.060	0.070	—
1,678	—	—	—	—	—	0.0984
2,000	0.050	0.060	—	0.080	0.080	—
2,500	0.060	0.060	—	0.100	0.100	—
2,678	—	—	—	—	—	0.1278
3,000	0.060	0.060	—	0.120	0.110	—
3,500	0.080	0.080	—	0.130	0.130	—
3,678	—	—	—	—	—	0.1570
4,000	0.090	0.080	—	0.140	0.140	—
4,500	0.090	0.100	—	0.150	0.160	—
4,678	—	—	—	—	—	0.1845
5,000	0.100	0.100	—	0.160	0.170	—
5,500	0.130	0.120	—	0.180	0.180	—
5,678	—	—	—	—	—	0.2093
6,000	0.150	0.150	—	0.190	0.200	—
6,050	—	—	—	—	0.200	—
6,100	—	—	—	—	0.200	—
6,150	—	—	—	—	0.200	—
6,200	—	—	—	—	0.210	—
6,250	—	—	—	—	0.210	—
6,300	—	—	—	—	0.210	—
6,350	—	—	—	—	0.210	—
6,400	—	—	—	—	0.220	—
6,450	—	—	—	—	0.220	—
6,500	0.160	0.160	—	0.210	0.220	—
6,550	—	—	—	—	0.220	—
6,600	—	—	—	—	0.220	—
6,650	—	—	—	—	0.220	—
6,678	—	—	—	—	—	0.2437
6,700	—	—	—	—	0.220	—
6,750	—	—	—	—	0.220	—

GP76-0803-21



**TABLE A-18 (Concluded)**  
**TRUNCATION VARIATION 6 CRACK GROWTH DATA**

Spectrum (hr)	Crack Length at Hole 1			Crack Length at Hole 2		
	Side A (in.)	Side B (in.)	Center (in.)	Side A (in.)	Side B (in.)	Center (in.)
6,800	—	—	—	—	0.220	—
6,850	—	—	—	—	0.220	—
6,900	—	—	—	—	0.230	—
6,950	—	—	—	—	0.230	—
7,000	0.170	0.160	—	0.220	0.230	—
7,500	0.180	0.180	—	0.240	0.240	—
7,678	—	—	—	—	—	0.2790
8,000	0.200	0.200	—	0.250	0.260	—
8,500	0.230	0.220	—	0.290	0.300	—
8,678	—	—	—	—	—	0.3109
9,000	0.240	0.240	—	0.300	0.320	—
9,500	0.260	0.260	—	0.320	0.340	—
9,678	—	—	—	—	—	0.3532
10,000	0.280	0.280	—	0.340	0.350	—
10,500	0.300	0.280	—	0.360	0.360	—
10,678	—	—	—	—	—	0.3972
11,000	0.320	0.300	—	0.380	0.380	—
11,500	0.340	0.320	—	0.420	0.420	—
11,678	—	—	—	—	—	0.4500
12,000	0.360	0.360	—	0.440	0.440	—
12,500	0.380	0.380	—	0.460	0.460	—
12,678	—	—	—	—	—	0.5212
13,000	0.400/0.040 (1)	0.400	—	0.520/0.080	0.520/0.100	—
13,500	0.420/0.040	0.440/0.050	—	0.560/0.120	0.560/0.120	—
13,678	—	—	—	—	—	0.6168
14,000	0.450/0.060	0.450/0.080	—	0.620/0.150	0.620/0.210	—
14,500	0.490/0.080	0.480/0.120	—	0.670/0.180	0.680/0.250	—
14,678	—	—	—	—	—	0.8010
15,000	0.520/0.120	0.510/0.150	—	0.820/0.250	0.810/0.320	—
15,500	0.570/0.160	0.550/0.180	—	1.040/0.440	1.030/0.430	1.0360

(1) Number on right side of "/" indicates crack growth from side of hole opposite intended flaw

GP76-0803-42

**TABLE A-19**  
**TRUNCATION VARIATION 8 CRACK GROWTH DATA**

Spectrum (hr)	Crack Length at Hole 1			Crack Length at Hole 2		
	Side A (in.)	Side B (in.)	Center (in.)	Side A (in.)	Side B (in.)	Center (in.)
0	0.018	0.004	—	0.032	0.032	0.0959
271	—	—	—	—	—	0.1211
500	0.018	0.004	—	0.032	0.040	—
782	—	—	—	—	—	0.1686
1000	0.061	0.060	—	0.083	0.090	—
1271	—	—	—	—	—	0.2111
1500	0.095	0.092	—	0.105	0.110	—
1782	—	—	—	—	—	0.2510
2000	0.140	0.125	—	0.160	0.160	—
2271	—	—	—	—	—	0.3031
2500	0.160	0.150	—	0.180	0.190	—
2782	—	—	—	—	—	0.3382
3000	0.190	0.200	—	0.200	0.220	—
3050	—	—	—	—	0.230	—
3100	—	—	—	—	0.240	—
3150	—	—	—	—	0.250	—
3200	—	—	—	—	0.260	—
3250	—	—	—	—	0.280	—
3271	—	—	—	—	—	0.4041
3300	—	—	—	—	0.300	—
3350	—	—	—	—	0.300	—
3400	—	—	—	—	0.310	—
3450	—	—	—	—	0.310	—
3500	0.270	0.280	—	0.300	0.320	—
3550	—	—	—	—	0.330	—
3600	—	—	—	—	0.330	—
3650	—	—	—	—	0.340	—
3700	—	—	—	—	0.340	—
3750	—	—	—	—	0.350	—
3782	—	—	—	—	—	0.4608
3800	—	—	—	—	0.350	—
3850	—	—	—	—	0.350	—
3900	—	—	—	—	0.350	—
3950	—	—	—	—	0.360	—
4000	0.320	0.320	—	0.350	0.360	—
4271	—	—	—	—	—	0.5228
4500	0.380	0.380	—	0.440	0.450	—
4782	—	—	—	—	—	0.5961
5000	0.430	0.440	—	0.520	0.520	—
5271	—	—	—	—	—	0.6918
5500	0.500	0.500	—	0.620/0.080 (1)	0.620/0.120	—
5782	—	—	—	—	—	0.8275
6000	0.580/0.080	0.600/0.100	—	0.740/0.220	0.750/0.250	—
6271	—	—	—	—	—	1.0021
6465	0.740/0.250	0.750/0.260	—	1.000/0.520	1.000/0.520	1.0500

(1) Number on right side of "/" indicates crack growth from side of hole opposite intended flaw

GP76-0803-22

**TABLE A-20**  
**TRUNCATION VARIATION 14 CRACK GROWTH DATA**

Spectrum (hr)	Crack Length at Hole 1			Crack Length at Hole 2		
	Side A (in.)	Side B (in.)	Center (in.)	Side A (in.)	Side B (in.)	Center (in.)
0	0.028	0.005	—	0.022	0.005	0.0141
500	0.040	0.010	—	0.040	0.010	—
1,000	0.050	0.010	—	0.040	0.010	0.0693
1,500	0.060	0.020	—	0.060	0.020	—
2,000	0.100	0.069	—	0.074	0.052	0.0915
2,500	0.130	0.090	—	0.090	0.070	—
3,000	0.150	0.110	—	0.110	0.090	0.1131
3,500	0.160	0.140	—	0.130	0.120	—
4,000	0.200	0.170	—	0.160	0.140	0.1600
4,050	0.200	—	—	—	—	—
4,100	0.205	—	—	—	—	—
4,150	0.210	—	—	—	—	—
4,200	0.215	—	—	—	—	—
4,250	0.220	—	—	—	—	—
4,300	0.220	—	—	—	—	—
4,350	0.225	—	—	—	—	—
4,400	0.225	—	—	—	—	—
4,450	0.230	—	—	—	—	—
4,500	0.230	0.200	—	0.170	0.155	—
4,550	0.235	—	—	—	—	—
4,600	0.235	—	—	—	—	—
4,650	0.240	—	—	—	—	—
4,700	0.240	—	—	—	—	—
4,750	0.245	—	—	—	—	—
4,800	0.250	—	—	—	—	—
4,850	0.250	—	—	—	—	—
4,900	0.255	—	—	—	—	—
4,950	0.255	—	—	—	—	—
5,000	0.260	0.230	—	0.210	0.190	0.2033
5,500	0.300	0.270	—	0.240	0.230	—
6,000	0.320/0.015 (1)	0.305	—	0.270	0.260	0.2475
6,500	0.355/0.020	0.350	—	0.310/0.010	0.290	—
7,000	0.400/0.030	0.380	—	0.330/0.020	0.330	0.3055
7,500	0.450/0.050	0.420/0.010	—	0.370/0.035	0.370/0.020	—
8,000	0.500/0.080	0.470/0.010	—	0.440/0.040	0.400/0.020	0.3718
8,500	0.550/0.110	0.590/0.070	—	0.450/0.100	0.450/0.070	—
9,000	0.630/0.110	0.600/0.140	—	0.520/0.150	0.500/0.110	0.4520
9,500	0.700/0.240	0.680/0.250	—	0.570/0.170	0.560/0.190	—
10,000	0.880/0.380	0.830/0.350	—	0.660/0.260	0.680/0.300	0.6194
10,306	1.100/0.530	1.080/0.530	—	0.760/0.350	0.750/0.400	0.7647

(1) Number on right side of / indicates crack growth from side of hole opposite intended flaw

GP76-0803-23

**TABLE A-21**  
**TRUNCATION VARIATION 18 CRACK GROWTH DATA**

Spectrum (hr)	Crack Length at Hole 1			Crack Length at Hole 2		
	Side A (in.)	Side B (in.)	Center (in.)	Side A (in.)	Side B (in.)	Center (in.)
0	0.016	0.001	0.0335	0.015	0.015	—
500	0.028	0.011	—	0.036	0.032	—
1,000	0.042	0.023	0.0705	0.053	0.049	—
1,500	0.054	0.030	—	0.069	0.060	—
2,000	0.058	0.035	0.0920	0.072	0.070	—
2,500	0.062	0.037	—	0.082	0.075	—
3,000	0.067	0.037	0.1057	0.082	0.075	—
3,500	0.075	0.055	—	0.090	0.095	—
4,000	0.094	0.064	0.1178	0.120	0.100	—
4,500	0.100	0.082	—	0.130	0.120	—
5,000	0.100	0.090	0.1278	0.130	0.120	—
5,500	0.100	0.090	—	0.130	0.120	—
6,000	0.100	0.090	0.1355	0.130	0.120	—
6,500	0.100	0.090	—	0.130	0.120	—
7,000	0.100	0.100	0.1445	0.130	0.130	—
7,500	0.100	0.100	—	0.130	0.130	—
8,000	0.100	0.100	0.1530	0.130	0.130	—
8,500	0.100	0.100	—	0.130	0.130	—
9,000	0.100	0.100	0.1615	0.130	0.130	—
9,500	0.100	0.100	—	0.130	0.130	—
10,000	0.100	0.100	0.1683	0.130	0.130	—
10,500	0.100	0.100	—	0.130	0.130	—
11,000	0.100	0.100	—	0.130	0.130	—
11,500	0.100	0.100	—	0.130	0.130	—
12,000	0.110	0.100	—	0.135	0.140	—
12,500	0.110	0.100	—	0.140	0.140	—
13,000	0.115	0.100	0.1918	0.150	0.150	—
13,500	0.120	0.100	—	0.150	0.150	—
14,000	0.120	0.100	—	0.160	0.160	—
14,500	0.120	0.100	—	0.160	0.165	—
15,000	0.125	0.100	—	0.165	0.170	—
15,500	0.125	0.105	—	0.170	0.170	—
16,000	0.130	0.105	—	0.170	0.175	—
16,500	0.130	0.105	—	0.170	0.175	—
17,000	0.130	0.110	0.2232	0.175	0.180	—
17,500	0.135	0.110	—	0.180	0.180	—
18,000	0.140	0.110	—	0.185	0.180	—
18,500	0.145	0.110	—	0.190	0.180	—
19,000	0.150	0.110	—	0.195	0.185	—
19,500	0.150	0.115	—	0.198	0.185	—
20,000	0.155	0.120	0.2490	0.200	0.192	—
20,050	—	—	—	0.200	—	—
20,100	—	—	—	0.200	—	—
20,150	—	—	—	0.205	—	—
20,200	—	—	—	0.205	—	—
20,250	—	—	—	0.205	—	—
20,300	—	—	—	0.205	—	—
20,350	—	—	—	0.205	—	—
20,400	—	—	—	0.205	—	—
20,450	—	—	—	0.210	—	—

GP76 0803 24

**TABLE A-21 (Concluded)**  
**TRUNCATION VARIATION 18 CRACK GROWTH DATA**

Spectrum (hr)	Crack Length at Hole 1			Crack Length at Hole 2		
	Side A (in.)	Side B (in.)	Center (in.)	Side A (in.)	Side B (in.)	Center (in.)
20,500	0.160	0.120	—	0.210	0.200	—
20,550	—	—	—	0.210	—	—
20,600	—	—	—	0.215	—	—
20,650	—	—	—	0.215	—	—
20,700	—	—	—	0.215	—	—
20,750	—	—	—	0.215	—	—
20,800	—	—	—	0.215	—	—
20,850	—	—	—	0.215	—	—
20,900	—	—	—	0.215	—	—
20,950	—	—	—	0.215	—	—
21,000	0.170	0.130	—	0.215	0.205	—
21,500	0.180	0.135	—	0.220	0.210	—
22,000	0.180/0.010 (1)	0.135/0.025	—	0.220/0.010	0.215	—
22,500	0.180/0.020	0.140/0.030	—	0.225/0.025	0.220/0.015	—
23,000	0.190/0.020	0.150/0.030	0.2158	0.225/0.025	0.220/0.015	—
23,500	0.210/0.020	0.180/0.030	—	0.240/0.020	0.240/0.020	—
24,000	0.210/0.050	0.180/0.040	0.2840	0.240/0.030	0.240/0.020	—
24,500	0.210/0.050	0.180/0.050	—	0.240/0.040	0.240/0.030	—
25,000	0.210/0.050	0.190/0.050	0.2921	0.240/0.040	0.250/0.030	—
25,500	0.220/0.060	0.190/0.060	—	0.240/0.050	0.250/0.030	—
26,000	0.240/0.060	0.190/0.060	—	0.240/0.050	0.250/0.050	—
26,500	0.240/0.080	0.190/0.070	—	0.240/0.050	0.250/0.050	—
27,000	0.240/0.080	0.190/0.070	—	0.270/0.060	0.260/0.050	—
27,500	0.260/0.080	0.210/0.070	—	0.270/0.060	0.290/0.070	—
28,000	0.260/0.090	0.220/0.070	0.3242	0.270/0.070	0.290/0.070	—
28,500	0.260/0.100	0.230/0.090	—	0.300/0.090	0.290/0.100	—
29,000	0.270/0.100	0.230/0.090	—	0.300/0.090	0.300/0.100	—
29,500	0.280/0.120	0.250/0.110	—	0.300/0.090	0.300/0.100	—
30,000	0.290/0.120	0.260/0.110	—	0.300/0.090	0.300/0.100	—
30,500	0.300/0.150	0.270/0.110	—	0.300/0.120	0.330/0.100	—
31,000	0.300/0.150	0.280/0.110	—	0.330/0.120	0.320/0.100	—
31,500	0.310/0.150	0.290/0.120	—	0.330/0.120	0.330/0.110	—
32,000	0.310/0.150	0.290/0.150	0.3742	0.350/0.120	0.330/0.120	—
32,500	0.310/0.150	0.290/0.150	—	0.350/0.120	0.340/0.130	—
33,000	0.310/0.150	0.290/0.150	0.3890	0.350/0.120	0.340/0.130	—
33,500	0.310/0.150	0.290/0.150	—	0.350/0.120	0.340/0.130	—
34,000	0.310/0.150	0.290/0.150	0.4062	0.350/0.120	0.340/0.130	—
34,500	0.320/0.180	0.320/0.200	—	0.360/0.160	0.360/0.150	—
35,000	0.340/0.200	0.340/0.210	0.4229-0.4268 (2)	0.370/0.200	0.380/0.180	—
35,500	0.380/0.200	0.360/0.210	—	0.400/0.200	0.400/0.180	—
36,000	0.380/0.200	0.360/0.210	0.4478-0.4410	0.420/0.210	0.420/0.200	—
36,500	0.380/0.200	0.380/0.210	—	0.420/0.210	0.420/0.200	—
37,000	0.380/0.200	0.380/0.210	0.4667-0.4758	0.420/0.210	0.420/0.200	—
37,500	0.380/0.200	0.380/0.210	—	0.420/0.210	0.420/0.200	—
38,000	0.400/0.220	0.400/0.210	0.5067-0.4895	0.440/0.220	0.440/0.220	—
38,500	0.420/0.250	0.420/0.240	—	0.460/0.250	0.460/0.260	—
39,000	0.420/0.260	0.430/0.250	0.5221-0.5585	0.460/0.260	0.460/0.260	—
39,500	0.420/0.260	0.440/0.260	—	0.460/0.260	0.460/0.260	—
40,000	0.480/0.300	0.480/0.300	0.5728-0.6111	0.520/0.320	0.520/0.320	—
40,500	0.500/0.310	0.500/0.300	—	0.540/0.320	0.540/0.320	—
41,000	0.520/0.330	0.520/0.340	0.6292-0.6888	0.560/0.340	0.560/0.340	—
41,500	0.580/0.390	0.580/0.390	—	0.620/0.400	0.620/0.460	—
41,995	0.700/0.510	0.670/0.500	0.7196	0.730/0.500	0.700/0.460	—

(1) Number on right side of "/" indicates crack growth from side of hole opposite intended flaw

(2) Crack lengths separated by a "-" indicate a static burst between these values

GP76-0803-25

**TABLE A-22**  
**COMPRESSION LOADS VARIATION 4 CRACK GROWTH DATA**

Spectrum (hr)	Crack Length at Hole 1			Crack Length at Hole 2		
	Side A (in.)	Side B (in.)	Center (in.)	Side A (in.)	Side B (in.)	Center (in.)
0	0.37	0.047	0.0599	0.004	0.035	—
500	0.04	0.050	—	0.004	0.035	—
714	—	—	0.0850	—	—	—
1,000	0.05	0.060	—	0.020	0.040	—
1,500	0.06	0.080	—	0.030	0.050	—
1,714	—	—	0.1271	—	—	—
2,000	0.08	0.120	—	0.040	0.070	—
2,500	0.10	0.140	—	0.050	0.080	—
2,714	—	—	0.1827	—	—	—
3,000	0.12	0.160	—	0.060	0.100	—
3,500	0.16	0.180	—	0.100	0.120	—
3,714	—	—	0.2453	—	—	—
4,000	0.18	0.210	—	0.120	0.140	—
4,050	—	0.210	—	—	—	—
4,100	—	0.210	—	—	—	—
4,150	—	0.220	—	—	—	—
4,200	—	0.220	—	—	—	—
4,250	—	0.230	—	—	—	—
4,300	—	0.230	—	—	—	—
4,350	—	0.240	—	—	—	—
4,400	—	0.240	—	—	—	—
4,450	—	0.250	—	—	—	—
4,500	0.21	0.260	—	0.160	0.170	—
4,550	—	0.260	—	—	—	—
4,600	—	0.260	—	—	—	—
4,650	—	0.270	—	—	—	—
4,700	—	0.270	—	—	—	—
4,714	—	—	0.3411	—	—	—
4,750	—	0.270	—	—	—	—
4,800	—	0.280	—	—	—	—
4,850	—	0.280	—	—	—	—
4,900	—	0.280	—	—	—	—
4,950	—	0.280	—	—	—	—
5,000	0.24	0.290	—	0.180	0.200	—
5,500	0.28	0.320	—	0.270	0.300	—
5,714	—	—	0.4380	—	—	—
6,000	0.40	0.400	—	0.340	0.340	—
6,500	0.42	0.430	—	0.350	0.350	—
6,714	—	—	0.5481	—	—	—
7,000	0.48	0.490	—	0.420	0.410	—
7,500	0.51	0.530	—	0.450	0.450	—
7,714	—	—	0.7080	—	—	—
8,000	0.57	0.580	—	0.490	0.490	—
8,500	0.62	0.660	—	0.540	0.560	—
8,714	—	—	0.8288	—	—	—
9,000	0.66	0.690	—	0.580	0.580	—
9,500	0.780/0.100 (1)	0.820/0.100	—	0.620	0.660/0.080	—
9,714	—	—	0.9483	—	—	—
10,000	0.920/0.240	0.930/0.260	—	0.760/0.080	0.760/0.150	—
10,120	0.980/0.320	1.000/0.320	1.0118	0.800/0.200	0.800/0.220	—

(1) Number on right side of "/" indicates crack growth from side of hole opposite intended flaw

GP76-0803-26

**TABLE A-23**  
**COMPRESSION LOADS VARIATION 7 CRACK GROWTH DATA**

Spectrum (hr)	Crack Length at Hole 1			Crack Length at Hole 2		
	Side A (in.)	Side B (in.)	Center (in.)	Side A (in.)	Side B (in.)	Center (in.)
0	0.042	0.045	0.0535	0.005	0.008	—
500	0.060	0.050	—	0.005	0.010	—
714	—	—	0.1175	—	—	—
1000	0.080	0.070	—	0.010	0.010	—
1500	0.100	0.110	—	0.040	0.030	—
1714	—	—	0.1860	—	—	—
2000	0.140	0.150	—	0.060	0.100	—
2500	0.180	0.190	—	0.100	0.130	—
2714	—	—	0.2638	—	—	—
3000	0.200	0.220	—	0.160	0.160	—
3050	—	0.240	—	—	—	—
3100	—	0.250	—	—	—	—
3150	—	0.260	—	—	—	—
3200	—	0.260	—	—	—	—
3250	—	0.270	—	—	—	—
3300	—	0.270	—	—	—	—
3350	—	0.270	—	—	—	—
3400	—	0.270	—	—	—	—
3450	—	0.280	—	—	—	—
3500	0.270	0.280	—	0.220	0.220	—
3550	—	0.290	—	—	—	—
3600	—	0.300	—	—	—	—
3650	—	0.310	—	—	—	—
3700	—	0.310	—	—	—	—
3714	—	—	0.3487	—	—	—
3750	—	0.310	—	—	—	—
3800	—	0.320	—	—	—	—
3850	—	0.325	—	—	—	—
3900	—	0.325	—	—	—	—
3950	—	0.325	—	—	—	—
4000	0.330	0.330	—	0.250	0.250	—
4500	0.380	0.380	—	0.310	0.310	—
5000	0.450/0.070 (1)	0.450/0.070	—	0.350	0.350	—
5500	0.540/0.150	0.540/0.150	—	0.420/0.030	0.430/0.030	—
5714	—	—	0.6645	—	—	—
6000	0.650/0.270	0.650/0.270	—	0.480/0.130	0.480/0.130	—
6500	0.900/0.480	0.900/0.480	—	0.580/0.220	0.580/0.220	—
6570	1.040/0.580	1.040/0.580	1.0351	0.600/0.250	0.600/0.250	—

(1) Number on right side of "/" indicates crack growth from side of hole opposite intended flaw

GP76-0803-27

**TABLE A-24**  
**COMPRESSION LOADS VARIATION 10 CRACK GROWTH DATA**

Spectrum (hr)	Crack Length at Hole 1			Crack Length at Hole 2		
	Side A (in.)	Side B (in.)	Center (in.)	Side A (in.)	Side B (in.)	Center (in.)
0	0.020	0.020	—	0.024	0.023	0.0425
500	0.038	0.023	—	0.044	0.027	—
714	—	—	—	—	—	0.0888
1000	0.060	0.067	—	0.069	0.062	—
1500	0.070	0.069	—	0.079	0.089	—
1714	—	—	—	—	—	0.1514
2000	0.103	0.090	—	0.129	0.115	—
2500	0.156	0.171	—	0.171	0.140	—
2714	—	—	—	—	—	0.2180
3000	0.175	0.180	—	0.190	0.200	—
3050	—	—	—	—	0.200	—
3100	—	—	—	—	0.200	—
3150	—	—	—	—	0.210	—
3200	—	—	—	—	0.210	—
3250	—	—	—	—	0.210	—
3300	—	—	—	—	0.220	—
3350	—	—	—	—	0.220	—
3400	—	—	—	—	0.230	—
3450	—	—	—	—	0.230	—
3500	0.190	0.210	—	0.220	0.240	—
3550	—	—	—	—	0.240	—
3600	—	—	—	—	0.250	—
3650	—	—	—	—	0.250	—
3700	—	—	—	—	0.250	—
3714	—	—	—	—	—	0.2895
3750	—	—	—	—	0.260	—
3800	—	—	—	—	0.260	—
3850	—	—	—	—	0.270	—
3900	—	—	—	—	0.270	—
3950	—	—	—	—	0.270	—
4000	0.240	0.230	—	0.270	0.280	—
4500	0.260	0.280	—	0.300	0.310	—
4714	—	—	—	—	—	0.3683
5000	0.320	0.320	—	0.340	0.350	—
5500	0.360	0.360	—	0.380	0.380	—
5714	—	—	—	—	—	0.4570
6000	0.400	0.400	—	0.430	0.440	—
6500	0.430	0.420	—	0.520/0.060 (1)	0.500	—
6714	—	—	—	—	—	0.5902
7000	0.560	0.580	—	0.620/0.150	0.600/0.140	—
7500	0.610/0.060	0.600/0.050	—	0.660/0.250	0.660/0.220	—
7714	—	—	—	—	—	0.7772
8000	0.680/0.180	0.660/0.200	—	0.800/0.440	0.820/0.420	—
8240	0.820/0.220	0.800/0.240	—	0.950/0.700	1.020/0.460	1.0081

(1) Number on right side of "/" indicates crack growth from side of hole opposite intended flaw

GP76-0803-28



**TABLE A-25  
EXCEEDANCE CURVE VARIATION 2 CRACK GROWTH DATA**

Spectrum (hr)	Crack Length at Hole 1			Crack Length at Hole 2		
	Side A (in.)	Side B (in.)	Center (in.)	Side A (in.)	Side B (in.)	Center (in.)
0	0.015	0.035	0.0500	0.003	0.029	—
500	0.044	0.070	—	0.030	0.060	—
780	—	—	0.1040	—	—	—
1000	0.080	0.100	—	0.060	0.080	—
1500	0.120	0.130	—	0.080	0.100	—
1780	—	—	0.1753	—	—	—
2000	0.150	0.160	—	0.120	0.140	—
2500	0.180	0.190	—	0.160	0.170	—
2780	—	—	0.2567	—	—	—
3000	0.220	0.220	—	0.190	0.200	—
3050	—	0.230	—	—	—	—
3100	—	0.230	—	—	—	—
3150	—	0.240	—	—	—	—
3200	—	0.240	—	—	—	—
3250	—	0.250	—	—	—	—
3300	—	0.250	—	—	—	—
3350	—	0.260	—	—	—	—
3400	—	0.270	—	—	—	—
3450	—	0.280	—	—	—	—
3500	0.280	0.280	—	0.240	0.240	—
3550	—	0.290	—	—	—	—
3600	—	0.290	—	—	—	—
3650	—	0.300	—	—	—	—
3700	—	0.310	—	—	—	—
3750	—	0.310	—	—	—	—
3780	—	—	0.3490	—	—	—
3800	—	0.310	—	—	—	—
3850	—	0.320	—	—	—	—
3900	—	0.320	—	—	—	—
3950	—	0.330	—	—	—	—
4000	0.330	0.330	—	0.290	0.300	—
4500	0.380	0.380	—	0.340	0.340	—
4780	—	—	0.4548	—	—	—
5000	0.440	0.440	—	0.380	0.390	—
5500	0.500	0.500	—	0.450	0.450	—
5780	—	—	0.6140	—	—	—
6000	0.570	0.570	—	0.500	0.500	—
6500	0.640/0.130	0.650/0.110	—	0.550	0.560	—
6780	—	—	0.7495	—	—	—
7000	0.770/0.190	0.760/0.220	—	0.620	0.650	—
7500	0.910/0.340	0.910/0.340	—	0.680/0.020	0.680/0.040	—
7770	1.280/0.700	1.280/0.700	1.3063	0.780/0.150	0.800/0.130	—

(1) Number on right side of "/" indicates crack growth from side of hole opposite intended flaw

GP78-0803-28

**TABLE A-26**  
**EXCEEDANCE CURVE VARIATION 5 CRACK GROWTH DATA**

Spectrum (hr)	Crack Length at Hole 1			Crack Length at Hole 2		
	Side A (in.)	Side B (in.)	Center (in.)	Side A (in.)	Side B (in.)	Center (in.)
0	0.017	0.021	0.0338	0.009	0.018	—
500	0.061	0.068	—	0.048	0.058	—
830	—	—	0.1183	—	—	—
1000	0.105	0.106	—	0.086	0.102	—
1500	0.145	0.150	—	0.120	0.140	—
1830	—	—	0.2095	—	—	—
2000	0.190	0.190	—	0.160	0.180	—
2500	0.230	0.250	—	0.200	0.230	—
2550	—	0.250	—	—	—	—
2600	—	0.250	—	—	—	—
2650	—	0.250	—	—	—	—
2700	—	0.250	—	—	—	—
2750	—	0.260	—	—	—	—
2800	—	0.270	—	—	—	—
2830	—	—	0.3021	—	—	—
2850	—	0.280	—	—	—	—
2900	—	0.290	—	—	—	—
2950	—	0.300	—	—	—	—
3000	0.290/0.050 (1)	0.310/0.090	—	0.250	0.280	—
3050	—	0.320	—	—	—	—
3100	—	0.320	—	—	—	—
3150	—	0.320	—	—	—	—
3200	—	0.320	—	—	—	—
3250	—	0.330	—	—	—	—
3300	—	0.330	—	—	—	—
3350	—	0.330	—	—	—	—
3400	—	0.340	—	—	—	—
3450	—	0.340	—	—	—	—
3500	0.350/0.110	0.360/0.140	—	0.280	0.300	—
3830	—	—	0.4641	—	—	—
4000	0.480/0.250	0.480/0.260	—	0.360/0.060	0.380/0.100	—
4500	0.560/0.390	0.560/0.380	—	0.440/0.160	0.440/0.180	—
4830	0.900/0.680	0.900/0.680	0.8939	0.550/0.300	0.550/0.300	—

(1) Number on right side of "/" indicates crack growth from side of hole opposite intended flaw

GP76-0803-30

**TABLE A-27**  
**EXCEEDANCE CURVE VARIATION 6 CRACK GROWTH DATA**

Spectrum (hr)	Crack Length at Hole 1			Crack Length at Hole 2		
	Side A (in.)	Side B (in.)	Center (in.)	Side A (in.)	Side B (in.)	Center (in.)
0	0.037	0.030	—	0.008	0.031	0.0418
500	0.065	0.053	—	0.035	0.057	—
994	—	—	—	—	—	0.1528
1000	0.140	0.120	—	0.120	0.130	—
1500	0.170	0.160	—	0.160	0.170	—
1994	—	—	—	—	—	0.2342
2000	0.220	0.210	—	0.190	0.210	—
2050	0.240	—	—	—	—	—
2100	0.245	—	—	—	—	—
2150	0.250	—	—	—	—	—
2200	0.255	—	—	—	—	—
2250	0.260	—	—	—	—	—
2300	0.260	—	—	—	—	—
2350	0.265	—	—	—	—	—
2400	0.265	—	—	—	—	—
2450	0.275	—	—	—	—	—
2500	0.280/0.130 (1)	0.275/0.115	—	0.240/0.050	0.230/0.060	—
2550	0.285	—	—	—	—	—
2600	0.290	—	—	—	—	—
2650	0.295	—	—	—	—	—
2700	0.300	—	—	—	—	—
2750	0.305	—	—	—	—	—
2800	0.305	—	—	—	—	—
2850	0.310	—	—	—	—	—
2900	0.320	—	—	—	—	—
2950	0.330	—	—	—	—	—
2994	—	—	—	—	—	0.3438
3000	0.360/0.240	0.370/0.240	—	0.320/0.120	0.320/0.140	—
3500	0.530/0.380	0.520/0.420	—	0.400/0.200	0.400/0.220	—
3825	0.830/0.710	0.800/0.700	—	0.480/0.250	0.470/0.280	0.4720

(1) Number on right side of "/" indicates crack growth from side of hole opposite intended flaw

GP78-0803-31

**TABLE A-28**  
**COUPLING OF PEAKS AND VALLEYS VARIATION 5 CRACK GROWTH DATA**

Spectrum (hr)	Crack Length at Hole 1			Crack Length at Hole 2		
	Side A (in.)	Side B (in.)	Center (in.)	Side A (in.)	Side B (in.)	Center (in.)
0	0.008	0.010	—	0.023	0.018	0.0343
424	—	—	—	—	—	0.0757
500	0.013	0.015	—	0.031	0.026	—
1000	0.041	0.042	—	0.057	0.066	—
1424	—	—	—	—	—	0.1562
1500	0.085	0.079	—	0.118	0.118	—
2000	0.095	0.120	—	0.145	0.150	—
2424	—	—	—	—	—	0.2525
2500	0.175	0.165	—	0.200	0.210	—
2550	—	—	—	—	0.220	—
2600	—	—	—	—	0.220	—
2650	—	—	—	—	0.240	—
2700	—	—	—	—	0.240	—
2750	—	—	—	—	0.250	—
2800	—	—	—	—	0.250	—
2850	—	—	—	—	0.250	—
2900	—	—	—	—	0.250	—
2950	—	—	—	—	0.250	—
3000	0.200	0.200	—	0.240	0.250	—
3050	—	—	—	—	0.250	—
3100	—	—	—	—	0.250	—
3150	—	—	—	—	0.250	—
3200	—	—	—	—	0.260	—
3250	—	—	—	—	0.260	—
3300	—	—	—	—	0.270	—
3350	—	—	—	—	0.270	—
3400	—	—	—	—	0.280	—
3424	—	—	—	—	—	0.4711
3450	—	—	—	—	0.290	—
3500	0.270	0.260	—	0.290	0.300	—
4000	0.300	0.290	—	0.360	0.370	—
4424	—	—	—	—	—	0.7189
4500	0.360	0.320	—	0.460/0.120 (1)	0.460	—
5000	0.460/0.150	0.460/0.100	—	0.560/0.240	0.580/0.260	—
5097	—	—	—	—	—	0.8532-0.8700 (2)
5424	—	—	—	—	—	0.9685-0.9870
5500	0.580/0.240	0.540/0.150	—	0.800/0.380	0.800/0.400	—
5800	0.600/0.250	0.580/0.200	—	1.040/0.720	1.050/0.700	1.0415

(1) Number on right side of "/" indicates crack growth from side of hole opposite intended flaw

GP78-0803-32

(2) Crack lengths separated by a "-" indicate a static burst between these values

**TABLE A-29**  
**COUPLING OF PEAKS AND VALLEYS VARIATION 7 CRACK GROWTH DATA**

Spectrum (hr)	Crack Length at Hole 1			Crack Length at Hole 2		
	Side A (in.)	Side B (in.)	Center (in.)	Side A (in.)	Side B (in.)	Center (in.)
0	0.029	0.032	0.0417	0.010	0.005	—
500	0.062	0.064	—	0.054	0.012	—
714	—	—	0.1012	—	—	—
1000	0.100	0.100	—	0.084	0.064	—
1500	0.120	0.120	—	0.090	0.100	—
1714	—	—	0.1740	—	—	—
2000	0.130	0.140	—	0.100	0.110	—
2500	0.150	0.160	—	0.120	0.120	—
2714	—	—	0.2523	—	—	—
3000	0.210	0.220	—	0.160	0.160	—
3050	—	0.220	—	—	—	—
3100	—	0.230	—	—	—	—
3150	—	0.240	—	—	—	—
3200	—	0.240	—	—	—	—
3250	—	0.250	—	—	—	—
3300	—	0.250	—	—	—	—
3350	—	0.250	—	—	—	—
3400	—	0.250	—	—	—	—
3450	—	0.260	—	—	—	—
3500	0.240	0.260	—	0.200	0.200	—
3550	—	0.260	—	—	—	—
3600	—	0.270	—	—	—	—
3650	—	0.270	—	—	—	—
3700	—	0.280	—	—	—	—
3714	—	—	0.3380	—	—	—
3750	—	0.280	—	—	—	—
3800	—	0.280	—	—	—	—
3850	—	0.290	—	—	—	—
3900	—	0.290	—	—	—	—
3950	—	0.300	—	—	—	—
4000	0.290	0.300	—	0.260	0.260	—
4500	0.330	0.340	—	0.260	0.280	—
4714	—	—	0.4278	—	—	—
5000	0.380	0.380	—	0.290	0.300	—
5500	0.440	0.440	—	0.350	0.350	—
5714	—	—	0.5373	—	—	—
6000	0.500	0.500	—	0.400	0.400	—
6500	0.560/0.100 (1)	0.560/0.120	—	0.450	0.450	—
6714	—	—	0.7834	—	—	—
7000	0.700/0.250	0.700/0.270	—	0.500/0.060	0.500/0.100	—
7500	0.820/0.370	0.820/0.380	—	0.570/0.120	0.570/0.170	—
7665	1.030/0.560	1.040/0.570	1.0560	0.640/0.150	0.640/0.180	—

(1) Number on right side of "/" indicates crack growth from side of hole opposite intended flaw

GP76-0803-33

**TABLE A-30**  
**COMBINED VARIATION 3 CRACK GROWTH DATA**

Spectrum (hr)	Crack Length at Hole 1			Crack Length at Hole 2		
	Side A (in.)	Side B (in.)	Center (in.)	Side A (in.)	Side B (in.)	Center (in.)
0	0.020	0.033	0.0405	0.005	0.028	—
500	0.045	0.061	—	0.034	0.060	—
727	—	—	0.0784	—	—	—
1000	0.070	0.100	—	0.050	0.090	—
1500	0.100	0.120	—	0.090	0.110	—
1727	—	—	0.1125	—	—	—
2000	0.140	0.150	—	0.120	0.130	—
2500	0.150	0.160	—	0.150	0.160	—
2727	—	—	0.2292	—	—	—
3000	0.190	0.190	—	0.180	0.180	—
3500	0.220	0.220	—	0.200	0.200	—
3550	—	0.230	—	—	—	—
3600	—	0.240	—	—	—	—
3650	—	0.240	—	—	—	—
3700	—	0.250	—	—	—	—
3727	—	—	0.3521	—	—	—
3750	—	0.270	—	—	—	—
3800	—	0.270	—	—	—	—
3850	—	0.270	—	—	—	—
3900	—	0.270	—	—	—	—
3950	—	0.270	—	—	—	—
4000	0.270	0.280	—	0.240	0.250	—
4050	—	0.280	—	—	—	—
4100	—	0.300	—	—	—	—
4150	—	0.300	—	—	—	—
4200	—	0.300	—	—	—	—
4250	—	0.320	—	—	—	—
4300	—	0.320	—	—	—	—
4350	—	0.320	—	—	—	—
4400	—	0.320	—	—	—	—
4450	—	0.320	—	—	—	—
4500	0.320/0.140 (1)	0.330/0.140	—	0.280/0.080	0.270/0.070	—
4727	—	—	0.5229	—	—	—
5000	0.410/0.240	0.410/0.220	—	0.320/0.140	0.320/0.130	—
5500	0.510/0.030	0.480/0.320	—	0.390/0.190	0.410/0.180	—
5727	—	—	0.7195-0.7533 (2)	—	—	—
5950	0.750/0.530	0.730/0.550	0.7722	0.520/0.280	0.560/0.280	—

(1) Number on right side of "/" indicates crack growth from side of hole opposite intended flaw

GP78-0803-34

(2) Crack lengths separated by a "-" indicate a static burst between these values

**TABLE A-31**  
**COMBINED VARIATION 4 CRACK GROWTH DATA**

Spectrum (hr)	Crack Length at Hole 1			Crack Length at Hole 2		
	Side A (in.)	Side B (in.)	Center (in.)	Side A (in.)	Side B (in.)	Center (in.)
0	0.014	0.021	0.0528	0.018	0.002	—
500	0.014	0.046	—	0.022	0.012	—
980	—	—	0.0924	—	—	—
1000	(1)	0.072	—	0.058	0.046	—
1500	(1)	0.104	—	0.079	0.069	—
1980	—	—	0.1535	—	—	—
2000	0.125	0.135	—	0.104	0.097	—
2500	0.170	0.170	—	0.130	0.120	—
2980	—	—	0.2148	—	—	—
3000	0.190	0.180	—	0.170	0.160	—
3500	0.220	0.210	—	0.200	0.200	—
3550	0.230	—	—	—	—	—
3600	0.240	—	—	—	—	—
3650	0.250	—	—	—	—	—
3700	0.250	—	—	—	—	—
3750	0.260	—	—	—	—	—
3800	0.260	—	—	—	—	—
3850	0.260	—	—	—	—	—
3900	0.270	—	—	—	—	—
3950	0.270	—	—	—	—	—
3980	—	—	0.3221	—	—	—
4000	0.280	0.270	—	0.240	0.240	—
4050	0.280	—	—	—	—	—
4100	0.290	—	—	—	—	—
4150	0.290	—	—	—	—	—
4200	0.290	—	—	—	—	—
4250	0.300	—	—	—	—	—
4300	0.300	—	—	—	—	—
4350	0.310	—	—	—	—	—
4400	0.310	—	—	—	—	—
4450	0.320	—	—	—	—	—
4500	0.320	0.320	—	0.280	0.280	—
4980	—	—	0.4317	—	—	—
5000	0.360	0.360	—	0.330	0.320	—
5500	0.400	0.400	—	0.360	0.360	—
5980	—	—	0.5522	—	—	—
6000	0.460	0.460	—	0.410	0.400	—
6500	0.540/0.040 (2)	0.540	—	0.480	0.480	—
6980	—	—	0.6970	—	—	—
7000	0.600/0.080	0.600	—	0.540	0.550	—
7500	0.660/0.120	0.660/0.120	—	0.580	0.580	—
7980	—	—	0.8528	—	—	—
8000	0.850/0.260	0.850/0.260	—	0.640/0.060	0.640	—
8400	1.000/0.360	1.000/0.360	1.0212	0.740/0.090	0.720	—

(1) Crack grew into a shallow hole in the specimen and could not be read.

GP78-0803-35

(2) Number on right side of "/" indicates crack growth from side of hole opposite intended flaw.

**TABLE A-32**  
**COMPOSITE BASELINE SPECTRUM AT 19.8 KSI CRACK GROWTH DATA**

Spectrum (hr)	Crack Length at Hole 1			Crack Length at Hole 2		
	Side A (in.)	Side B (in.)	Center (in.)	Side A (in.)	Side B (in.)	Center (in.)
0	0.002	0.004	—	0.022	0.017	0.0207
500	0.008	0.005	—	0.025	0.020	—
714	—	—	—	—	—	0.0305
1,000	0.015	0.012	—	0.032	0.024	—
1,500	0.015	0.012	—	0.032	0.026	—
1,714	—	—	—	—	—	0.0463
2,000	0.022	0.022	—	0.047	0.038	—
2,500	0.030	0.028	—	0.053	0.045	—
2,714	—	—	—	—	—	0.0673
3,000	0.040	0.030	—	0.055	0.047	—
3,500	0.043	0.042	—	0.068	0.055	—
3,714	—	—	—	—	—	0.0838
4,000	0.043	0.048	—	0.075	0.070	—
4,500	0.060	0.050	—	0.084	0.074	—
4,714	—	—	—	—	—	0.1041
5,000	0.066	0.065	—	0.085	0.088	—
5,500	0.086	0.082	—	0.101	0.097	—
5,714	—	—	—	—	—	0.1273
6,000	0.096	0.092	—	0.110	0.110	—
6,500	0.110	0.100	—	0.130	0.120	—
6,714	—	—	—	—	—	0.1488
7,000	0.120	0.110	—	0.140	0.130	—
7,500	0.120	0.120	—	0.140	0.130	—
7,714	—	—	—	—	—	0.1697
8,000	0.120	0.120	—	0.150	0.130	—
8,500	0.120	0.120	—	0.150	0.140	—
8,714	—	—	—	—	—	0.1946
9,000	0.120	0.120	—	0.150	0.140	—
9,500	0.140	0.140	—	0.180	0.170	—
9,714	—	—	—	—	—	0.2190
10,000	0.160	0.160	—	0.200	0.190	—
10,050	—	—	—	0.200	—	—
10,100	—	—	—	0.200	—	—
10,150	—	—	—	0.210	—	—
10,200	—	—	—	0.210	—	—

GP76-0803-37



**TABLE A-32 (Continued)**  
**COMPOSITE BASELINE SPECTRUM AT 19.8 KSI CRACK GROWTH DATA**

Spectrum (hr)	Crack Length at Hole 1			Crack Length at Hole 2		
	Side A (in.)	Side B (in.)	Center (in.)	Side A (in.)	Side B (in.)	Center (in.)
10,250	—	—	—	0.210	—	—
10,300	—	—	—	0.210	—	—
10,350	—	—	—	0.210	—	—
10,400	—	—	—	0.210	—	—
10,450	—	—	—	0.210	—	—
10,500	0.160	0.160	—	0.210	0.200	—
10,550	—	—	—	0.220	—	—
10,600	—	—	—	0.220	—	—
10,650	—	—	—	0.220	—	—
10,700	—	—	—	0.220	—	—
10,714	—	—	—	—	—	0.2420
10,750	—	—	—	0.220	—	—
10,800	—	—	—	0.220	—	—
10,850	—	—	—	0.220	—	—
10,900	—	—	—	0.220	—	—
10,950	—	—	—	0.220	—	—
11,000	0.180	0.180	—	0.220	0.220	—
11,500	0.180	0.190	—	0.220	0.220	—
11,714	—	—	—	—	—	0.2735
12,000	0.200	0.200	—	0.220	0.220	—
12,500	0.200	0.200	—	0.230	0.220	—
12,714	—	—	—	—	—	0.3020
13,000	0.230	0.220	—	0.260	0.260	—
13,500	0.260	0.260	—	0.300	0.300	—
13,714	—	—	—	—	—	0.3313
14,000	0.280	0.280	—	0.320	0.310	—
14,500	0.280	0.280	—	0.320	0.320	—
14,714	—	—	—	—	—	0.3580
15,000	0.300	0.300	—	0.350	0.340	—
15,500	0.320	0.320	—	0.360	0.360	—
15,714	—	—	—	—	—	0.3986
16,000	0.340	0.340	—	0.370	0.370	—
16,500	0.350	0.350	—	0.380	0.380	—
16,714	—	—	—	—	—	0.4337
17,000	0.360	0.360	—	0.410	0.420	—

GP76-0803-36

**TABLE A-32 (Concluded)**  
**COMPOSITE BASELINE SPECTRUM AT 19.8 KSI CRACK GROWTH DATA**

Spectrum (hr)	Crack Length at Hole 1			Crack Length at Hole 2		
	Side A (in.)	Side B (in.)	Center (in.)	Side A (in.)	Side B (in.)	Center (in.)
17,500	0.360	0.370	—	0.410	0.430	—
17,714	—	—	—	—	—	0.4706
18,000	0.400	0.400	—	0.450	0.450	—
18,500	0.400	0.400	—	0.450	0.450	—
18,714	—	—	—	—	—	0.5106
19,000	0.430	0.430	—	0.480	0.480	—
19,500	0.450	0.450	—	0.490	0.490	—
19,714	—	—	—	—	—	0.5512
20,000	0.470	0.470	—	0.530	0.530	—
20,500	0.490	0.490	—	0.550	0.550	—
20,714	—	—	—	—	—	0.5935
21,000	0.530	0.530	—	0.580	0.580	—
21,500	0.530	0.530	—	0.590	0.590	—
21,714	—	—	—	—	—	0.6438
22,000	0.560	0.560	—	0.620	0.620/0.020 (1)	—
22,500	0.570	0.570	—	0.630	0.630/0.040	—
22,714	—	—	—	—	—	0.7015
23,000	0.610	0.600	—	0.680	0.680/0.080	—
23,500	0.620	0.620	—	0.690	0.700/0.090	—
23,714	—	—	—	—	—	0.7691
24,000	0.660	0.660	—	0.740/0.070	0.740/0.130	—
24,500	0.700	0.690	—	0.760/0.100	0.760/0.150	—
24,714	—	—	—	—	—	0.8300
25,000	0.720	0.720	—	0.810/0.150	0.810/0.200	—
25,500	0.720	0.750	—	0.850/0.200	0.850/0.240	—
25,714	—	—	—	—	—	0.9158
26,000	0.770	0.770	—	0.900/0.230	0.860/0.250	—
26,500	0.820	0.770	—	0.920/0.260	0.920/0.280	—
27,000	0.84/0.10	0.840	—	0.970/0.340	1.000/0.350	1.0278

(1) Number on right side of "/" indicates crack growth from side of hole opposite intended flaw

GP76-0803-39

**TABLE A-33**  
**COMPOSITE BASELINE SPECTRUM AT 40.2 KSI CRACK GROWTH DATA**

Spectrum (hr)	Crack Length at Hole 1			Crack Length at Hole 2		
	Side A (in.)	Side B (in.)	Center (in.)	Side A (in.)	Side B (in.)	Center (in.)
0	0.02	0.004	—	0.035	0.033	0.0398
14	—	—	—	—	—	0.0433
23	—	—	—	—	—	0.0460
27	—	—	—	—	—	0.0488
93	—	—	—	—	—	0.0512
94	—	—	—	—	—	0.0544
109	—	—	—	—	—	0.0567
135	—	—	—	—	—	0.0602
138	—	—	—	—	—	0.0638
167	—	—	—	—	—	0.0688
186	—	—	—	—	—	0.0730
251	—	—	—	—	—	0.0767
253	—	—	—	—	—	0.0803
500	0.08	0.028	—	0.090	0.080	—
519	—	—	—	—	—	0.0855
552	—	—	—	—	—	0.0920
588	—	—	—	—	—	0.0981
695	—	—	—	—	—	0.1054
614	—	—	—	—	—	0.1152
648	—	—	—	—	—	0.1263
714	—	—	—	—	—	0.1462
1000	0.12	0.080	—	0.150	0.150	—
1500	0.15	0.130	—	0.180	0.180	—
1552	—	—	—	—	—	0.1880
1614	—	—	—	—	—	0.2254
1714	—	—	—	—	—	0.2728
2000	0.21	0.200	—	0.280	0.250	—
2050	—	—	—	0.290/0.080 (1)	—	—
2100	—	—	—	0.300/0.100	—	—
2150	—	—	—	0.330/0.130	—	—
2200	—	—	—	0.350/0.150	—	—
2250	—	—	—	0.380/0.160	—	—
2300	—	—	—	0.380/0.180	—	—
2350	—	—	—	0.380/0.180	—	—
2400	—	—	—	0.380/0.180	—	—
2450	—	—	—	0.380/0.190	—	—
2500	0.28/0.07	0.260/0.060	—	0.400/0.190	0.380/0.190	—
2550	—	—	—	0.420/0.230	—	—
2552	—	—	—	—	—	0.4307
2600	—	—	—	0.480/0.280	—	—
2605	—	—	—	—	—	0.5235
2614	—	—	—	—	—	0.6023
2650	—	—	—	0.570/0.370	—	—
2700	—	—	—	0.620/0.450	—	—
2711	0.40/0.23	0.370/0.200	—	0.650/0.450	0.650/0.370	0.6468

(1) Number on right side of "/" indicates crack growth from side of hole opposite intended flaw

GP76-0803-38